



ELSEVIER

TREATISE ON COASTAL AND ESTUARINE SCIENCE- CONTRIBUTORS' INSTRUCTIONS

PROOFREADING

The text content for your contribution is in final form when you receive proofs. Please read proofs for accuracy and clarity, as well as for typographical errors, but please **DO NOT REWRITE**.

At the beginning of your chapter there is a page containing any author queries, keywords, and the authors' full address details.

Please address author queries as necessary. While it is appreciated that some chapters will require updating/revising, please try to keep any alterations to a minimum. Excessive alterations may be charged to the contributors.

The shorter version of the address at the beginning of the chapter will appear under your author/co-author name(s) in the published work and also in a List of Contributors. The longer version shows full contact details and will be used to keep our internal records up-to-date (they will not appear in the published work). For the lead author, this is the address that the honorarium and any offprints will be sent to. Please check that these addresses are correct.

Titles and headings should be checked carefully for spelling and capitalization. Please be sure that the correct typeface and size have been used to indicate the proper level of heading. Review numbered items for proper order – e.g., tables, figures, footnotes, and lists. Proofread the captions and credit lines of illustrations and tables. Ensure that any material requiring permissions has the required credit line, and that the corresponding documentation has been sent to Elsevier.

Note that these proofs may not resemble the image quality of the final printed version of the work, and are for content checking only. Artwork will have been redrawn/relabelled as necessary, and is represented at the final size.

PLEASE KEEP A COPY OF ANY CORRECTIONS YOU MAKE.

DESPATCH OF CORRECTIONS

Proof corrections should be returned in one communication to **Laura Jackson, at the Elsevier MRW Production Dept**, by **18-Jan-2011** using one of the following methods:

1. **PREFERRED:** Corrections should be listed in an e-mail to **Laura Jackson** at Elsevier MRW Dept at ESCO-Proofs@elsevier.com. Please do not send corrections to the Editors.

The e-mail should state the chapter code number in the subject line. Corrections should be consecutively numbered and should state the paragraph number, line number within that paragraph, and the correction to be made.

2. If corrections are substantial, send the amended hardcopy by courier to **Laura Jackson, Elsevier MRW Production Department, The Boulevard, Langford Lane, Kidlington, Oxford, OX5 1GB, UK**. If it is not possible to courier your corrections, please fax the relevant marked pages to the Elsevier MRW Production Department (**fax number: +44 (0)1865 843974**) with a covering note clearly stating the chapter code number and title.

Note that a delay in the return of proofs could mean a delay in publication. Should we not receive corrected proofs within 10 days, Elsevier may proceed without your corrections.

CHECKLIST

- | | |
|--|--------------------------|
| Author queries addressed/answered? | <input type="checkbox"/> |
| Affiliations, names and addresses checked and verified? | <input type="checkbox"/> |
| 'References' section checked and completed?
<i>Please take this opportunity to bring the critical references in your chapter up to date</i> | <input type="checkbox"/> |
| Permissions details checked and completed? | <input type="checkbox"/> |
| Outstanding permissions letters attached/enclosed? | <input type="checkbox"/> |
| Figures and tables checked? | <input type="checkbox"/> |

If you have any questions regarding these proofs please contact the Elsevier MRW Production Department at: ESCO-Proofs@elsevier.com.

Author Query Form

Treatise on Estuarine and Coastal Science

Article: 00504

Dear Author,

Please respond to the queries listed below. You may write your comments on this page, but please write clearly as illegible mark-ups may delay publication. If returning the proof by fax do not write too close to the paper's edge.

Thank you for your assistance.

AUTHOR QUERIES

-
- AU1 Please check the long affiliations for accuracy. These are for Elsevier's records and will not appear in the printed work.
-
- AU2 Perils (1995) is not listed in the References section (cited more than once). Please provide complete details of this reference.
-
- AU3 The references Gosh et al. (1987), Hunt et al. (2009), and Ortega et al. (2004) are cited in the tables, but not listed. Please provide full reference details for these references.
-
- AU4 Chanton et al. (1988) or Chanton et al. (1989)? Please check. If the cross reference is Chanton et al. (1988), then please provide complete details of the reference.
-
- AU5 Please provide color photo for author, Gwenaël Abril.
-
- AU6 Do Figures 1–28 and Tables 1–11 require permission? If yes, please provide the relevant correspondence granting permission and the source of the figure/table. [If you have already provided this information, please ignore this query.]
-
- AU7 Blair and Aller (2005) is not listed in the References section. Please check.
-
- AU8 Battin et al. (2009) or Battin et al. (2008)? Please check. If the cross reference is Battin et al. (2009), then please provide complete details of the reference.
-

-
- AU9 Biswas et al. (2006) or Biswas et al. (2007)? Please check. If the cross reference is Biswas et al. (2006), then please provide complete details of the reference.
-
- AU10 Chanton et al. (1986) is not listed in the References section. Please provide complete details of the reference.
-
- AU11 Agosta (1983) is not listed in the References section. Please check.
-
- AU12 Bouillon et al. (2008) is not listed in the References section. Please check.
-
- AU13 Sansone and Martens (1978) or Sansone and Martens (1977)? Please check. If the cross reference is Sansone and Martens (1978), then please provide complete details of the reference.
-
- AU14 OK as edited?
-
- AU15 OK as edited?
-
- AU16 Please provide in-text citation for Table 11.
-
- AU17 References Aller (1998), Bange (2006), Battin et al. (2008), Chanton and Whiting (1995), Hunt et al. (2010), Ivanov et al. (2002), Martens and Goldhaber (1978), Meybeck et al. 2006., Ortega et al. (2005), and Sansone and Martens (1977) are not cited in the text. Please check.
-
- AU18 Please update the references 'Deborde et al. (2010)', 'Dürr et al. (2010)', 'Hunt et al. (2010)', and 'Koné et al. (2010)', 'Laruelle et al. (2010)'.
-
- AU19 Van der Nat and Middelburg, 1998a or 1998b? Please check.
-
- AU20 Kristensen (2008) is not listed in the References section (cited more than once). Please check.
-
- AU21 Chen et al. (2009) is not listed in the References section (cited more than once). Please check.
-
- AU22 Bouillon et al., 2007a or 2007b or 2007c? Please check.
-

Non-print Items

Author's Contact Information

[AU1]

AV Borges

Chemical Oceanography Unit
University of Liège
Liège
Belgium
E-mail: alberto.borges@ulg.ac.be

G Abril

Environnements et Paléoenvironnements Océaniques
Université Bordeaux 1
Bordeaux
France
E-mail: g.abril@epoc.u-bordeaux1.fr

Keywords: Atmospheric fluxes; Carbon cycle; Carbon dioxide; Community respiration; Estuaries; Gross primary production; Intertidal areas; Methane; Net ecosystem production; Nitrification; Oxygen; pH; Rivers; Sediments; Total alkalinity

ELSEVIER AUTHOR PROOF

Biographical Sketches



Alberto Vieira Borges was born in Portugal in 1972, graduated in biology from the Université Libre de Bruxelles in 1994, graduated in oceanology from the Université de Liège in 1996, and obtained his PhD from the Université de Liège in 2001. His master thesis and PhD were supervised by Michel Frankignoulle (1957–2005). In 2005, he became a Research Associate at the Fonds National de la Recherche Scientifique, and since then he heads the Chemical Oceanography Unit of the University of Liège. His research interest is on carbon cycling across aquatic ecosystems (freshwaters, coastal environments, continental- shelf seas, and open ocean) with an emphasis on the exchange of CO₂ with the atmosphere, and the coupling between inorganic carbon dynamics and biological processes.

AU5

Gwenaël Abril was born in France in 1969, obtained his PhD in environmental biogeochemistry from the University Bordeaux 1 in 1999. His thesis dealt with the biogeochemistry of highly turbid estuaries. After a postdoctoral study dedicated to methane dynamics in aquatic systems at the Aalborg University, Denmark, he became research associate at the Centre National de la Recherche Scientifique in France in 2001. He worked for 9 years at the EPOC laboratory (Environnements et Paléoenvironnements OCéaniques) in Bordeaux, comparing the carbon cycle of various temperate and tropical aquatic systems and their respective CO₂ and CH₄ dynamics. He worked in temperate European rivers, estuaries, and lagoons, in a tropical hydroelectric reservoir in French Guiana, and more recently, in the Amazon River system. A large part of his time was also dedicated to the application of new methodological approaches. He is currently Researcher at the French Institut de Recherche et Développement (IRD), and affiliated to the Universidade Federal de Amazonas (UFAM), Manaus, Brazil, where he develops and coordinates research dealing with the greenhouse gas budget of Amazonian aquatic systems, both natural and artificial.

a0005

5.04 Carbon Dioxide and Methane Dynamics in Estuaries

AV Borges, University of Liège, Liège, Belgium

G Abril, Université Bordeaux 1, Bordeaux, France

© 2012 Elsevier Inc. All rights reserved.

5.04.1	Estuarine Definitions and Classifications from the Perspective of CO₂ and CH₄ Dynamics	1
5.04.2	Dynamics of CO₂ and Atmospheric CO₂ Fluxes in Estuarine Environments	2
5.04.2.1	Spatial and Temporal Variability of CO ₂ in Estuaries	2
5.04.2.2	Drivers of the Emission of CO ₂ to the Atmosphere from Estuaries	4
5.04.2.2.1	Net ecosystem production in estuaries	5
5.04.2.2.2	Riverine inputs of CO ₂ and CH ₄ to estuaries	12
5.04.3	Dynamics of CH₄ and Atmospheric CH₄ Fluxes in Estuarine Environments	18
5.04.3.1	Occurrence of High CH ₄ Concentrations in Estuarine Sediments: Combined Controls of Methanogenesis by Organic Matter Supply and Salinity	18
5.04.3.2	Pathways and Fluxes of CH ₄ from Sediment to Water and to the Atmosphere	22
5.04.3.3	Distribution and Fate of CH ₄ in Estuarine Waters: Oxidation versus Degassing	27
5.04.4	Gas Transfer Velocities of CO₂ and CH₄ in Estuarine Environments: Multiple Drivers and A Large Source of Uncertainty in Flux Evaluations	31
5.04.5	Significance of CO₂ and CH₄ Emission from Estuaries in the Global Carbon Cycle	33
5.04.6	Summary and Perspectives	37
References		38

Abstract

Estuaries profoundly transform the large amounts of carbon delivered from rivers before their transfer to the adjacent coastal zone. As a consequence of the complex biogeochemical reworking of allochthonous carbon in the sediments and the water column, CO₂ and CH₄ are emitted into the atmosphere. We attempt to synthesize available knowledge on biogeochemical cycling of CO₂ and CH₄ in estuarine environments, with a particular emphasis on the exchange with the atmosphere. Unlike CH₄, the global emission of CO₂ to the atmosphere from estuaries is significant compared to other components of the global carbon cycle.

p0010 Estuaries are dynamic ecosystems that host some of the highest biodiversity and biological production in the world (Bianchi, 2007). At the land–ocean interface, estuaries receive large amounts of dissolved and particulate carbon (C), nitrogen (N), phosphorous (P), and silica from rivers. This riverine material undergoes profound transformations in estuaries before being transferred to the adjacent coastal zone (Wollast, 1983). Since the pioneering studies of Park et al. (1969) and Reeburgh (1969), it is known that estuarine environments emit carbon dioxide (CO₂) and methane (CH₄) to the atmosphere. Yet, it is only during the last decade that the dynamics of these two potent green-house gases has been investigated in greater depth in estuarine environments. In the present chapter, we summarize the available knowledge on the multiple drivers of biogeochemical cycling of CO₂ and CH₄ in estuarine environments, with a particular emphasis on the exchange with the atmosphere.

s0005 5.04.1 Estuarine Definitions and Classifications from the Perspective of CO₂ and CH₄ Dynamics

p0015 Estuaries are commonly defined as “semi-enclosed coastal bodies of water that have a free connection with the open sea and within which sea water is measurably diluted with fresh

water derived from land drainage” (Pritchard, 1967). This definition, based on salinity, was extended by Perils (1995) including geomorphological, physical, and biological information, whereby an estuary is defined as “a semi-enclosed coastal body of water that extends to the effective limit of tidal influence, within which sea water entering from one or more free connections with the open sea, or any saline coastal body of water, is significantly diluted with fresh water derived from land drainage, and can sustain euryhaline biological species from either part or the whole of the life cycle.” This definition allows to set the upstream limit of estuaries to the tidal river and to include within estuaries the intertidal areas. Although from the point of view of, for example, estuarine ecology, coastal management, and legislation, the definitions of Pritchard (1967) and Perillo (1995) might be ambiguous or incomplete (e.g., Elliott and McLusky, 2002), these definitions provide the basis for the analysis of CO₂ and CH₄ biogeochemistry examined in this chapter. However, there is a need to further classify estuarine systems into different types that are characterized by different physical settings that strongly influence organic carbon dynamics and, ultimately, CO₂ and CH₄ dynamics.

The first estuarine classifications were based on physiography. Pritchard (1952, 1955) classified estuaries based on physical mixing. Fairbridge (1980) provided a classification

AU2

p0020

based on circulation and relief with the following types: coastal plain, bar-built, delta, blind, ria, tectonic, and fjord. Perillo (1995) provided a morphogenetic classification based on the genesis of the systems. Primary estuaries correspond to former river valleys (coastal plain estuaries and rias), former glacier valleys (fjords and fjärds), and river-dominated (tidal river estuaries and delta fronts), and structural estuaries; secondary estuaries correspond to coastal lagoons divided into choked, restricted, and leaky lagoons. The classification of Perillo (1995) does not take into account the tidal regime of estuaries. Tidal systems can be classified into micro-, meso-, and macro-tidal estuaries corresponding to tidal amplitudes <2 m, 2–4 m, and >4 m, respectively (Davies, 1964). Tidal regime will, to a large extent, regulate the freshwater residence time and stratification of the water column. These physical settings will strongly influence organic carbon cycling in surface waters and oxygen levels and, ultimately, CO₂ and CH₄ fluxes. The physical characteristics of different estuarine types relevant for the present chapter are summarized in **Table 1**.

^{p0025} In the following, we adopt the simplified estuarine classification given by the typology of Dürr et al. (2010), whereby systems are aggregated into four types: small deltas and estuaries (type I), tidal systems and embayments (type II), lagoons (type III), and fjords and fjärds (type IV). This estuarine classification is relevant to the present chapter because it is associated with surface areas estimated by latitudinal bands based on a geographical information system analysis (Dürr et al., 2010). This will allow to scale globally CO₂ and CH₄ fluxes using a more precise and detailed estuarine surface area than previous studies (Bange et al., 1994; Middelburg et al., 2002; Abril and Borges, 2004; Borges, 2005; Borges et al., 2005; Chen and Borges, 2009).

^{s0010} **5.04.2 Dynamics of CO₂ and Atmospheric CO₂ Fluxes in Estuarine Environments**

^{s0015} **5.04.2.1 Spatial and Temporal Variability of CO₂ in Estuaries**

^{p0030} Estuaries are characterized by a dynamic range of the partial pressure of CO₂ (*p*CO₂) in terms of cross-system variability, spatial gradients, and seasonal variability much higher than other coastal environments such as nearshore environments, coastal upwelling systems, and marginal seas (**Figure 1**). The high variability of *p*CO₂ in estuaries reflects the similarly high

variability of organic carbon standing stocks and organic carbon production and degradation compared to other coastal environment exemplified by chlorophylla (Chl *a*), dissolved organic carbon (DOC), and oxygen saturation level (%O₂) in **Figure 2**. **Figure 3** shows the seasonality and spatial variability in 2008 of *p*CO₂ in the Scheldt estuary, as an example of an eutrophic macrotidal estuary. Whatever the season, *p*CO₂ values are higher upstream and decrease downstream as salinity increases. Upstream, two seasonal maxima of *p*CO₂ coinciding with %O₂ minima occur in May and October. This corresponds to the periods of high O₂ consumption and CO₂ production due to bacterial respiration and to nitrification (stimulated by high temperatures compared to winter), and low primary production due to relatively lower light availability. In midsummer (July–August), light availability is maximum upstream, leading to a phytoplankton bloom in the freshwater reaches (as indicated by the increase of Chl *a*). Hence, in midsummer, phytoplanktonic gross primary production (GPP) compensates, to some extent, the O₂ consumption and CO₂ production by bacterial respiration and nitrification (that releases protons and generates CO₂), leading to the decrease of *p*CO₂ and an increase of O₂ compared to April–May. Downstream, the major seasonal feature is the marked spring phytoplanktonic bloom (late April), leading to an increase of Chl *a* and %O₂ and a decrease of *p*CO₂ (below atmospheric equilibrium, ~380 ppm). This feature extends from the mouth of the estuary to about salinity 5 where the downstream limit of the estuarine maximum turbidity (EMT) zone is located. In fall, there is a slight decrease of %O₂ and an increase of *p*CO₂ downstream related to the collapse of primary production due to light limitation, and degradation of organic matter. Similar spatial gradients and seasonal variations, as described above for the Scheldt, have been also reported in other tidal estuaries in Europe (e.g., Frankignoulle et al., 1998), in the US (e.g., Raymond et al., 2000) and in China (e.g., Guo et al., 2009).

The seasonality of *p*CO₂ and %O₂ described earlier in the ^{p0035} Scheldt estuary in 2008 is in general agreement with the GPP, community respiration (CR), and net community production (NCP) seasonal variations measured in 2003 (**Figure 4**). In the lower estuary (salinity 18), GPP peaks in May earlier than in the upper estuary (salinity 0), where GPP peaks in August when light availability is the highest annually. In the lower estuary, CR generally tracks GPP, while in the upper estuary,

^{t0005} **Table 1** Major features relevant for CO₂ and CH₄ cycling in estuarine environments

Type	Length (km)	Depth (m)	Residence time (yr)	Total suspended solids (TSS)	Stratification	O ₂	Sensitivity to river flow
Delta	1–100	≤10	10 ⁻³ –10 ⁻²	Medium	Limited	high O ₂	High
Lagoon	1–100	<10	10 ⁻² –10 ⁻¹	Low/medium	Limited	variable O ₂	Medium
Macrotidal/ria	10–100	≤10	10 ⁻² –10 ⁻¹	ETM*	None	low O ₂ at ETM*	Medium
Fjord	10>100	>100	10 ¹ –10 ²	Very low	High	high O ₂ in surface, anoxic bottom layer**	Very low
Fjärd	1–10	≥10	10 ²	Low	Medium	Medium O ₂	Low

* Estuarine turbidity maximum: TSS > 0.1 to 10.0 g l⁻¹ depending on depth

** In fjörds with sills

Adapted from Meybeck, M., Abril, G., Roussennac, S., Behrendt, H., Billett, M.F., Billen, G., Borges, A.V., Casper, P., Garnier, J., Hinderer, M., Huttunen, J., Johansson, T., Kastowski, M.F., Manø, S., 2006. Specific study on freshwater greenhouse gas budget. CarboEurope – GHG – Concerted Action: Synthesis of the European Greenhouse Gas Budget. Report 1.1.5.

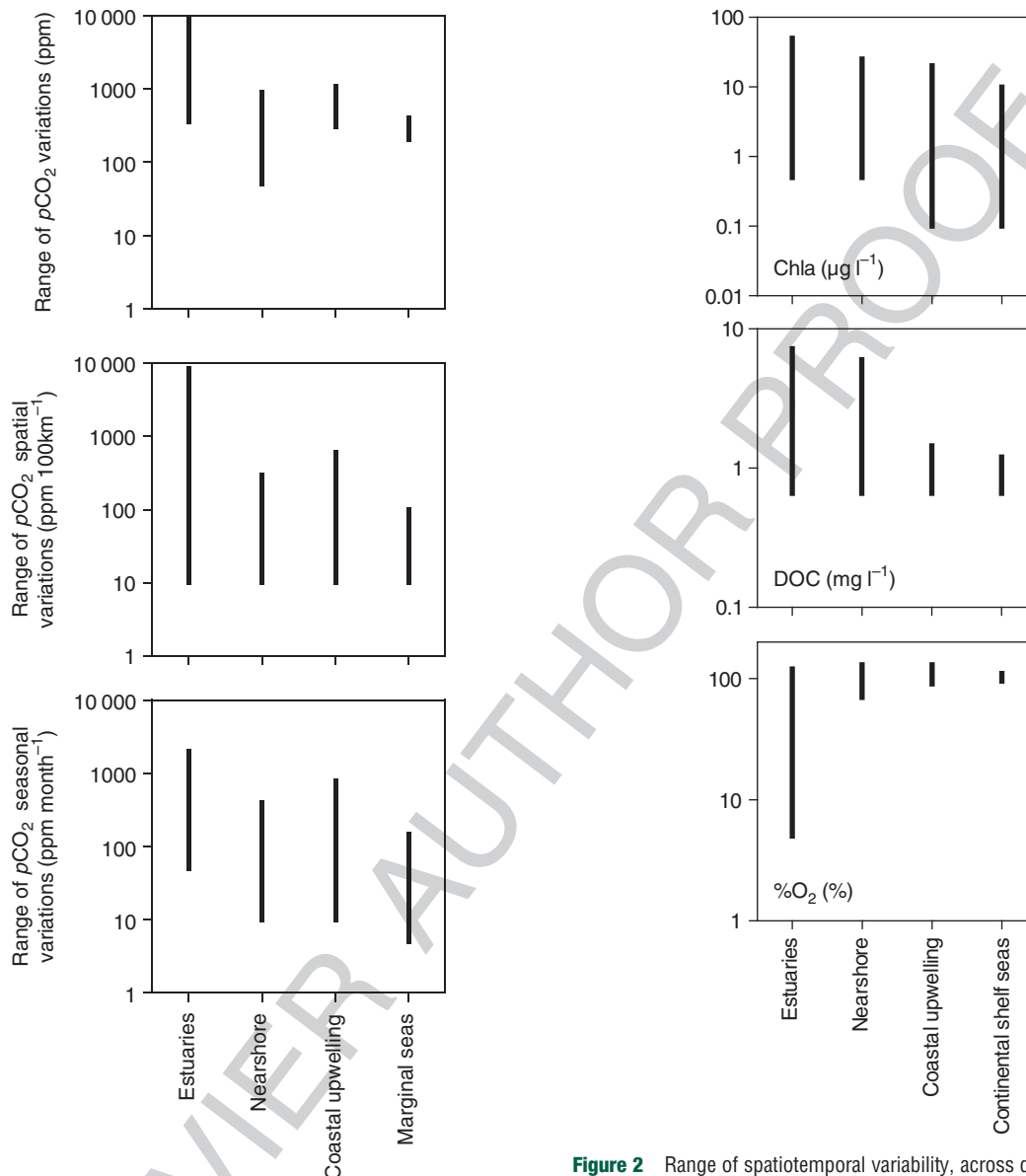


Figure 1 Dynamic range of the partial pressure of CO_2 ($p\text{CO}_2$ in ppm) variations across coastal ecosystems, of $p\text{CO}_2$ spatial gradients, and of $p\text{CO}_2$ seasonal changes in estuaries (based on Frankignoulle et al., 1998; Bouillon et al., 2003), in nearshore ecosystems (based on Borges and Frankignoulle 2002a; Cai et al., 2003), and in coastal upwelling systems (based on Friederich et al., 2002, 2008; Goyet et al., 1998; Borges and Frankignoulle 2002b).

Figure 2 Range of spatiotemporal variability, across different coastal environments, of oxygen saturation level ($\% \text{O}_2$ in %), chlorophyll *a* (Chla in $\mu\text{g l}^{-1}$), and dissolved organic carbon (DOC in mg l^{-1}), based on Borges and Frankignoulle (2002a, 2002b, 2002c), Bouillon et al. (2003), Cai et al. (2003), Chavez and Messié (2009), Cloern and Jassby (2008), Frankignoulle et al. (1998, 1996), Frankignoulle and Borges (2001), Abril et al. (2002), Friederich et al. (2002, 2008), García-Muñoz et al. (2005), Goyet et al. (1998), Kuliński and Pempkowiak (2008), Okkonen et al. (2004), Raimbault et al. (2007), Shin and Tanaka (2004).

CR seems uncoupled from GPP and remains at levels $>60 \text{ mmol-C m}^{-2} \text{ d}^{-1}$ throughout the year. This would suggest that, in the upper estuary, CR is sustained by allochthonous organic carbon inputs, while, in the lower estuary, CR is coupled to GPP.

In 2008, salinity at the mouth of the Scheldt estuary showed relatively modest seasonal variations ranging between 25.0 and 30.0, with maximal salinity intrusion into the estuary in summer when freshwater discharge is lowest (Figure 3). In the Mekong Delta, the seasonal variability of salinity at the mouth of the estuary is much larger with freshwater extending

beyond the mouth of delta during the high-water period (October 2004) and salinity ranging between ~ 24 and ~ 28 at the mouth of the estuary during the low-water period (April 2004) (Figure 5). The different behavior of salinity distribution in these two estuaries results from the lower freshwater discharge of the Scheldt ($\sim 100 \text{ m}^3 \text{ s}^{-1}$, ranging seasonally between ~ 15 and $\sim 715 \text{ m}^3 \text{ s}^{-1}$) compared to the Mekong ($\sim 7700 \text{ m}^3 \text{ s}^{-1}$, ranging seasonally between 420 and $17100 \text{ m}^3 \text{ s}^{-1}$). The strong changes in the spatial distribution of salinity in the Mekong Delta have a strong impact on $p\text{CO}_2$, with values at the mouth of the delta ranging between ~ 500 and ~ 600 ppm during the

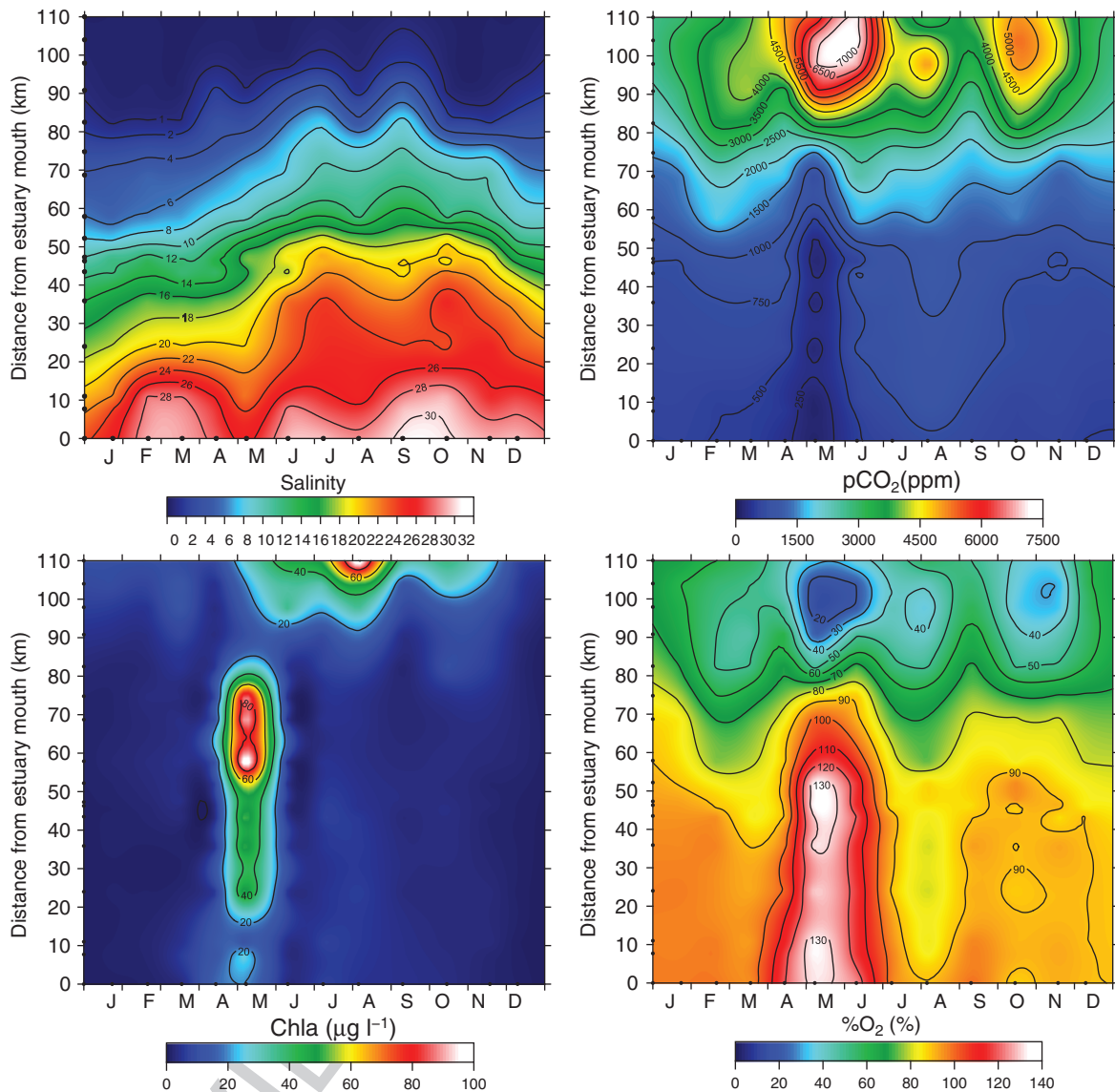


Figure 3 Seasonal and spatial variations of salinity, partial pressure of CO₂ ($p\text{CO}_2$ in ppm), chlorophyll a (Chla in $\mu\text{g l}^{-1}$) in the surface waters of the Scheldt estuary, based on monthly sampling in 2008 by Centre for Estuarine and Marine Ecology (Yerseke, the Netherlands) and University of Liège (Belgium) (A.V. Borges and J.J. Middelburg, unpublished). Dots on y - and x -axis indicate the spatial and temporal sampling coverage, respectively.

low-water period (April 2004) and between ~ 1900 and ~ 2850 ppm during the high-water period (October 2004). In October 2004, $p\text{CO}_2$ values were generally below atmospheric equilibrium (with values down to 280 ppm) for salinities above 10 in conjunction with oxygen levels above saturation (with $\%O_2$ values up to 114%). In April 2004, for salinities above 10, $p\text{CO}_2$ ranged between 420 and 1400 ppm, and O_2 was below atmospheric equilibrium. The occurrence of a phytoplankton bloom at salinities above 10 in October 2004, as indicated by lower $p\text{CO}_2$ and higher $\%O_2$ values than in April, could be related to the more extended river plume offshore. Indeed, the offshore extension of the river plume in October 2004 allowed the settling on suspended matter, enhancing light availability in the water column, as indicated by the lower average total suspended solid (TSS) concentration ($8.6 \pm 4.8 \text{ mg l}^{-1}$) than in April 2004 ($54.4 \pm 47.9 \text{ mg l}^{-1}$).

Similar $p\text{CO}_2$ spatial patterns in large river plumes have been also reported elsewhere as in the Amazon River plume (Körtzinger, 2003) and the Changjiang River plume (Zhai and Dai, 2009).

5.04.2.2 Drivers of the Emission of CO₂ to the Atmosphere from Estuaries s0020

The values of $p\text{CO}_2$ are usually above atmospheric equilibrium p0045 in the large majority of estuaries, and, consequently, these systems are sources of CO₂ to the atmosphere (Table 2; Figure 6). Of the 62 estuaries where, to our best knowledge, air–water CO₂ fluxes have been reported, only one system (the Aby Lagoon) behaved as a sink for atmospheric CO₂. The Aby Lagoon is a strongly and permanently stratified choked lagoon. This particular physical feature strongly enhances the AU3

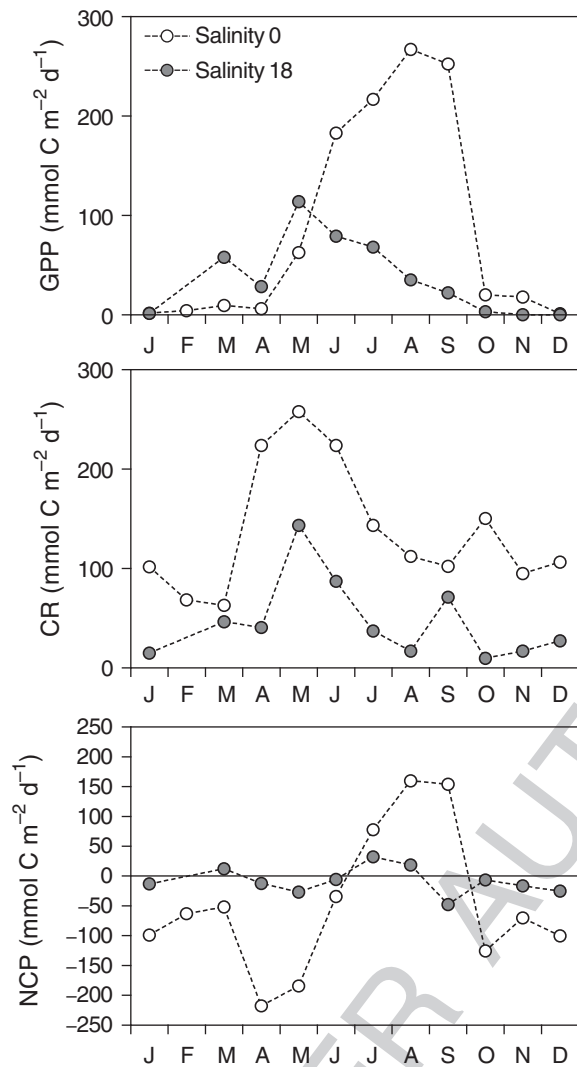


Figure 4 Seasonal variations of planktonic gross primary production (GPP in $\text{mmol C m}^{-2} \text{d}^{-1}$), community respiration (CR in $\text{mmol C m}^{-2} \text{d}^{-1}$) and net community production (NCP in $\text{mmol C m}^{-2} \text{d}^{-1}$) at salinity 0 and 18 in the Scheldt estuary based on a monthly sampling in 2003. Adapted from Gazeau, F., Gattuso, J.-P., Middelburg, J.J., Brion, N., Schiettecatte, L.-S., Frankignoulle, M., Borges, A.V., 2005b. Planktonic and whole system metabolism in a nutrient-rich estuary (the Scheldt estuary). *Estuaries* 28 (6), 868–883.

transfer of organic matter from surface waters across the pycnocline, hence sequestering CO_2 from surface waters (Koné et al., 2009).

There are two main drivers of the emission of CO_2 to the atmosphere from estuaries: the net heterotrophy at ecosystem level, and the inputs from rivers of freshwater rich in CO_2 .

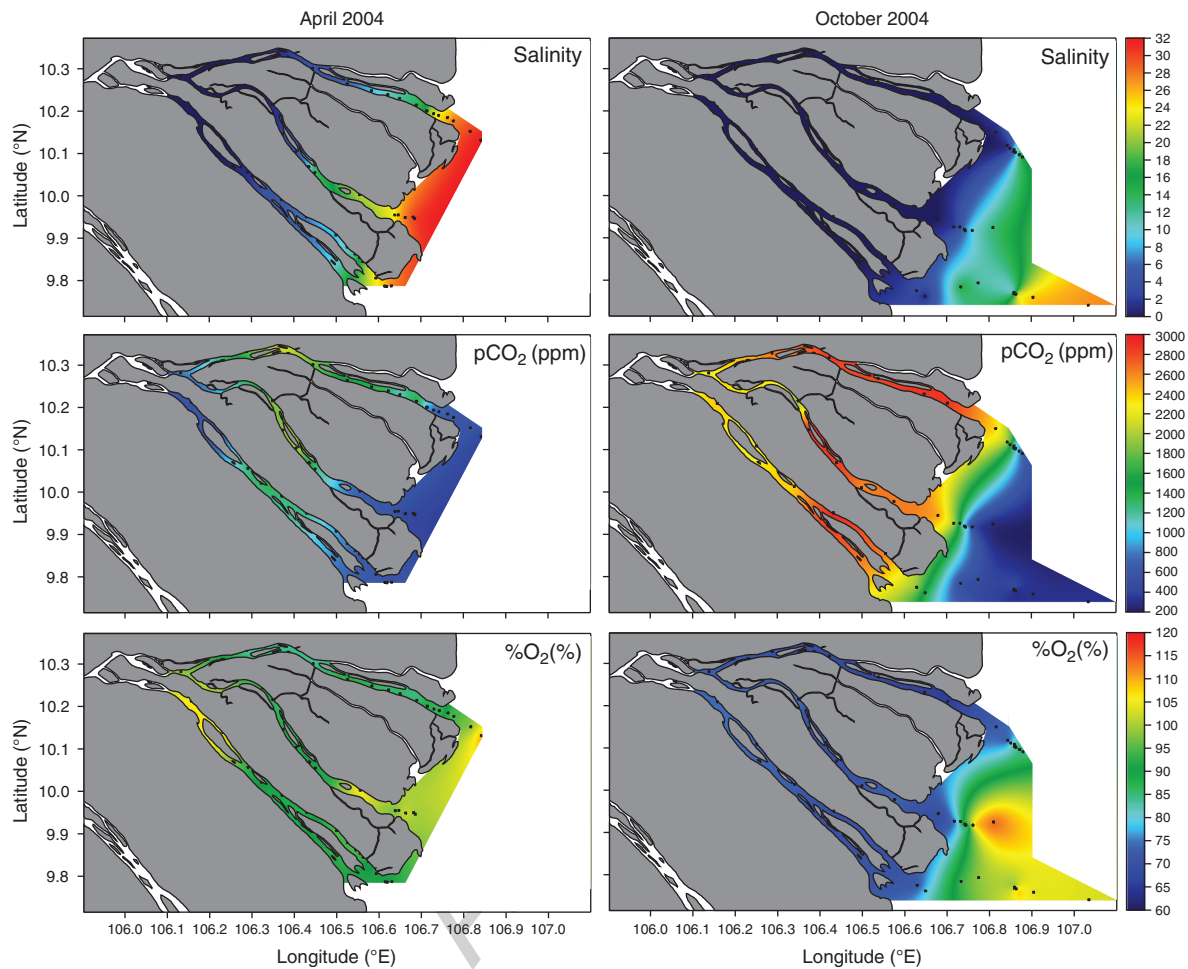
5.04.2.2.1 Net ecosystem production in estuaries

Net ecosystem production (NEP) is the difference between GPP and CR, the latter including autotrophic and heterotrophic respiration (see also 00706). The evaluation of NEP requires the determination of GPP and CR in both planktonic and benthic communities. NCP refers to the difference between GPP and CR in one of these communities (e.g., planktonic). A net autotrophic ecosystem or community is characterized by

a positive NEP or NCP ($\text{GPP} > \text{CR}$), and exports or stores the excess of organic carbon. A net heterotrophic ecosystem or community is characterized by a negative NEP or NCP ($\text{GPP} < \text{CR}$), and the ecosystem metabolism is supported by external inputs of organic matter.

In the 79 estuaries where, to our best knowledge, GPP, CR, NEP, and NCP estimates have been reported, about 66 are net heterotrophic, 12 net autotrophic, and one balanced (Table 3; Figure 7). The estuarine system where the most marked net autotrophy has been reported (Bojorquez Lagoon) corresponds to a very shallow lagoon with extensive and dense macrophyte cover (Reyes and Merino, 1991). The general pattern of net heterotrophy in estuaries is to a large extent related to large inputs of labile organic matter from rivers that fuel CR, while in most systems GPP is limited by light availability due to high suspended matter content despite a large availability of nutrients (Smith and Hollibaugh, 1993; Heip et al., 1995; Gattuso et al., 1998; Gazeau et al., 2004). Despite diverse shortcomings associated to the different methods to evaluate NEP or NCP (e.g., Gazeau et al., 2005a) and in particular GPP (e.g., Gazeau et al., 2007), a general pattern emerges of increasing net heterotrophy with increasing GPP (Figure 8) in agreement with previous analysis (Smith and Hollibaugh, 1993; Heip et al., 1995; Caffrey, 2004). This general pattern is due to the fact that allochthonous inputs of nutrients and allochthonous inputs of organic carbon (riverine and lateral) to estuaries are more or less coupled, enhancing simultaneously GPP and CR, respectively (Smith and Hollibaugh, 1993). The remineralization of allochthonous organic matter (fueling part of the CR) can provide inorganic nutrients to sustain GPP. Indeed, the delivery of N and P by rivers to estuaries is largely (62% and 90%, respectively) in the organic (dissolved and particulate) form rather than in the inorganic dissolved form (Seitzinger et al., 2005). Finally, the C:N and C:P ratios of terrestrial organic matter (the bulk of allochthonous organic matter inputs) is higher than the respective ratios of phytoplankton (Hopkinson and Vallino, 1995; Kemp et al., 1997). Hence, the remineralization of allochthonous organic matter in estuaries can sustain a larger carbon demand (enhancing CR) while releasing relatively lower quantities of N and P to sustain GPP.

The general pattern of increasing heterotrophy with increasing GPP in estuaries is opposed to the one reported for the open ocean by, for example, Duarte and Agustí (1998), whereby net heterotrophy increases with decreasing GPP from eutrophic to oligotrophic systems. This difference could be due to the marked decoupling of allochthonous inputs of inorganic nutrients and allochthonous inputs of organic carbon in the open ocean. This could also be due to the fact that, in the open ocean, allochthonous organic matter inputs have C:N and C:P ratios closer to those of phytoplankton. Yet, the relation between NEP or NCP and GPP in estuaries shows a considerable scatter that could be explained by either the variable degree of light limitation in different estuaries (Heip et al., 1995), or the ratio of inorganic nutrient to organic carbon allochthonous inputs (Kemp et al., 1997) as depicted in Figure 8. The scatter could also be due to differences in the size of estuarine systems, with smaller systems showing more marked heterotrophy than larger ones (Hopkinson, 1988; Caffrey, 2004).



f0025 **Figure 5** Spatial variations of salinity, partial pressure of CO_2 ($p\text{CO}_2$ in ppm), and oxygen saturation level ($\% \text{O}_2$ in %) in the Mekong delta during the low-water period (April 2004) and the flooding period (October 2004) (A.V. Borges, unpublished).

p0070 Net heterotrophy leads to a buildup of CO_2 in surface waters, while net autotrophy leads to a removal of CO_2 from surface waters, and in principle, this should lead to a source of CO_2 to the atmosphere and a sink of atmospheric CO_2 , respectively. Yet, the link between the exchange of CO_2 with the atmosphere and the metabolic status of surface waters is not direct. Besides NEP, the net CO_2 flux between the water column and the atmosphere will be further modulated by other factors such as additional biogeochemical processes (e.g., CaCO_3 precipitation/dissolution); exchange of water with adjacent aquatic systems and the CO_2 content of the exchanged water mass; residence time of the water mass within the system; decoupling of organic carbon production; and degradation across the water column related to the physical settings of the system, in particular, the presence or absence of stratification (e.g., Borges et al., 2006).

p0075 Nevertheless, data sets that report both air–water CO_2 fluxes and NEP in estuaries show a consistent pattern of a CO_2 emission to the atmosphere coupled to net heterotrophy (Raymond et al., 2000; Gazeau et al., 2005a, 2005b; Borges et al., 2006; Gupta et al., 2008, 2009). This is confirmed by the cross-system analysis of $p\text{CO}_2$ and O_2 in estuarine systems (Figure 9). However, caution is needed when analyzing O_2 dynamics in estuaries because nitrification can be a significant

oxygen-consuming process (Vanderborght et al., 2002; Hofmann et al., 2008, 2009). Further, nitrification is a chemoautotrophic process contributing to GPP, and leading to the uptake of dissolved inorganic carbon (DIC); yet, the H^+ production leads to a decrease in pH and total alkalinity (TA), and an increase of $p\text{CO}_2$ (Frankignoulle et al., 1996). Nitrification in the Scheldt estuary can account for ~50% of O_2 consumption in the whole estuary (Soetaert and Herman, 1995; Vanderborght et al., 2002; Gazeau et al., 2005b). In the upper estuary (salinity ~2), high nitrification and CR rates (leading to marked net heterotrophy, $\text{NCP} < 1$) lead to an oxygen minimum that coincides with a distinct deviation of TA from conservative mixing and with a pH minimum (Figure 10).

In estuaries, the general patterns (Figure 9) of a positive p0080 relationships between apparent oxygen utilization (AOU) and $p\text{CO}_2$ normalized to a temperature of 20 °C ($p\text{CO}_2@20\text{ °C}$) and excess DIC (EDIC), and the negative relationship between AOU and pH normalized to a constant temperature ($\text{pH}@20\text{ °C}$) are indicative of O_2 consumption linked to CO_2 production, and hence, of a CO_2 production partly related to net heterotrophy and partly related to the acidification due to nitrification. Yet, most of EDIC and $p\text{CO}_2@20\text{ °C}$ data points are above the theoretical lines, while most of the $\text{pH}@20\text{ °C}$ data points are below the theoretical lines due to aerobic

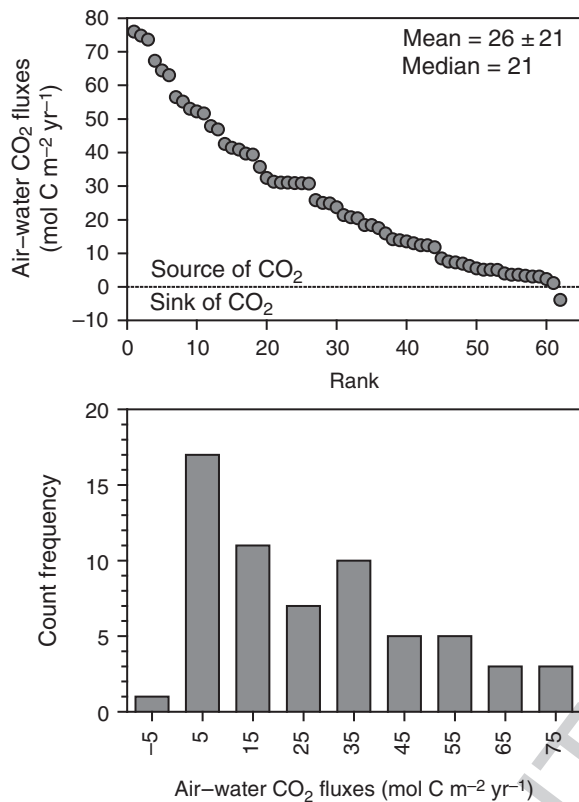
Table 2 Range of the partial pressure of CO₂ (pCO₂ in ppm) and air-water CO₂ fluxes (FCO₂ in mol C m⁻² yr⁻¹) in estuarine environments

	°E	°W	pCO ₂ range (ppm)	FCO ₂ (mol C m ⁻² yr ⁻¹)	References
Small deltas and estuaries (type I)					
Duplin River (US)	-81.3	31.5	500–3000	21.4	Wang and Cai (2004)
Gaderu creek (IN)	82.3	16.8	1380–4770	20.4	Borges et al. (2003)
Itacuraça creek (BR)	-44.0	-23.0	660–7700	41.4	Ovalle et al. (1990), Borges et al. (2003)
Khura River estuary (TH)	98.3	9.2	470–13830	35.7	Miyajima et al. (2009); T. Miyajima (pers. comm.)
Kidogweni creek (KE)	39.5	-4.4	1480–6435	23.7	Bouillon et al. (2007b)
Kiên Vâng creeks (wet season) (VN)	105.1	8.7	1435–8140	56.5	Koné and Borges (2008)
Kiên Vâng creeks (dry season) (VN)	105.1	8.7	705–4605	11.8	Koné and Borges (2008)
Matolo/Ndogwe/Kaloia/Mto Tana creeks (KE)	40.1	-2.1	490–10035	25.8	Bouillon et al. (2007a)
Mooranganga creek (IN)	89.0	22.0	800–1530	8.5	Ghosh et al. (1987), Borges et al. (2003)
Mtoni (TZ)	39.3	-6.9	400–1800	7.3	Kristensen et al. (2008)
Nagada creek (IN)	145.8	-5.2	540–1680	15.9	Borges et al. (2003)
Norman's Pond (BS)	-76.1	23.8	385–750	5.0	Borges et al. (2003)
Ras Dege creek (TZ)	39.5	-6.9	430–5050	12.4	Bouillon et al. (2007c)
Rio San Pedro (ES)	-5.7	36.6	380–3760	39.4	Ferrón et al. (2007)
Saptamukhi creek (IN)	89.0	22.0	1080–4000	20.7	Gosh et al. (1987), Borges et al. (2003)
Shark River (US)	-81.1	25.2	920–2910	18.4	Millero et al. (2001), Clark et al. (2004), Koné and Borges (2008)
Tam Giang creeks (dry season) (VN)	105.2	8.8	770–11480	51.6	Koné and Borges (2008)
Tam Giang creeks (wet season) (VN)	105.2	8.8	1210–7150	46.9	Koné and Borges (2008)
Trang River estuary (TH)	99.4	7.2	320–5580	30.9	Miyajima et al. (2009); T. Miyajima (pers. Comm.)
Tidal systems and embayments (type II)					
Altamaha Sound (US)	-81.3	31.3	390–3380	32.4	Jiang et al. (2008)
Bellamy (US)	-70.9	43.2	100–800	3.6	Hunt et al. (2009)
Betsiboka (MG)	46.3	-15.7	270–1530	3.3	Ralison et al. (2008)
Bothnian Bay (FI)	21.0	63.0	150–550	3.1	Algesten et al. (2004)
Changjiang (Yantze) (CN)	120.5	31.5	200–4600	24.9	Gao et al. (2005), Zhai et al. (2007), Chen et al. (2008)
Chilka (IN)	85.5	19.1	80–14640	25	Gupta et al. (2008)
Cocheo (US)	-70.9	43.2	80–900	3.1	Hunt et al. (2009)
Cochin (IN)	76	9.5	150–3800	55.1	Gupta et al. (2009)
Doboy Sound (US)	-81.3	31.4	390–2400	13.9	Jiang et al. (2008)
Douro (PT)	-8.7	41.1	1330–2200	76.0	Frankignoulle et al. (1998)
Eibe (DE)	8.8	53.9	580–1100	53.0	Frankignoulle et al. (1998)
Ems (DE)	6.9	53.4	560–3755	67.3	Frankignoulle et al. (1998)
Gironde (FR)	-1.1	45.6	465–2860	30.8	Frankignoulle et al. (1998)
Godavari (IN)	82.3	16.7	220–500	5.5	Bouillon et al. (2003)
Great Bay (US)	-70.9	43.1	100–2000	3.6	Hunt et al. (2009)
Guadalquivir (ES)	-6.0	37.4	520–3606	31.1	De La Paz et al. (2007)
Hooghly (IN)	88.0	22.0	80–1520	5.1	Mukhopadhyay et al. (2002)
Limingiantai Bay (FI)	25.4	64.9	10–2690	7.5	Silvennoinen et al. (2008)
Little Bay (US)	-70.9	43.1	100–1500	2.4	Hunt et al. (2009)
Loire (FR)	-2.2	47.2	630–2910	64.4	Abrié et al. (2003)

(Continued)

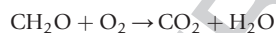
Table 2 (Continued)

	°E	°N	pCO ₂ range (ppm)	FCO ₂ (mol C m ⁻² yr ⁻¹)	References
Mandovi-Zuari (IN)	73.5	15.3	500–3500	14.2	Sarma et al. (2001)
Mekong (VN)	106.5	10.0	280–4105	30.8	Borges (unpublished)
Oyster (US)	-70.9	43.1	100–2000	4.0	Hunt et al. (2009)
Parker River estuary (US)	-70.8	42.8	500–4100	1.1	Raymond and Hopkinson (2003)
Piaui River estuary (BR)	-37.5	-11.5	285–10000	13.0	Souza et al. (2009)
Rhine (NL)	4.1	52.0	545–1990	39.7	Frankignoulle et al. (1998)
Sado (PT)	-8.9	38.5	575–5700	31.3	Frankignoulle et al. (1998)
Saja-Besaya (ES)	-2.7	43.4	264–9728	52.2	Ortega et al. (2004)
Sapelo Sound (US)	-81.3	31.6	390–2400	13.5	Jiang et al. (2008)
Satilla River (US)	-81.5	31.0	360–8200	42.5	Cai and Wang (1998)
Scheldt (BE/NL)	3.5	51.4	125–9425	63.0	Frankignoulle et al. (1998)
Tana (KE)	40.1	-2.1	2240–5305	47.9	Bouillon et al. (2007a)
Tamar (UK)	-4.2	50.4	380–2200	74.8	Frankignoulle et al. (1998)
Thames (UK)	0.9	51.5	505–5200	73.6	Frankignoulle et al. (1998)
York River (US)	-76.4	37.2	350–1900	6.2	Raymond et al. (2000)
Zhujiang (Pearl River) (CN)	113.5	22.5	560–8350	6.9	Guo et al. (2009)
Lagoons (type III)					
Aby lagoon (CI)	-3.3	4.4	60–325	-3.9	Koné et al. (2009)
Aveiro lagoon (PT)	-8.7	40.7	143–11335	12.4	Borges and Frankignoulle (unpublished)
Ebré lagoon (CI)	-4.3	4.5	1365–3575	31.1	Koné et al. (2009)
Potou lagoon (CI)	-3.8	4.6	1235–5120	40.9	Koné et al. (2009)
Tagba lagoon (CI)	-5.0	4.4	800–4250	18.4	Koné et al. (2009)
Tendo lagoon (CI)	-3.2	4.3	90–3600	5.1	Koné et al. (2009)
Fjords and fjårds (type IV)					
Randers Fjord (DK)	10.3	56.6	220–3440	17.5	Gazeau et al. (2005a)



f0030 **Figure 6** Air–water CO₂ fluxes (mol C m⁻² yr⁻¹) in estuarine environments (Table 2).

respiration and nitrification computed from simplified overall equations of these processes:



One explanation of these discrepancies could be due to allochthonous inputs of CO₂ either from freshwaters or from lateral inputs that can be significant in estuarine environments (e.g., Cai and Wang, 1998; Cai et al., 1999, 2000; Abril et al., 2002; Neubauer and Anderson, 2003; Gazeau et al., 2005b). Indeed, the theoretical lines were computed assuming atmospheric CO₂ equilibrium ($p\text{CO}_2 = 380$ ppm) at AOU = 0, while the y -intercept of the linear regression between $p\text{CO}_2@20^\circ\text{C}$ and AOU (not shown) indicates a higher $p\text{CO}_2$ value (~740 ppm). Further, O₂ has a faster equilibration time than CO₂ (due to the buffering capacity of the carbonate system). The contribution of anoxic organic carbon degradation in submerged and intertidal estuarine sediments could also partly explain these discrepancies. Finally, some of the scatter in the pH@20 °C, $p\text{CO}_2@20^\circ\text{C}$, and EDIC versus AOU plots could be due to the dissolution of allochthonous CaCO₃, although in the water column this process is independent of O₂ consumption processes. However, in sediments, metabolic-driven CaCO₃ dissolution is due to acidification of pore waters linked to oxygen consumption (e.g., Emerson and Bender, 1981). Nevertheless, the effect of dissolution of CaCO₃ on carbonate chemistry in estuarine environments has been seldom documented, with the exception of the Loire (Abril et al., 2003, 2004).

There has been some concern on the impacts of acidification of surface waters due to the uptake of anthropogenic CO₂ from the atmosphere in estuarine environments (Salisbury et al., 2008). Changes of allochthonous organic carbon and nutrients inputs due to human activities can change heterotrophic or nitrification activities and oxygen levels in estuarine environments. Besides potentially leading to suboxic or even anoxic conditions with dramatic consequences on biota (e.g., Diaz and Rosenberg, 2008), the relationship between pH@20 °C and AOU in Figure 9 would indicate that changes in oxygen levels are also coupled to changes in carbonate chemistry that are probably stronger than the acidification of surface waters due to the uptake of anthropogenic CO₂ from the atmosphere. The relationship between $p\text{CO}_2@20^\circ\text{C}$ and AOU also indicates that changes in the air–water $p\text{CO}_2$ gradient due to the rise in atmospheric CO₂ would be negligible in comparison to changes in water $p\text{CO}_2$ in response to estuarine biogeochemical processes.

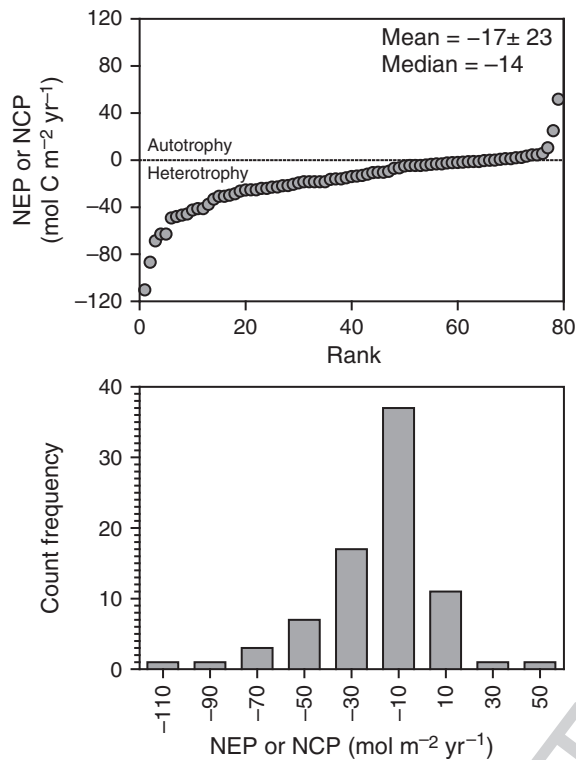
The modulation of air–water CO₂ fluxes by NEP is also, to a large extent, a function of the physical settings of estuaries, in particular with respect to the occurrence of vertical stratification, and residence time of the water mass. These two physical characteristics are, to a large extent, functions of the tidal amplitude. Figure 11 compares NEP and DIC fluxes in two contrasted European estuaries, the microtidal and permanently stratified Randers Fjord, and the macrotidal well-mixed Scheldt estuary. Although, on the whole, the Randers Fjord is a net heterotrophic system; the mixed layer shows a net heterotrophy less marked than in the Scheldt estuary. The air–sea CO₂ fluxes computed to close the budget (Figure 11) and those estimated from field $p\text{CO}_2$ measurements (Table 2) show that the emission of CO₂ is more intense in the Scheldt estuary than in Randers Fjord. This can be attributed, at least partly, to the decoupling in the Randers Fjord of the production of organic matter in the surface layer and its degradation in the bottom layer. In this way, the CO₂ produced by organic matter degradation processes will not be immediately available for exchange with the atmosphere in the Randers Fjord, unlike in the Scheldt estuary. Further, the residence time of freshwater is much longer in the Scheldt (30–90 d) than in the Randers Fjord (5–10 d). Thus, even for a similar NEP, the enrichment in DIC of estuarine waters and corresponding ventilation of CO₂ to the atmosphere will be more intense in long residence-time systems such as the Scheldt than short residence-time systems such as the Randers Fjord. Indeed, NEP in the Scheldt estuary is of the same order of magnitude as the emission of CO₂ to the atmosphere, while the advection of DIC to the North Sea is close to the sum of riverine and lateral DIC inputs. In the Randers Fjord, the emission of CO₂ to the atmosphere is lower than mixed layer NCP, while the export of DIC to the Baltic Sea is higher than the river inputs of DIC. This would suggest that DIC produced by NCP in the Randers Fjord is, to a large extent, exported rather than emitted to the atmosphere due to the shorter residence time than in the Scheldt where DIC produced by NEP is, to a larger extent, emitted to the atmosphere rather than exported.

The cross-system comparison of $p\text{CO}_2$ and CH₄ in estuaries also provides information regarding the role of physical settings in the control of organic carbon cycling and production of CO₂ and CH₄ (Figure 12). In well-mixed large estuarine systems, there is a positive relationship between CH₄ and $p\text{CO}_2$,

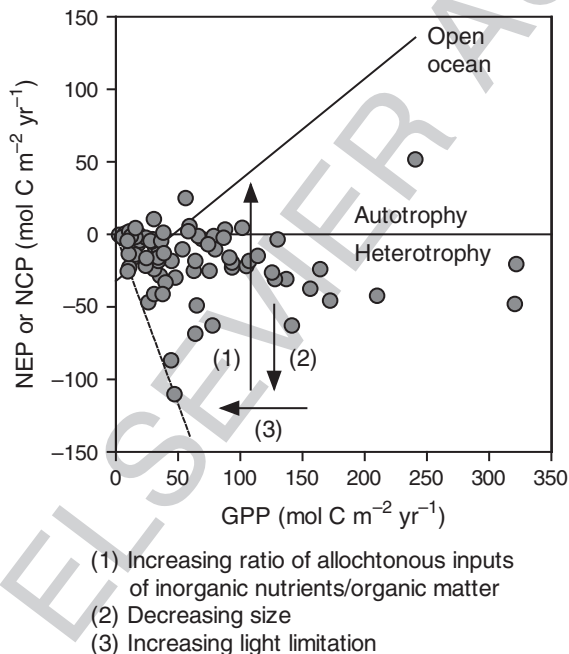
Table 3 Compilation of gross primary production (GPP in $\text{mol C m}^{-2} \text{yr}^{-1}$), community respiration (CR in $\text{mol C m}^{-2} \text{yr}^{-1}$), and net ecosystem production (NEP in $\text{mol C m}^{-2} \text{yr}^{-1}$), or net community production (NCP in $\text{mol C m}^{-2} \text{yr}^{-1}$) in estuarine environments

	GPP ($\text{mol C m}^{-2} \text{yr}^{-1}$)	CR ($\text{mol C m}^{-2} \text{yr}^{-1}$)	NEP or NCP ($\text{mol C m}^{-2} \text{yr}^{-1}$)	References
ACE Big Bay Creek (US)	141.4	204.2	-62.7	Caffrey (2004)
ACE St. Pierre (US)	136.9	167.7	-30.8	Caffrey (2004)
Apalachicola Bottom (US)	35.4	63.9	-28.5	Caffrey (2004)
Apalachicola Surface (US)	31.9	50.2	-18.3	Caffrey (2004)
Apex NY Bight (US)	31.7	41.1	-9.4	Garside and Malone (1978)
Bojorquez lagoon, Mexico	240.6	188.8	51.8	Reyes and Merino (1991)
Chesapeake Bay Maryland Jug Bay (US)	77.6	140.3	-62.7	Caffrey (2004)
Chesapeake Bay Maryland Patuxent Park (US)	93.5	116.3	-22.8	Caffrey (2004)
Chesapeake Bay Virginia Goodwin Island (US)	59.3	53.6	5.7	Caffrey (2004)
Chesapeake Bay Virginia Taskinas Creek (US)	101.5	97.0	4.6	Caffrey (2004)
Cochin (IN)	9.4	13.8	-4.5	Gupta et al. (2009)
Columbia River Estuary (US)	5.1	7.1	-2.0	Small et al. (1990)
Copano Bay (US)	24.1	45.7	-21.6	Russell and Montagna (2007)
Delaware Bay Blackwater Landing (US)	127.8	158.5	-30.8	Caffrey (2004)
Delaware Bay Scotton Landing (US)	107.2	125.5	-18.3	Caffrey (2004)
Douro (PT)	9.7	35.1	-25.4	Azevedo et al. (2006)
Elkhorn Slough Azevedo Pond (US)	125.5	151.7	-26.2	Caffrey (2004)
Elkhorn Slough South Marsh (US)	34.2	50.2	-16.0	Caffrey (2004)
Ems-Dollar	10.4	23.9	-13.5	Van Es (1977)
Estero Pargo, Mexico	28.8	33.8	-5.0	Day et al. (1988)
Fourteague Bay (US)	34.8	45.3	-10.4	Randall and Day (1987)
Georgia Coast (US)	44.9	63.3	-18.3	Hopkinson (1985)
Great Bay Great Bay Buoy (US)	86.7	89.0	-2.3	Caffrey (2004)
Great Bay Squamscott River (US)	74.1	81.0	-6.8	Caffrey (2004)
Hudson River Tivoli South (US)	34.2	52.5	-18.3	Caffrey (2004)
Jobs Bay 09 (US)	65.0	114.1	-49.0	Caffrey (2004)
Jobs Bay 10 (US)	47.9	77.6	-29.7	Caffrey (2004)
Laguna Madre	69.2	72.4	-3.1	Odum and Hoskin (1958), Odum and Wilson (1962), Ziegler and Benner (1998)
Lavaca Bay (US)	24.5	40.7	-16.2	Russell and Montagna (2007)
MERL control microcosm	14.8	15.0	-0.3	Frithsen et al. (1985)
Mitla Lagoon (Mexico)	321.7	342.2	-20.5	Mee (1977)
Mullica River Buoy 126 (US)	66.2	67.3	-1.1	Caffrey (2004)
Mullica River Lower Bank (US)	30.8	54.8	-24.0	Caffrey (2004)
Narragansett Bay Potters Cove (US)	93.5	112.9	-19.4	Caffrey (2004)
Narragansett Bay T-wharf (US)	91.3	107.2	-16.0	Caffrey (2004)
Newport River Estuary (US)	29.4	32.6	-3.2	Kenney et al. (1988)
Nordasvannet Fjord, Norway	15.8	14.5	1.3	Wassmann et al. (1986)

North Atlantic bight (US)	19.2	23.3	-4.2	Rowe et al. (1986)
North Carolina Masonboro Inlet (US)	62.7	87.8	-25.1	Caffrey (2004)
North Carolina Zeke's Island (US)	39.9	73.0	-33.1	Caffrey (2004)
North Inlet-Winyah Bay Oyster Landing (US)	79.8	90.1	-10.3	Caffrey (2004)
North Inlet-Winyah Bay Thousand Acre Creek (US)	53.6	63.9	-10.3	Caffrey (2004)
Nueces Bay (US)	30.6	20.0	10.6	Russell and Montagna (2007)
Ochlocknee Bay (US)	2.7	2.8	-0.2	Kaul and Froelich (1984)
Old Woman Creek State Route 2 (US)	26.2	73.0	-46.8	Caffrey (2004)
Old Woman Creek State Route 6 (US)	30.8	71.9	-41.1	Caffrey (2004)
Oosterschelde (NL)	24.2	26.3	-2.2	Scholten et al. (1990)
Padilla Bay Bay View (US)	130.0	133.5	-3.4	Caffrey (2004)
Randers Fjord	12.2	13.5	-1.3	Gazeau et al. (2005b)
Redfish Bay	156.3	193.8	-37.4	Odum and Hoskin (1958)
Ria de Vigo (ES)	10.7	8.7	2.0	Prego (1993)
Ria Formosa (PT)	15.8	11.3	4.4	Santos et al. (2004)
Rookery Bay Blackwater River (US)	44.5	131.2	-86.7	Caffrey (2004)
Rookery Bay Upper Henderson (US)	63.9	132.3	-68.4	Caffrey (2004)
S. Kaneohe Bay (US)	18.1	24.5	-6.4	Smith et al. (1981)
San Antonio Bay (US)	38.5	51.4	-12.9	Russell and Montagna (2007)
San Francisco Bay, North Bay (US)	10.7	33.3	-22.7	Jassby et al. (1993)
San Francisco Bay, South Bay (US)	15.8	17.5	-1.7	Jassby et al. (1993)
Sapelo Flume Dock (US)	209.9	252.1	-42.2	Caffrey (2004)
Sapelo Marsh Landing (US)	104.9	126.6	-21.7	Caffrey (2004)
Saquarema Lagoon, Brazil	38.3	37.1	1.2	Carmouze et al. (1991)
Scheldt estuary (BE/NL)	15.7	29.6	-13.9	Gazeau et al. (2005a)
South Slough Stengstacken Arm (US)	164.3	188.2	-24.0	Caffrey (2004)
South Slough Winchester Arm (US)	114.1	128.9	-14.8	Caffrey (2004)
Southampton water, United Kingdom	12.0	24.0	-12.0	Collins (1978)
Spencer Gulf, Australia	7.7	7.0	0.7	Smith and Veeh (1989)
Terminos lagoon, Mexico	18.3	18.3	0.0	Day et al. (1988)
Tijuana River Oneonta Slough (US)	172.2	217.9	-45.6	Caffrey (2004)
Tijuana River Tidal Linkage (US)	320.5	368.4	-47.9	Caffrey (2004)
Tornales Bay (US)	36.5	41.0	-4.5	Smith and Hollibaugh (1997)
Urdaibai	56.0	30.8	25.1	Revilla et al. (2002)
Venice Lagoon (IT)	47.2	157.3	-110.1	Ciavatta et al. (2008)
Waquoit Bay Central Basin (US)	75.3	100.4	-25.1	Caffrey (2004)
Waquoit Bay Metoxit Point (US)	63.9	82.1	-18.3	Caffrey (2004)
Weeks Bay Fish River (US)	87.8	84.4	3.4	Caffrey (2004)
Weeks Bay Weeks Bay (US)	78.7	79.8	-1.1	Caffrey (2004)
Wells Head of Tide (US)	37.6	78.7	-41.1	Caffrey (2004)
Wells Inlet (US)	58.2	55.9	2.3	Caffrey (2004)
West Wadden Sea, the Netherlands	27.9	32.3	-4.4	Hoppema (1991)



f0035 **Figure 7** Net ecosystem production (NEP in $\text{mol C m}^{-2} \text{yr}^{-1}$) or net community production (NCP in $\text{mol C m}^{-2} \text{yr}^{-1}$) in estuarine environments (Table 3).



f0040 **Figure 8** Net ecosystem production (NEP in $\text{mol C m}^{-2} \text{yr}^{-1}$) or net community production (NCP in $\text{mol C m}^{-2} \text{yr}^{-1}$) vs. gross primary production (GPP in $\text{mol C m}^{-2} \text{yr}^{-1}$) in estuarine environments (Table 3). The curve of NCP vs. GPP for the open ocean was derived from the relationship of GPP vs. community respiration given by Duarte and Agustí (1998), and the volumetric data were roughly integrated assuming a photic depth of 100 m. The dotted line indicates the lower boundary of the data. Arrows indicate biogeochemical processes that can conceptually explain the variability in the data based on Heip et al. (1995) and Kemp et al. (1997).

while in stratified estuarine systems, there is a more or less marked negative relationship between CH_4 and $p\text{CO}_2$. This could indicate that in well-mixed systems the increase of allochthonous carbon inputs sustaining increased CO_2 production also sustains increased CH_4 production. In stratified systems, the transfer of organic matter across the pycnocline leads to a decrease of CO_2 in surface waters while promoting suboxic or anoxic conditions in bottom layers favorable for methanogenesis in the sediments (Fenchel et al., 1995; Koné et al., 2010). In stratified systems, the large quantities of CH_4 produced in bottom waters will diffuse to the surface waters, and, despite bacterial oxidation, will lead to high CH_4 concentrations in surface waters. Hence, the more efficient transfer of organic matter from surface waters to bottom waters in stratified estuarine ecosystems than in well-mixed systems can explain the different patterns of the relationships between CH_4 and $p\text{CO}_2$ shown in Figure 12.

Among the large stratified estuarine systems, the Rhine p0100 stands above the linear regression between CH_4 and $p\text{CO}_2$ (Figure 12). The very short residence time of freshwater in the Rhine (~ 2 d) due to high freshwater discharge ($\sim 2200 \text{ m}^3 \text{ s}^{-1}$), and a moderate tidal range (2–3 m), as well as the low turbidity, reduces the loss of riverine CH_4 by evasion to the atmosphere and by bacterial oxidation, and leads to a lesser CO_2 production due to net heterotrophy compared to the other large stratified estuaries compiled in Figure 12 with higher freshwater residence time. Among the large mixed estuarine systems, the Sado stands above the positive linear regression between CH_4 and $p\text{CO}_2$. This could be due to the very large extent of intertidal areas and marshes in the Sado compared to other estuaries probably leading to higher lateral inputs of CH_4 by tidal pumping (cf. Section 5.04.3.2). Two of the three small mixed estuarine systems stand well above the positive linear regression between CH_4 and $p\text{CO}_2$ of the large mixed estuarine systems. In small estuarine systems, the lateral inputs from intertidal sediments due to tidal pumping (cf. Section 5.04.3.2), and the inputs from submerged sediments of both CH_4 and CO_2 into small water volumes can lead to a large accumulation of CH_4 and CO_2 in surface waters. Further, the large inputs of allochthonous organic carbon in vegetated systems (marshes or mangroves) and shading by vegetation that limits GPP (mangroves) will promote more intense net heterotrophy (Hopkinson, 1988). In the mangrove creeks of Ca Mau, there is a marked increase of $p\text{CO}_2$ and CH_4 , and a marked decrease of $\% \text{O}_2$ and $\delta^{13}\text{C}$ DIC with the decrease of width of creeks (Figure 13). Further, $p\text{CO}_2$ is well correlated with both CH_4 (positively) and $\% \text{O}_2$ (negatively). These patterns are consistent with larger impact in smaller systems of inputs of pore waters rich in CO_2 , CH_4 , and reduced solutes (that will lead to a decrease of O_2 in the water column) and poor in O_2 , and possibly of higher production of CO_2 and CH_4 in the water column and sediments sustained by allochthonous organic carbon inputs.

5.04.2.2.2 Riverine inputs of CO_2 and CH_4 to estuaries

Freshwater ecosystems are generally characterized by high p0105 $p\text{CO}_2$ values (Cole et al., 1994; Cole and Caraco, 2001). Hence, the input of freshwater with high CO_2 content could, to some extent, also contribute to the CO_2 emission from estuaries. Figure 14 compares $p\text{CO}_2$ and DOC in tidal rivers and rivers, an approach that has been frequently used in

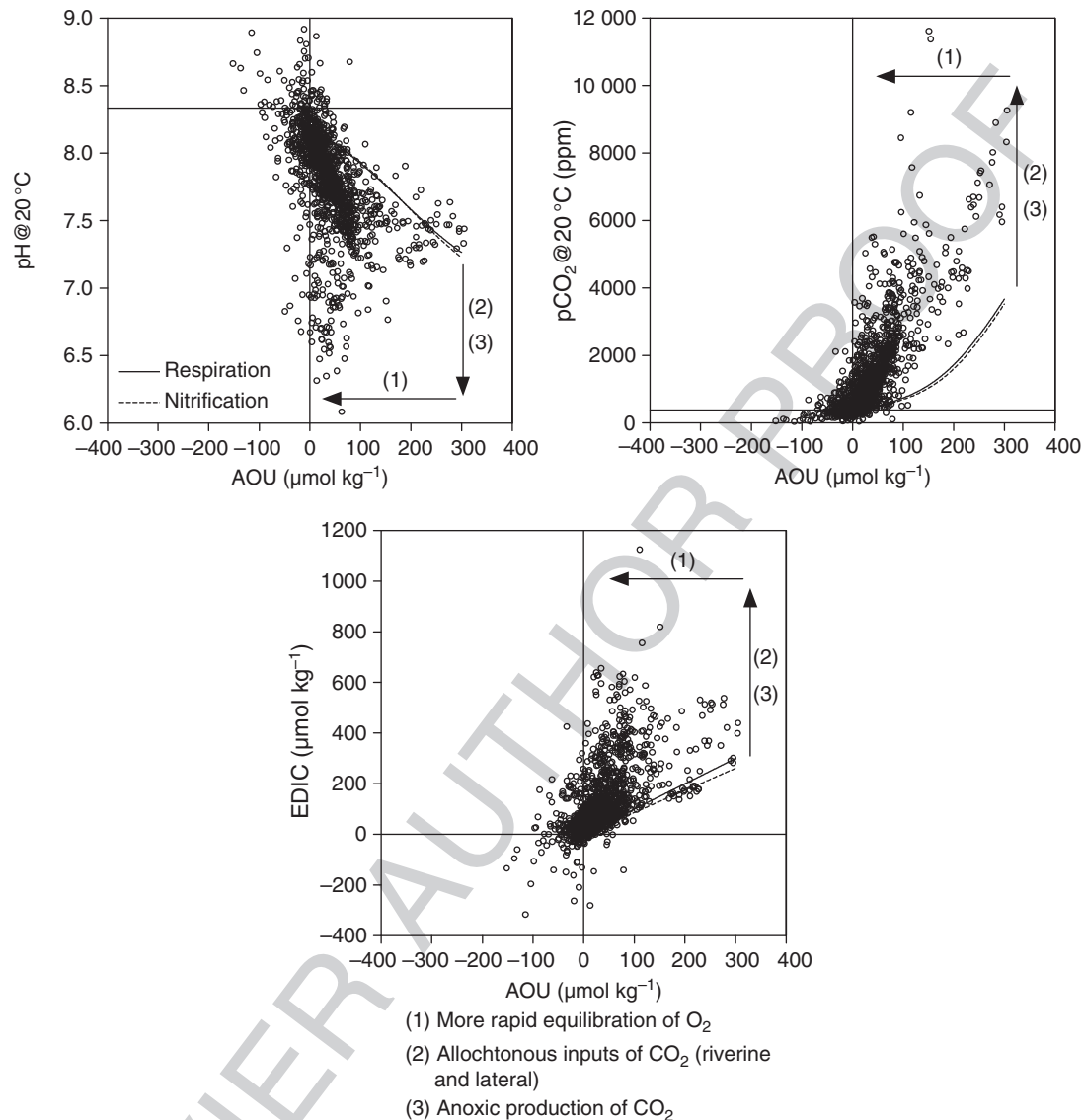


Figure 9 pH in the US National Bureau of Standards scale normalised to 20 °C (pH@20 °C), partial pressure of CO₂ normalized to 20 °C (pCO₂@20 °C in ppm), and excess dissolved inorganic carbon (EDIC in μmol kg⁻¹, computed according to Abril et al. (2000)) vs. apparent oxygen utilization (AOU in μmol kg⁻¹) compiling 1641 measurements in 24 estuarine environments : Aveiro lagoon (M. Frankignoulle, unpublished), Betsiboka (Ralison et al., 2008), Chilka Lake (Gupta et al., 2008), Cochin (Gupta et al., 2009), Douro (Frankignoulle et al., 1998), Elbe (Frankignoulle et al., 1998), Ems (Frankignoulle et al., 1998), Gironde (Frankignoulle et al., 1998), Godavari (Bouillon et al., 2003; Borges et al., 2003), Huangmaohai (Guo et al., 2009), Kidogoweni (Bouillon et al., 2007b), Kinondo (Bouillon et al., 2007b), Loire (Abril et al., 2003), Mekong (A.V. Borges, unpublished), Mkurumuji (Bouillon et al., 2007b), Mtoni (Kristensen et al., 2008), Pearl River (Zhujiang) (Guo et al., 2009), Ras Dege (Bouillon et al., 2007c), Rhine (Frankignoulle et al., 1998), Sado (Frankignoulle et al., 1998), Scheldt (Frankignoulle et al., 1998), Tamar (Frankignoulle et al., 1998), Tana (Bouillon et al., 2007a), and Thames (Frankignoulle et al., 1998). The solid line and dotted line correspond to the theoretical evolution of pH@20 °C, pCO₂@20 °C, and EDIC due aerobic respiration (CH₂O + O₂ → CO₂ + H₂O) and nitrification (NH₄⁺ + 2 O₂ → NO₃⁻ + 2 H⁺ + H₂O), respectively (for initial conditions of salinity = 0, temperature = 20 °C, TA = 2500 μmol kg⁻¹, DIC = 2303 μmol kg⁻¹, pH = 8.188, pCO₂ = 380 ppm, and using the carbonic acid dissociation constants of Millero et al. (2006)).

limnology for cross-system analysis of pCO₂ data (del Giorgio et al., 1999; Riera et al., 1999; Kelly et al., 2001; Sobek et al., 2003, 2005; Roehm et al., 2009; Teodoru et al., 2009). The positive relationship between pCO₂ and DOC in rivers and tidal rivers is remarkably consistent considering that data compiled in Figure 14 are from different climatic regions (from temperate to tropical), and from rivers with different catchment characteristics. The positive relationship between pCO₂ and DOC can be indicative of terrestrial organic matter inputs (as traced by DOC) sustaining net heterotrophy in the rivers (as

indicated by pCO₂). Alternatively, and not incompatibly, the positive relationship can also be indicative of lateral inputs of both DOC and CO₂ from soils by groundwaters and surface runoff. Data from peatland streams stand out, suggesting highly refractory DOC, and lower in-stream production of CO₂ in these systems. Further, peatland streams are very acid (due to the high content of humic substances), leading to a low buffering capacity due to low HCO₃⁻ content, with TA values ranging between 0 and 775 μmol kg⁻¹ (Dawson et al., 2001, 2002, 2004; Hope et al., 2001; Billett et al., 2004), while, in

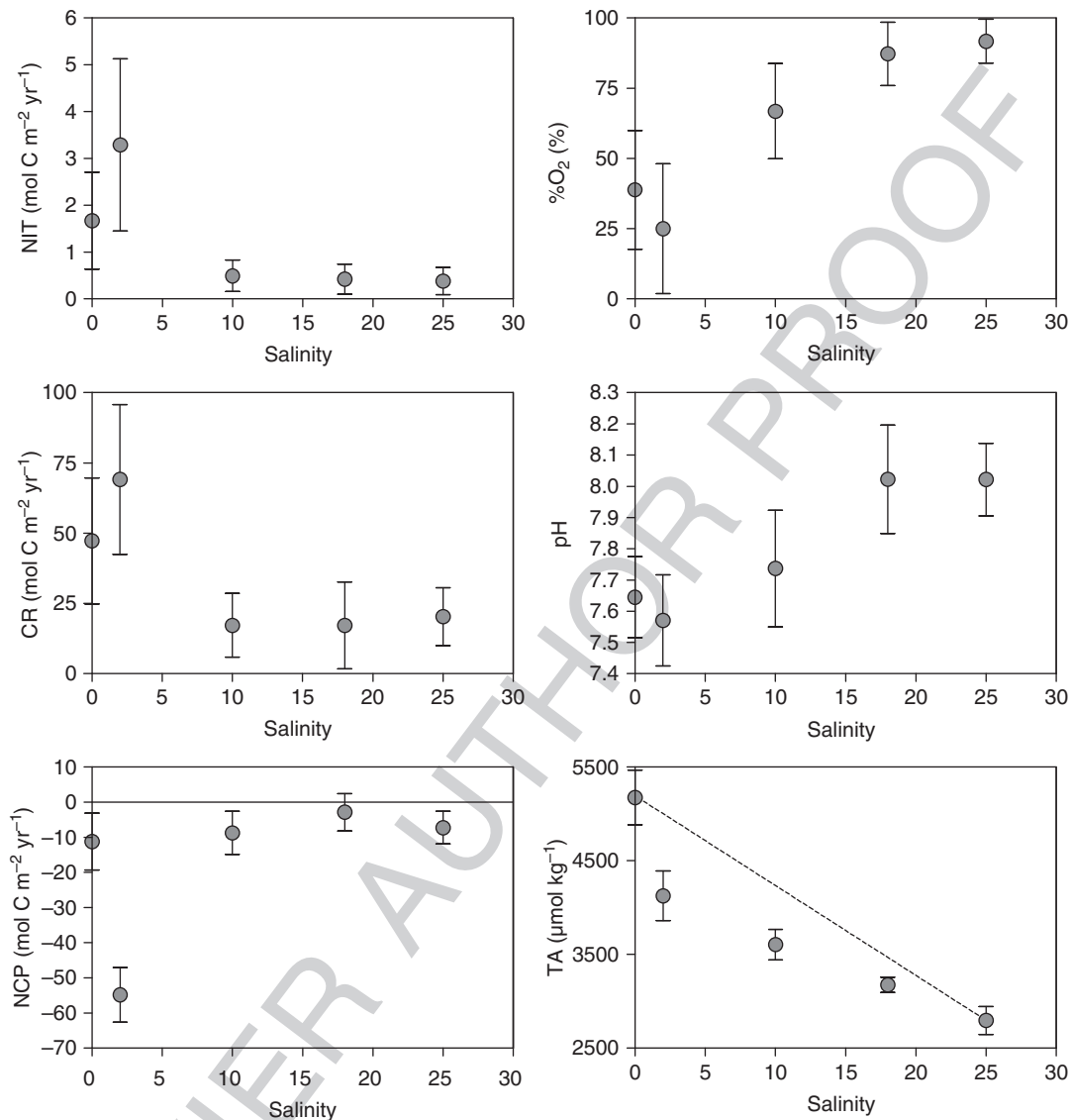


Figure 10 Annual averages of nitrification (NIT in mol C m⁻² yr⁻¹), community respiration (CR in mol C m⁻² yr⁻¹), net community production (NCP in mol C m⁻² yr⁻¹), oxygen saturation level (%O₂ in %), pH, and total alkalinity (TA in μmol kg⁻¹) versus salinity in the Scheldt estuary in 2003, based on a monthly monitoring covering the full annual cycle, adapted from Gazeau et al. (2005b). The dotted line indicates the dilution line of TA using the two extreme end members in the data set. The error bars are the standard deviations on the means, and indicate the range of seasonal variability at each salinity. Note that nitrification is expressed in carbon units (organic matter production), and the corresponding O₂ consumption is 14 times higher; hence, O₂ consumption due to nitrification is equivalent to CR throughout the estuary.

ivers, TA values range between 220 and 3115 μmol kg⁻¹ (e.g., Cai et al., 2008), with values > 4000 μmol kg⁻¹ in some tidal rivers (e.g., Frankignoulle et al., 1996). Note that the regression line of pCO₂ versus DOC from Quebec rivers reported by Teodoru et al. (2009) converges toward the data from peatland streams, and has a lower slope than the one based on temperate and tropical data. This can also be indicative of the more refractory nature of DOC in the catchment of the Quebec rivers and streams investigated by Teodoru et al. (2009), dominated by boreal forests and extensive bogs and peatlands. Further, the slope of the relationship between pCO₂ and DOC reported by Sobek et al. (2003) for Swedish (boreal) lakes is very consistent with the relationship of Teodoru et al. (2009) for Quebec rivers, confirming the refractory nature of DOC in rivers and lakes investigated in both studies. Finally,

the relationship between pCO₂ and DOC reported by Sobek et al. (2005) for global lakes has an even lower slope. While beyond the scope of the present chapter, this different relationship between pCO₂ and DOC is related to marked and multiple differences in overall organic and inorganic carbon cycling between rivers/streams and lakes, related, for instance, to residence time, surface area, ratio of allochthonous inputs to volume of water, photooxidation of DOC, gas transfer velocity, etc.

Cross-system analysis of CH₄ and pCO₂ in tidal rivers, rivers, and streams can also provide information on their origin and in-stream cycling. Despite large scatter, data could aggregate into two clusters, on the one hand small streams and headwaters, on the other hand lowland rivers and tidal rivers (Figure 15). For similar pCO₂ values, the CH₄ content is higher in streams and headwaters than in lowland rivers and tidal

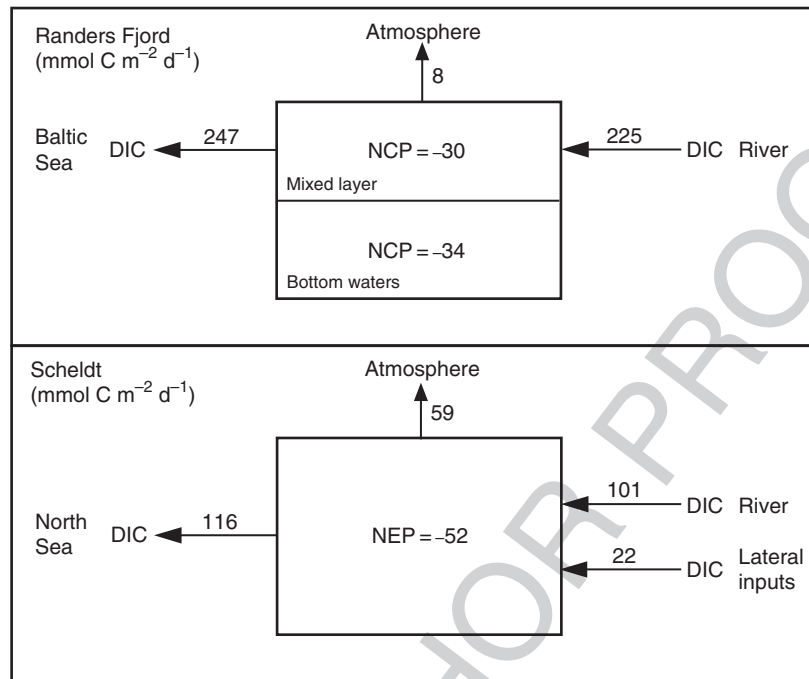


Figure 11 Dissolved inorganic carbon (DIC) mass balance in the Randers Fjord (April 2001 and August 2001) and the Scheldt estuary (annual coverage based on monthly sampling in 2003), based on Gazeau et al. (2005a, 2005b). Net ecosystem production (NEP) and net community production (NCP) are based on O₂ discrete incubations scaled at the level of whole estuary, except for the NCP value in the mixed layer for August 2001 in the Randers Fjord that was derived from the response-surface-difference method (Gazeau et al., 2005a). The flux of CO₂ across the air–water interface was computed as the closing term of the mass balance, and compares well in direction and magnitude with values derived from field measurements of the partial pressure of CO₂ (Gazeau et al., 2005a, 2005b; **Table 2**).

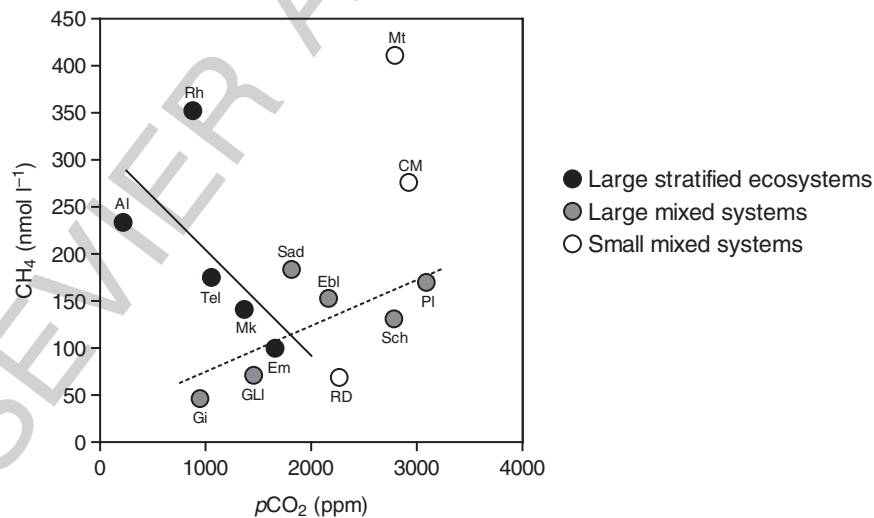


Figure 12 Average methane concentration (CH₄ in nmol l⁻¹) vs. average partial pressure of CO₂ (pCO₂ in ppm) in 14 estuarine systems: Aby lagoon (Al; Koné et al., 2009, 2010), Ca Mau mangrove creeks (CM; A.V. Borges and G. Abril, unpublished), Ebríe lagoon (Ebl; Koné et al., 2009, 2010), Ems (Em; Frankignoulle et al., 1998; Middelburg et al., 2002), Gironde (Gi; Frankignoulle et al., 1998; Middelburg et al., 2002), Grand-Lahou lagoon (GLI; Koné et al., 2009, 2010), Mekong (Mk; A.V. Borges and G. Abril, unpublished), Mtoni creek (Mt; Kristensen et al., 2008), Potou lagoon (Pl; Koné et al., 2009, 2010), Ras Dege creek (RD; Bouillon et al., 2007c), Rhine (Rh; Frankignoulle et al., 1998; Middelburg et al., 2002), Sado (Sad; Frankignoulle et al., 1998; Middelburg et al., 2002), Scheldt (Sch; Frankignoulle et al., 1998; Middelburg et al., 2002), and Tendo lagoon (Tel; Koné et al., 2009, 2010). The solid line corresponds to the regression line for large and stratified estuaries (CH₄ = 317 - 0.11 * pCO₂, r² = 0.39, p = 0.2604, n = 5), and the dotted line corresponds to the regression line for large and vertically mixed estuaries (CH₄ = 26 + 0.005 * pCO₂, r² = 0.51, p = 0.1124, n = 6).

rivers. This could be indicative of CH₄ degassing and bacterial oxidation of CH₄ in parallel to enrichment in CO₂ due to in-stream production as water moves downstream (from

headwaters to tidal rivers). Note also that the overall positive relationship between CH₄ and pCO₂ could be indicative of a common origin: from soils drained by groundwaters and

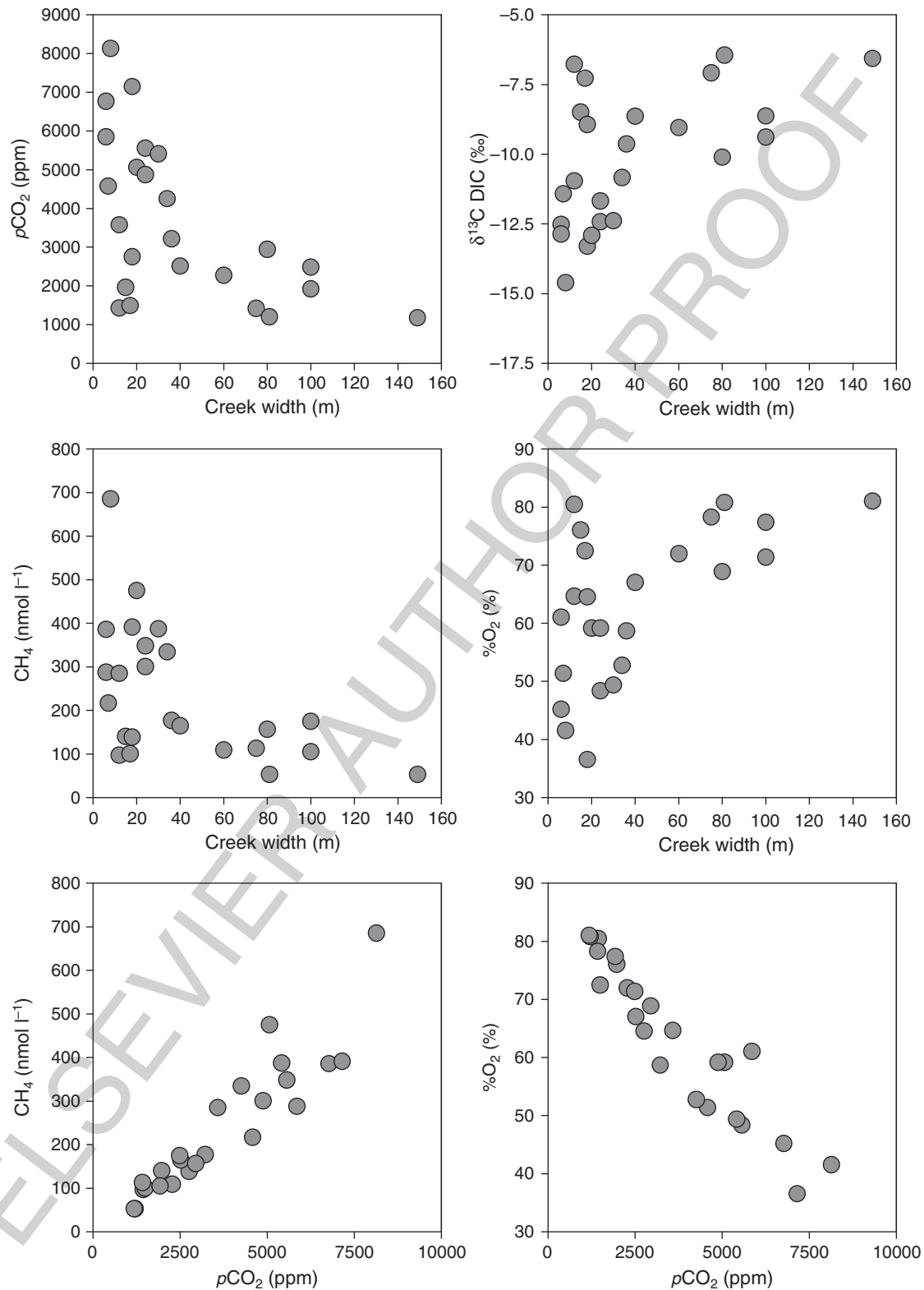


Figure 13 Partial pressure of CO₂ (pCO₂ in ppm), δ¹³C of dissolved inorganic carbon (δ¹³C DIC in ‰), methane concentration (CH₄ in nmol l⁻¹) and oxygen saturation level (%O₂ in %) vs. creek width (m), and CH₄ vs. pCO₂ and %O₂ vs. pCO₂ in the mangrove creeks of Ca Mau in October 2004 (Koné and Borges, 2008; A.V. Borges, G. Abril, and S. Bouillon, unpublished).

surface runoff in headwaters and small rivers, possibly from net heterotrophy in lowland rivers and tidal rivers. Along the river system, allochthonous and autochthonous organic carbon is

transported and transformed, with different fates along the stream-size continuum (Vannote et al., 1980; Battin et al., 2009). According to the river continuum concept, midreaches

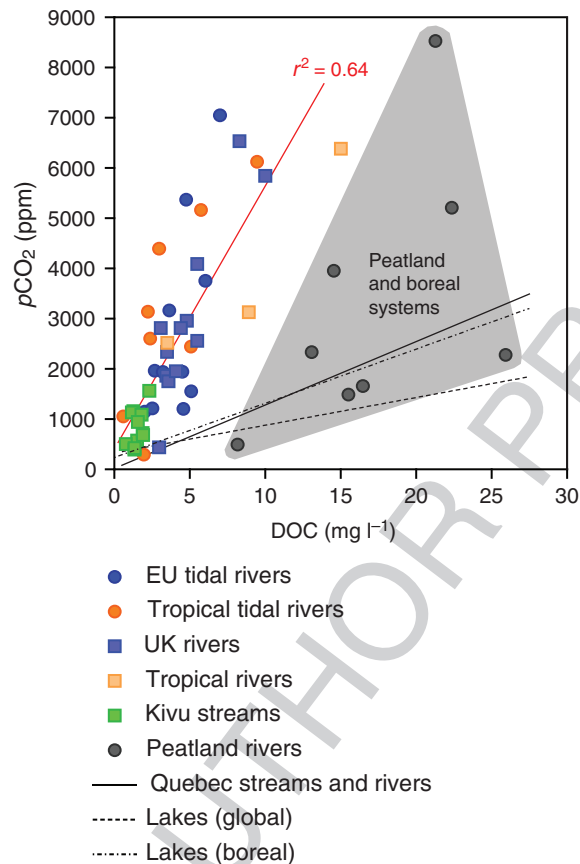


Figure 14 Partial pressure of CO₂ ($p\text{CO}_2$ in ppm) versus dissolved organic carbon (DOC in mg l^{-1}) in several tidal rivers, and nontidal rivers and streams: Auchencorth peatland stream (Billett et al., 2007), Aveiro (Frankignoulle, unpublished), Betsiboka (Ralison et al., 2008), Brocky Burn peatland stream (Dawson et al., 2004), Brocky Burn peatland stream (Hope et al., 2001), Chilka Lake (Gupta et al., 2008), Cochin (Gupta et al., 2009), Douro (Frankignoulle et al., 1998; Abril et al., 2002), Elbe (Frankignoulle et al., 1998; Abril et al., 2002), Ems (Frankignoulle et al., 1998; Abril et al., 2002), Gironde (Frankignoulle et al., 1998; Abril et al., 2002), Godavari (Bouillon et al., 2003), Kidogoweni (Bouillon et al., 2007b), Lake Kivu streams (Kakumbu, Kiraro, Koko, Magarama, Mpungwe, Mugada-Bwindi, Muregeya, Murhundu, Mushava, Nyabahanga; A.V. Borges and S. Bouillon, unpublished), Loch More peatland stream (Billett et al., 2007), Loire (Frankignoulle et al., 1998; Abril et al., 2002), Mekong (A.V. Borges and S. Bouillon, unpublished), Mer Bleue peatland streams (Billett and Moore, 2008), Migneint peatland stream (Billett et al., 2007), Mkurumuji (Bouillon et al., 2007b), Moor House peatland stream (Billett et al., 2007), Niger (Martins, 1982), Nyong (Brunet et al., 2009), Parana River (Depetris and Kempe, 1993), Randers (Gazeau et al., 2005a; Rochelle-Newall et al., 2007), Rhine (Frankignoulle et al., 1998; Abril et al., 2002), Scheldt (Frankignoulle et al., 1998; Abril et al., 2002), Tamar (Frankignoulle, unpublished), Tana (Bouillon et al., 2009), Thames (Frankignoulle et al., 1998; Abril et al., 2002), UK rivers (Neal et al., 1998), and Water of Dye peatland stream (Dawson et al., 2004). The solid black line represents the relationship for Quebec rivers and streams (Teodoru et al., 2009), the dash-dotted line represents the relationship from a compilation of Swedish boreal lakes (Sobek et al., 2003), the dotted black line represents the relationship from a global compilation in lakes (Sobek et al., 2005), and the solid red line is the linear regression for all data in the figure excluding peatland rivers ($p\text{CO}_2 = 407 + 523.1 \cdot \text{DOC}$, $r^2 = 0.64$, $p < 0.0001$, $n = 45$).

are net autotrophic, while headwaters and lower reaches are net heterotrophic fueled by allochthonous and autochthonous carbon, respectively (Vannote et al., 1980). The connectivity along the river system is more complex for CO₂ and CH₄ than for organic carbon due to lateral inputs from soils by groundwaters and surface runoff, variable *in situ* production and exchange with the atmosphere for both gases, and bacterial oxidation for CH₄. Yet, the increase of CO₂ from headwaters/streams to lowland and tidal rivers (Figure 15) agrees with pattern of increasing net heterotrophy with size given by the river continuum concept. Note that data in the Rhine tidal river stand out for the same reasons as for the overall estuarine analysis discussed above: the large discharge that leads to rapid flushing of freshwater minimizing CH₄ loss terms (evasion to the atmosphere and bacterial oxidation), and reduces the accumulation of CO₂ due to net heterotrophy.

Based on the approach given by Abril et al. (2000), the relative contribution of the ventilation of riverine CO₂ to the overall CO₂ emission was computed in several estuaries (Figure 16). This contribution decreases with the increase of the freshwater residence time. In estuaries with a long freshwater residence time, the riverine CO₂ will be fully ventilated to the atmosphere within the estuary, and the overall CO₂ emission from the estuary will be mostly related to net heterotrophy. In contrast, in estuaries with very short freshwater residence time, the enrichment of DIC from net heterotrophy will be less pronounced, and the contribution of the ventilation of riverine CO₂ will be larger. In the case of the Rhine estuary, the freshwater residence time is so short that all the riverine CO₂ is not ventilated to the atmosphere in the estuarine zone, and part of it is, instead, exported to the adjacent coastal ocean. Hence, the potential contribution of the

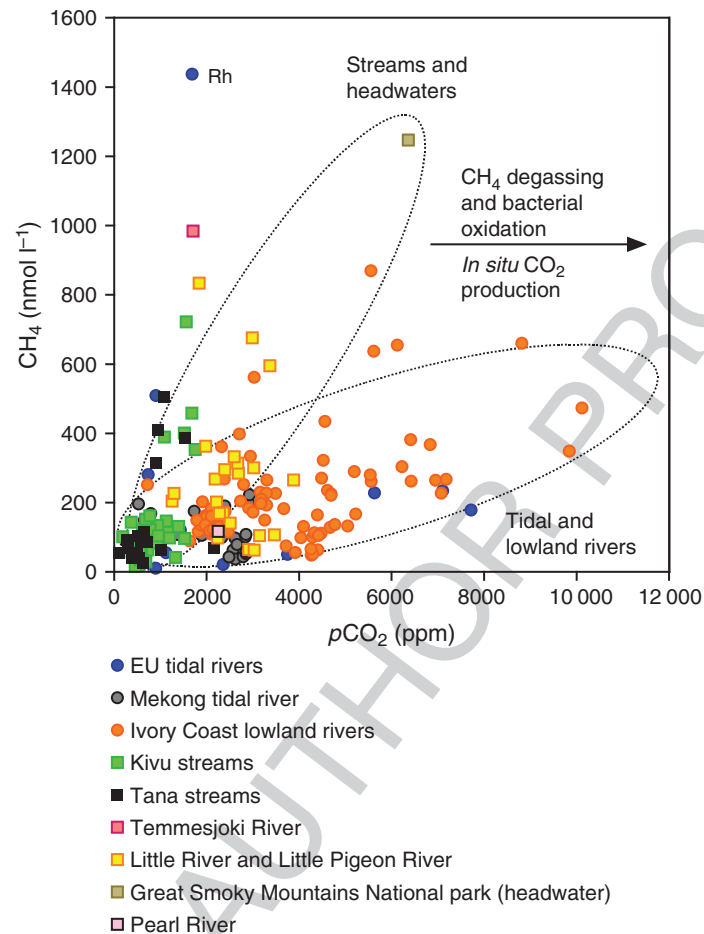


Figure 15 Methane (CH_4 in nmol l^{-1}) versus partial pressure of CO_2 (pCO_2 in ppm) in several tidal rivers, nontidal rivers and streams: E.U. tidal rivers (Ems, Gironde, Rhine (Rh), Scheldt; Frankignoulle et al., 1998; Middelburg et al. 2002), Great Smoky Mountains National park (headwater, Jones and Mulholland, 1998), Ivory coast lowland rivers (Bia, Comoé, Tanoé; Koné et al., 2009, 2010), Lake Kivu streams (Kakumbu, Kiraro, Koko, Magarama, Mpungwe, Mugada-Bwindi, Muregeya, Murhundu, Mushava, Nyabahanga; A.V. Borges and G. Abril, unpublished), Little Pigeon River (headwater; Jones and Mulholland, 1998), Little River (headwater; Jones and Mulholland, 1998), Mekong (A.V. Borges and G. Abril, unpublished), Pearl river (Chen et al., 2008), Tana streams (Chania, Maguru, Mara, Muringato, Mutundu, Nithi, Rojewero, Ruguti, Sagana, Tana, Thingithu, Thuchi; Bouillon et al., 2009), and Temmesjoki (Silvennoinen et al., 2008).

ventilation of riverine CO_2 is higher than the actual observed emission from the estuary. For the 11 estuaries in Figure 16, the median of the potential emission from riverine CO_2 amounts to about 10% of the total emission of CO_2 from the estuary. Hence, about 90% of the emission of CO_2 from these inner estuaries could be attributed to net heterotrophy. It remains to be established whether this is a general pattern, or if this conclusion is biased by the limited data set analyzed in Figure 16.

s0035 5.04.3 Dynamics of CH_4 and Atmospheric CH_4 Fluxes in Estuarine Environments

p0120 Fluxes of CH_4 from aquatic systems to the atmosphere result from the balance between the microbial processes of CH_4 production and CH_4 oxidation, and are also driven by the physical processes of gas transport. In estuaries, these microbial and physical processes are highly variable depending on the supply of labile organic matter to sediments, the availability of oxygen and other electron acceptors, the hydrodynamics, and the hydrostatic

pressure. The presence or absence of vegetation, the depth and vertical mixing of the water column, temperature, salinity, and turbidity are environmental variables that create spatial and temporal heterogeneity in CH_4 fluxes in estuaries. All studies converge to a seaward decrease in CH_4 fluxes, but these can differ by one order of magnitude from one site to another, depending on the combination of several biogeochemical processes. These processes differ from freshwater to saline waters, from the intertidal areas to the subtidal areas, and from well-mixed to stratified water columns (Figure 17).

5.04.3.1 Occurrence of High CH_4 Concentrations in Estuarine Sediments: Combined Controls of Methanogenesis by Organic Matter Supply and Salinity s0040

Production of CH_4 in aquatic systems occurs during the p0125 degradation of organic matter in anoxic sediments. Production of CH_4 in the water column of estuarine systems, even anoxic, is minor in comparison with production in sediments (Lindstrom, 1983; Fenchel et al., 1995).

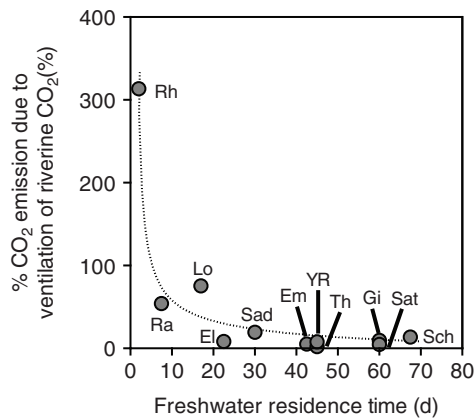


Figure 16 Contribution of the ventilation of river CO_2 to the overall emission of CO_2 from different estuaries to the atmosphere versus average residence time of freshwater, based on nine European and two US estuaries: Elbe (El; Frankignoulle et al., 1998; Frankignoulle and Middelburg, 2002), Ems (Em; Frankignoulle et al., 1998; Frankignoulle and Middelburg, 2002), Gironde (Gi; Frankignoulle et al., 1998; Frankignoulle and Middelburg, 2002), Loire (Lo; Abril et al., 2003; Frankignoulle and Middelburg, 2002), Randers Fjord (Ra; Frankignoulle et al., 1998; Frankignoulle and Middelburg, 2002), Rhine (Rh; Frankignoulle et al., 1998; Frankignoulle and Middelburg, 2002), Sado (Sad; Frankignoulle et al., 1998; Frankignoulle and Middelburg, 2002), Satilla (Sat; Cai and Wang, 1998), Scheldt (Sch; Frankignoulle et al., 1998; Frankignoulle and Middelburg, 2002), Thames (Th; Frankignoulle et al., 1998; Frankignoulle and Middelburg, 2002), and York River (YR; Raymond et al., 2000). Adapted from Borges, A.V., Schiettecatte, L.-S., Abril, G., Delille, B., Gazeau, F., 2006. Carbon dioxide in European coastal waters. *Estuarine, Coastal and Shelf Science* 70 (3), 375–387.

Environmental conditions favorable to methanogenesis in sediments are anoxia and depletion of alternative electron acceptors, nitrate, iron oxides, manganese oxides, and sulfate

(Conrad, 1989; Le Mer and Roger, 2001). In anoxic marine sediments, sulfate availability allows sulfate-reducing bacteria to outcompete methanogenic bacteria (Capone and Kiene, 1988). As a result, CH_4 concentrations are generally low in the top layers of the sediments where sulfate reduction occurs, and suddenly increase downward at the depth where sulfate concentration reaches zero (Reeburgh, 1969; Martens and Benner, 1977; Kelley et al., 1990; Blair and Aller, 1995). In addition, anaerobic CH_4 oxidation that occurs at the sulfate- CH_4 transition prevents CH_4 to diffuse upward, and generates a concave-up CH_4 profile (Martens and Benner, 1977; Blair and Aller, 1995). In estuaries, sulfate concentrations in the water column vary from a few $\mu\text{mol l}^{-1}$ in the freshwater end member to $\sim 28 \text{ mmol l}^{-1}$ in the marine end member. Consequently, the depth of sulfate depletion and of concomitant CH_4 rise in sediment generally increases seaward (Kelley et al., 1990). However, salinity and the associated sulfate availability, is not the only factor that controls the sulfate- CH_4 transition depth in the estuarine sediments. The rate of organic matter sedimentation and the availability of electron acceptors other than sulfate also play a major role. As shown in Table 4, high CH_4 concentrations can occur at depths from 10 cm to 7 m below the sediment-water interface. When the anaerobic degradation of organic matter raises the sum of the partial pressure of all dissolved gases above the hydrostatic pressure in the sediment, gas bubbles are formed (Chanton and Dacey, 1991). These bubbles start to form at CH_4 concentrations well below the gas solubility (roughly 1 mmol l^{-1}) and can contain between 40% and 100% of CH_4 , the second gas contained in these bubbles being molecular nitrogen (Chanton et al., 1989). In estuarine freshwater reaches like in the White Oak River estuary, which is organic-rich due to a supply from adjacent tidal marshes, CH_4 gas bubbles often

(a) Freshwaters and low-salinity regions

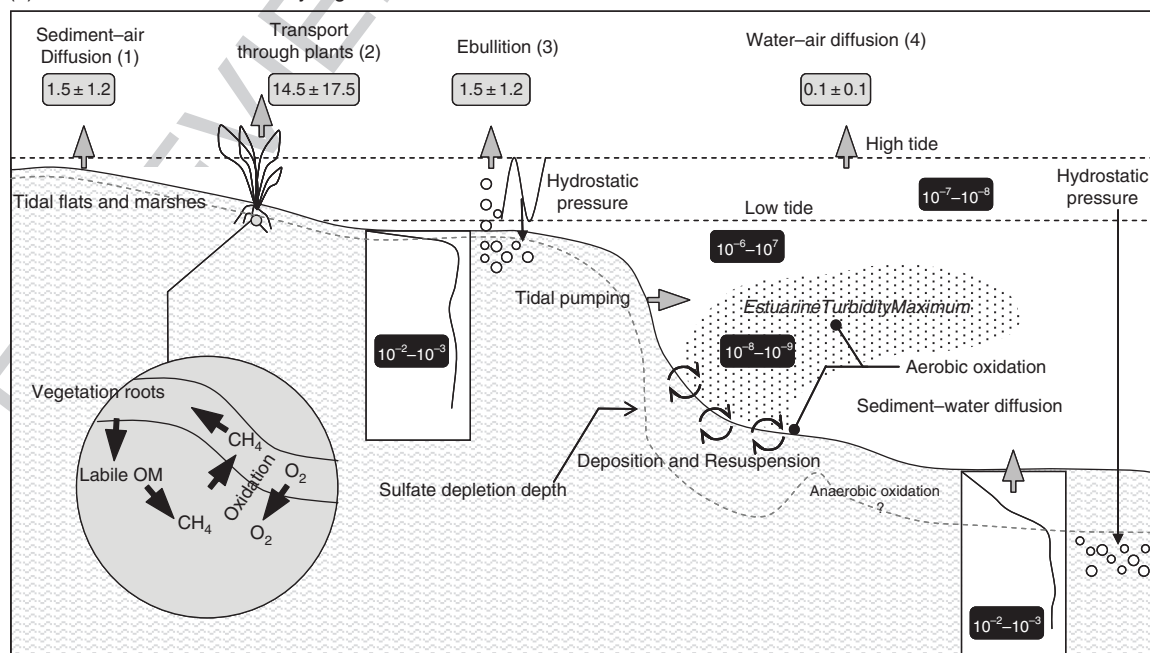


Figure 17 (Continued)

(b) High-salinity regions

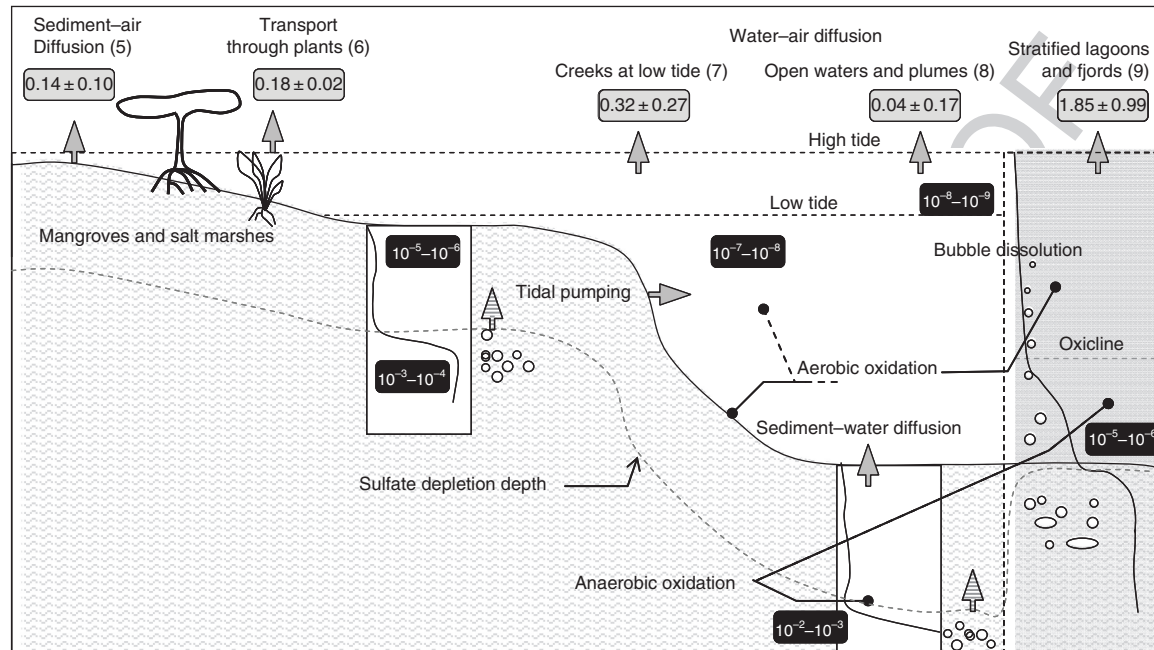


Figure 17 Summary of major processes controlling the CH_4 cycle in estuaries and associated concentrations and atmospheric fluxes. Order of magnitude of dissolved CH_4 concentrations in each compartment are shown in black boxes and expressed in mol l^{-1} ; CH_4 fluxes are shown in gray boxes and expressed in $\text{mmol C m}^{-2} \text{d}^{-1}$. (a) case of freshwaters; (1) average flux ($\pm \text{SD}$, $N=6$) from unvegetated sediments of tidal flats and marshes with salinities <5 from **Table 5** (Lipschultz, 1981; Chanton et al., 1989; Kelley et al., 1995; Van der Nat and Middelburg, 2000); outlying data influenced by sewage inputs (Middelburg et al., 1996) were excluded; (2) average flux ($\pm \text{SD}$, $N=12$) from vegetated sediments of tidal marshes with salinities <5 from **Table 5**, transport through plants contribution or total fluxes measured over dense vegetation (Delaune et al., 1983; Bartlett et al., 1985, 1987; Alford et al., 1997; Van der Nat and Middelburg, 1998, 2000); (3) average ($\pm \text{SD}$, $N=4$) from unvegetated sediments of tidal marshes with salinities <5 from **Table 5** (Chanton et al., 1989; Van der Nat and Middelburg, 2000); and (4) average flux ($\pm \text{SD}$, $N=9$) from inner estuarine channels from **Table 7** (De Angelis and Lilley, 1987; De Angelis and Scranton, 1993; Bange et al., 1998; Sansone et al., 1998; Middelburg et al., 2002; Abril and Iversen, 2002; Shalini et al., 2006; Ferrón et al., 2007; Zhang et al., 2008); (b) case of saline waters. (5) average flux ($\pm \text{SD}$, $N=5$) from unvegetated sediments of salt marshes and mangroves with salinities >25 from **Table 5** (Magenheimer et al., 1996; Sotomayor et al., 1994; Kristensen et al., 2008); (6) average flux ($\pm \text{SD}$, $N=4$) from tidal marshes with dense vegetation and pneumatophore contribution in mangrove sediments in systems with salinities >20 from **Table 5** (Bartlett et al., 1985; Kristensen, 2008; Chen et al., 2009); (7) average flux ($\pm \text{SD}$, $N=5$) from marsh and mangrove creeks at low tide in **Table 7** (Bartlett et al., 1985; Kristensen, 2008; Chen et al., 2009; Bouillon et al., 2007); (8) average flux ($\pm \text{SD}$, $N=4$) in estuarine plumes (Scranton and McShane, 1991; Bange et al., 1996; Amouroux et al., 2002; Zhang et al., 2008); and (9) average flux ($\pm \text{SD}$, $N=2$) from a stratified tropical lagoon and a small fjord (Fenchel et al., 1995; Koné et al., 2010); note that two arctic stratified fjords without anoxic bottom waters had much lower surface CH_4 concentrations (Damm et al., 2005).

occur in unvegetated sediments at depths of no more than 10–20 cm (Chanton et al., 1989; Kelley et al., 1995). In contrast, in marine regions of estuaries such as the Amazon shelf, where organic matter sedimentation is much lower, and where most of the organic decomposition occurs by reduction of iron oxides and of sulfate, CH_4 concentrations reach few hundred $\mu\text{mol l}^{-1}$ only at depths of more than 5 m in the sediment (Blair and Aller, 1995). Between these two extremes (cases A and D in **Figure 18**), all possible intermediate situations can occur.

The general spatial pattern is a seaward decrease in near-surface CH_4 pore-water concentrations, as the sulfate concentration and depletion depth increase, and as the organic matter supply to the sediment decreases (Bartlett et al., 1985, 1987; Kelley et al., 1990; Middelburg et al., 1996). There are, however, several exceptions both in the high- and low salinity regions of estuarine environments. First, in the low salinity region of macrotidal estuaries, the strong hydrodynamics generates repetitive sediment resuspension, and makes oxic and suboxic conditions to prevail in fluid mud and sediments. Nitrate, Mn

oxides, and, eventually, Fe oxides become the predominant electron acceptors and a very minor fraction of the organic matter is decomposed by sulfate reduction and methanogenesis (Abril et al., 1999, 2010; Robert et al., 2004; Audry et al., 2006). Hence, no high CH_4 concentrations have been observed in these freshwater sediments, even deep below the water-sediment interface. Second, at high salinity in shallow eutrophic and quiescent coastal bays, extremely high organic sedimentation can lead to a sulfate depletion in the top layers of the sediment, and CH_4 rises to several mmol l^{-1} at depths of less than 1 m below the sediment-water interface (case B in **Figure 18**). This has been reported, for instance, in the Cape Lookout Bight (Martens and Klump, 1980) and the Eckernförde Bay sediments (Albert et al., 1998; Martens et al., 1998), where CH_4 gas bubbles at a few decimeters below the sediment-water interface are a common feature. Third, groundwater flows of sulfate-depleted freshwater also favor methanogenesis and the occurrence of CH_4 bubbles in coastal marine sediments (Albert et al., 1998).

Measurements of CH_4 production performed so far in estuarine sediment revealed maximum values at distinct depths,

Table 4 Porewater maximal CH₄ concentration ($\mu\text{mol l}^{-1}$), corresponding depth (cm) and water or porewater salinity in various estuarine sediments

	Maximum porewater CH ₄ observed ($\mu\text{mol l}^{-1}$)	Corresponding depth in the sediment (cm)	Water or porewater salinity	Comment	References
Queen's Creek, York River (US Virginia)	300	60	5.1	Selected date: November 1983	Bartlett et al. (1987)
Queen's Creek, York River (US Virginia)	500	20	12.8	Selected date: November 1983	
Queen's Creek, York River (US Virginia)	180	20	16.6	Selected date: November 1983	
Long Island Sound (US NY/ connecticut)	1 000	20–40	30	Sampling date not specified, salinity assumed from water sulfate concentration	Martens and Benner (1977)
Cape Lookout Bight (US North Carolina)	1 700	10–30	30–35	Salinity assumed from water sulfate concentration	Martens and Klump (1980)
White Oak River estuary	800–1200	5–10	0	Two subtidal stations, two seasons	Chanton et al. (1986) and Kelley et al (1995)
White Oak River estuary	600–700	40–60	18.9	One subtidal station, two seasons	Kelley et al (1990)
Amazon Shelf	120–240	600–700	15–23	cc $\mu\text{mol l}^{-1}$ wet sediment converted using a water content of ww 66%	Blair and Aller (1995)
Sundarban mangrove, Bay of Bengal	1.5	0–20	12–27	Only surface values (integrated in the top 20 cm sediments)	Biswas et al. (2007)
Eckernförde Bay, Baltic Sea (Germany)	4000–6000	50–150	17–25	Fresh groundwater inputs from the aquifer	Albert et al. (1998)
Tidal Flat Janssand, Wadden Sea (Germany)	200	400	33		Grunald et al. (2009)

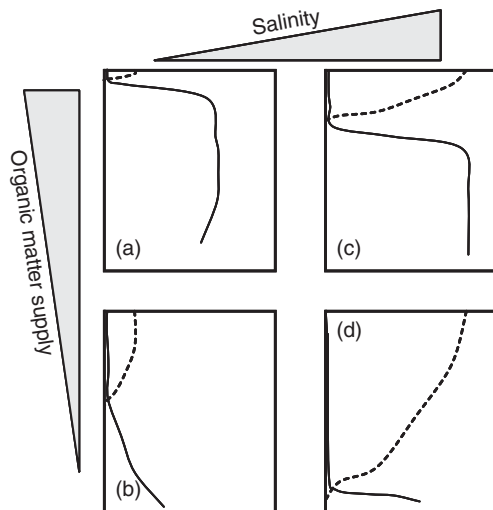


Figure 18 Typical depth distributions of CH_4 (bold lines) and sulfate (dotted lines) in estuarine sediments, along gradients of salinity (increasing from left to right) and of organic matter supply (decreasing from top to bottom). The horizontal scale is roughly $0\text{--}20\text{ mmol l}^{-1}$ for sulfate and about $0\text{--}1\text{ mmol l}^{-1}$ for CH_4 . The vertical scale is $0\text{--}1\text{ m}$ to $0\text{--}5\text{ m}$. Examples of the four situations are: (a) unvegetated sediments in freshwater tidal marshes and quiescent adjacent channels (Chanton et al., 1988; Kelley et al., 1995), freshwater tidal flats affected by sewage loads (Middelburg et al., 1996); (b) freshwater channel of highly energetic macrotidal estuaries; (c) quiescent organic-rich coastal bays (Martens and Klump, 1980; Albert et al., 1998; Martens et al., 1998); and (d) highly dynamic estuarine plumes (Blair and Aller, 2005).

depending on the organic matter availability and the presence of alternative oxidants: in the top $10\text{--}20\text{ cm}$ of sediment cores from a freshwater tidal flat (Kelley et al., 1995), in the top 2 cm and also at 40 cm depth in freshwater and Fe-rich vegetated tidal marsh sediments (van der Nat and Middelburg, 2000), at $10\text{--}20\text{ cm}$, close to and below the sulfate-depletion depth in organic-rich coastal marine sediments (Crill and Martens, 1983). Cases of CH_4 production (though at low rates) in the presence of other electron acceptors also occur and could account for most of the CH_4 produced at some sites. In an *in vitro* experiment with fluid mud from the Gironde estuary turbidity maximum (ETM), a slow but constant CH_4 production was measured in the presence of nitrate and sulfate (Abril et al., 2010). Peaks of CH_4 in the first centimeters below the sediment surface have also been observed at high salinity associated with diatom mats (Abril and Iversen, 2002; Deborde et al., 2010). Such CH_4 production suggests a supply of specific substrates for methanogen bacteria. Noncompetitive substrates for methanogens in marine sediments include methylamines (Oremland and Polcin, 1982) and dimethyl sulfide (Van der Maarel and Hansen, 1997). In coastal sediments, these compounds are present in algae, benthic animals, and bacteria, and are also produced during decomposition of organic material (Oremland and Polcin, 1982; Wang and Lee, 1994).

5.04.3.2 Pathways and Fluxes of CH_4 from Sediment to Water and to the Atmosphere

There are four distinct pathways in estuaries for CH_4 to reach the atmosphere (Figure 17): (1) diffusion at the sediment–air, sediment–water, and water–air interfaces; (2) ebullition from

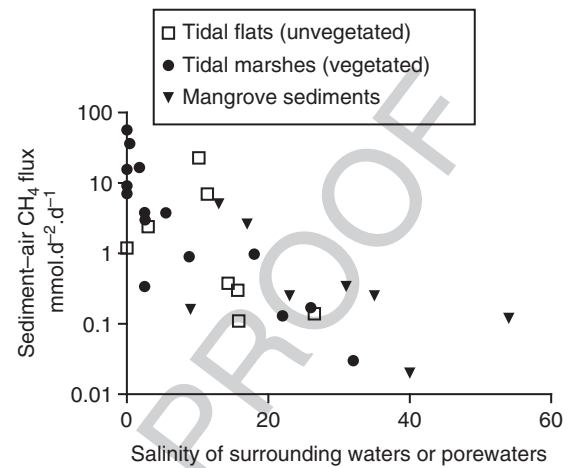


Figure 19 Sediment–air CH_4 fluxes measured around low tide in intertidal areas versus salinity in surrounding water or pore waters based on data from Table 5. Two outlying high values from the Scheldt estuary tidal flats at very low salinity, which corresponded to sites affected by sewage loads (Middelburg et al., 1996) are not shown.

sediment to water and air; (3) transport through plants in vegetated tidal marshes; and (4) lateral tidal pumping followed by water–air diffusion. Figure 19 shows reported CH_4 fluxes from intertidal areas to the atmosphere versus salinity. These fluxes have been measured with static chambers close to low tide in a wide spectrum of intertidal systems, with or without vegetation. Therefore, they include the three types of CH_4 transport in the absence of water, sediment–air diffusion, ebullition, and transport through plants. A general decrease with salinity is observed (Bartlett et al., 1987), but CH_4 fluxes can vary by two orders of magnitude at a given salinity. Median fluxes reported in Table 5 decrease from vegetated tidal marshes (with highest values in freshwater, and where most of the CH_4 flux occurs through plants), to unvegetated tidal flats (where diffusion and ebullition dominate), and to mangrove sediments (where salinity is generally high).

The presence of macrophytes rooted in sediments strongly affects the CH_4 cycle and fluxes in tidal marshes by three processes: (1) plants release labile organic compounds through plant litter production and root exudation, and may so stimulate methanogenesis; (2) plants transport atmospheric oxygen to the rhizosphere and favor CH_4 oxidation; and (3) plants act as gas conduits and transport CH_4 from the sediments to the atmosphere (Chanton and Dacey, 1991; van der Nat and Middelburg, 1998a, 2000). This CH_4 transport through plants is passive (due to molecular diffusion) and active (due to convective flow generated by pressure differences) (for an overview of the literature on gas transport through plants, refer to van der Nat et al. (1998)). Fluxes of CH_4 are maximal during the growing season of plants and, depending on the capacity of plants for active gas transport, daytime fluxes are greater than nighttime fluxes (van der Nat et al., 1998; van der Nat and Middelburg, 2000). As shown in Figure 20, the presence of marsh vegetation strongly affects the shape of CH_4 profiles in sediments, decreasing the concentration at depths of the rhizosphere, by stripping out CH_4 by transport, and by favoring CH_4 oxidation. In the presence of plants, CH_4 oxidation can occur

Table 5 Sediment-air CH₄ fluxes (in mmol m⁻² d⁻¹) in estuarine intertidal areas around low tide

	CH ₄ flux (mmol m ⁻² d ⁻¹)	Comment	References
Tidal flats			
White Oak (US–North Carolina)	1.2 1–45	Annual average from four bank stations (freshwater sites) Seasonal range from four bank stations (freshwater sites)	Kelley et al. (1995)
Choptank river estuary	2.5–6.3	Tidal variation at a single bank station in August 1991	Lipschultz (1981)
Scheidt Estuary (Belgium/the Netherlands)	2.4 550 190 23 7 0.3 0.38 0.11 0.14	Annual average, salinity 1–10 Annual average, fresh water site affected by sewage Annual average, salinity 1.6, site affected by sewage Annual average, salinity 10 Annual average, salinity 11 Annual average, salinity 16 Annual average, salinity 14 Annual average, salinity 15 Annual average, salinity 26	Middelburg et al. (1996)
Tidal marshes			
White Oak freshwater (US–North Carolina)	7.1 3.5 3.5 36.5 16.6 0.9 0.17 3.0 3.8 0.9 0.13 0.03 15.7 9.1 57 0.3 3.8	Total, annual average, freshwaters Ebullition Diffusion Annual average, salinity 0.4 Annual average, salinity 1.8 Annual average, salinity 18 Annual averages, one site, salinity 26, <i>Spartina alterniflora</i> Annual average, salinity 2.6, <i>Spartina cynosuroides</i> Annual average, salinity 5.5, <i>S. cynosuroides</i> and <i>S. alterniflora</i> Annual average, salinity 8.8, <i>S. alterniflora</i> Annual average, salinity 20–23 Annual average, salinity 31–35 Annual average, freshwater, <i>Sagittaria lancifolia</i> Annual average, freshwater, forested by <i>Taxodium distichum</i> / <i>Nyssa aquatica</i> Annual average, freshwater, <i>Sagittaria lancifolia</i> / <i>Spartina patens</i> Annual average, salinity 2.5, <i>Scirpus lacustris</i> Annual average, salinity 2.5, <i>Phragmites australis</i>	Chanton et al. (1989) DeLaune et al. (1983) Bartlett et al. (1985) Bartlett et al. (1987) Magenheimer et al. (1996) Alford et al. (1997) Van der Nat and Middelburg (1998) Van der Nat and Middelburg (2000)
Dipper Harbor (Canada–New Brunswick)	1.9–7.8	Total, seasonal range, freshwater, <i>Scirpus lacustris</i>	
Mississippi deltaic plain	1.3–7.8 0.14–0.6 0–0.1	Through plants Diffusive Ebullitive	
Scheidt estuary (Belgium)			
Constructed bulrush wetlands			

(Continued)

Table 5 (Continued)

	CH_4 flux ($mmol\ m^{-2}\ d^{-1}$)	Comment	References
Constructed reed wetlands	3.3–17.7	Total, seasonal range, freshwater, Phragmites australis	Cheng et al. 2009
	1.2–17.3	Through plants	
	0.4–0.6	Diffusive	
	0.9–5.9	Ebullitive	
Constructed wetlands unvegetated	0.7–14.3	Annual average, Freshwater, unvegetated control	Cheng et al. 2009
	0.4–0.7	Diffusive	
Jiuduansha wetlands Yantze River (China)	0.03–0.4	Seasonal range, invasive <i>Spartina alterniflora</i>	Cheng et al. 2009
	0.01–0.34	Seasonal range, native <i>Scirpus maritimus</i>	
Mangroves			
Brisbane River Estuary (Queensland, Australia) Southwestern Coast of Puerto Rico	0.04–0.022	Seasonal range at two sites of gray mangrove (<i>Avicennia marina</i>)	Allen et al. (2007) Sotomayor et al. (1994)
	0.019	Annual average, Red mangrove, salinity 38–44	
	0.119	Annual average, Transition zone, salinity 52–56	
	2.6	Annual average, Red mangrove, salinity 11–25	
	5.1	Annual average, Transition, salinity 7–18	
	0.25	Annual average, White mangrove, salinity 19–27	
	0.16	Annual average, Mangrove Site affected by sewage, salinity 9	
	0.022–0.088	Dry season, diffusion two stations	
	0.114	Dry season, pneumatophores contribution, one station	
	0.018–0.168	Dry season crab burrows contribution, two stations	
	0.34	Total	
Mtoni (Tanzania)	0–25	Dry season, diffusion two stations	Kristensen et al. (2008)
	0.153	Dry season, pneumatophores contribution, one station	
	0.064–0.085	Dry season, crab burrows contribution, two stations	
Ras Dege (Tanzania)	0.253	Total	Kristensen et al. (2008)

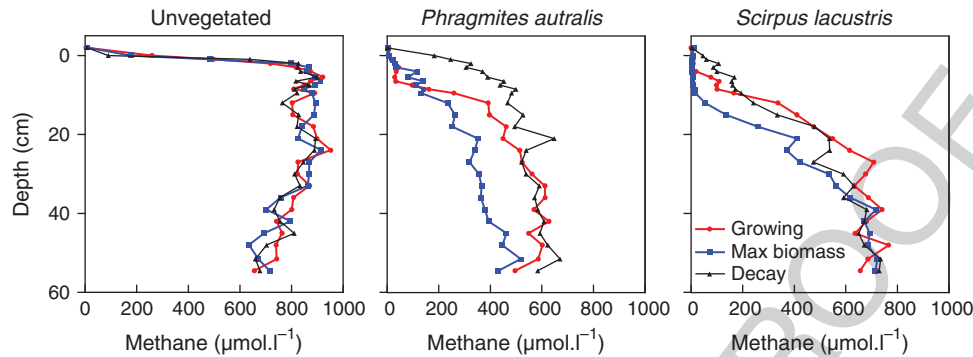


Figure 20 Effect of vegetation on depth distributions of dissolved CH_4 in freshwater marsh sediments. The profiles were obtained in constructed wetland mesocosms, which consisted of *Phragmites australis*, *Scirpus lacustris*, and an unvegetated control. Blue, red, and black symbols correspond to the growing, maximal biomass, and plant decay periods, respectively. Adapted from van der Nat, F.J.W.A., Middelburg, J.J., 1998a. Effect of two common macrophytes on methane dynamics in freshwater sediments. *Biogeochemistry* 43, 79–104.

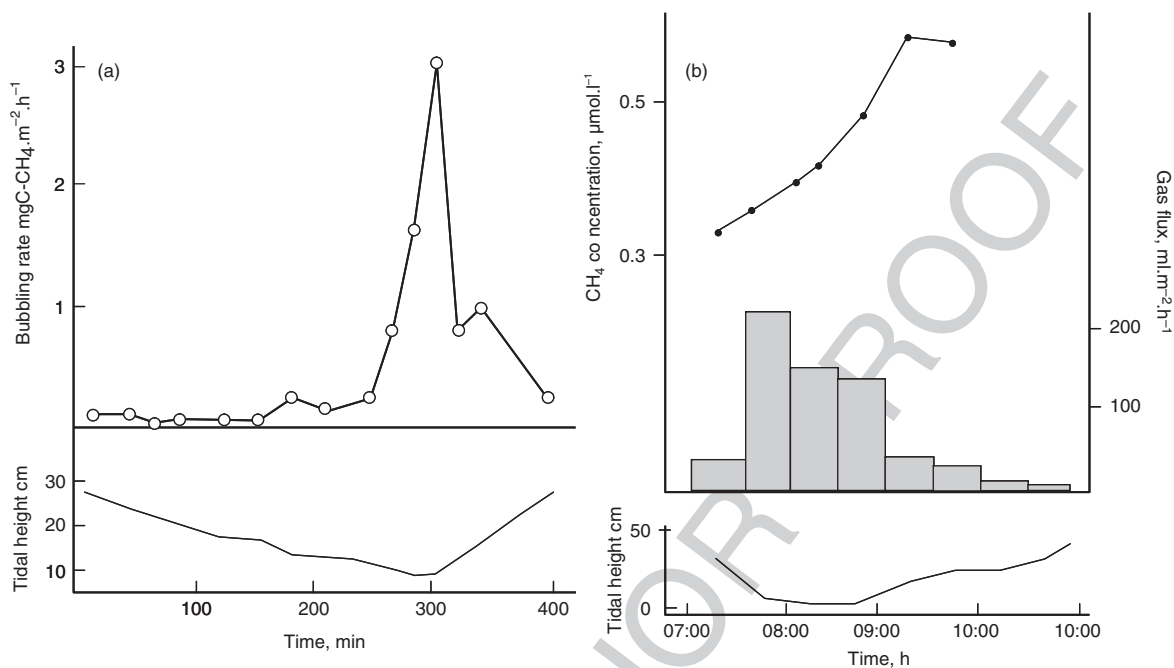
deeper in the sediments, where methanotrophs live near or even within the roots of macrophytes (Gerard and Chanton, 1993; King, 1994). As a major consequence, CH_4 is almost exclusively emitted by plant-mediated transport in vegetated sediment, and by ebullition in unvegetated, otherwise identical sediment. As in the case of rice paddies, it has been suggested that, in tidal marshes, plant-mediated CH_4 transport and CH_4 ebullition may be mutually exclusive processes (van der Nat and Middelburg, 1998a, 2000). Similarly, in mangrove sediments, the presence of aerial roots (pneumatophores) is believed to act as gas conduits for CH_4 to the atmosphere and as a source of oxygen to the sediment, and contribute to low CH_4 concentrations in the top layers of the sediments (Biswas et al., 2006). In two Tanzanian mangrove sites, Kristensen et al. (2008) observed a three- to fivefold enhancement of CH_4 sediment-atmosphere fluxes in the presence of pneumatophores, and estimated that transport through this pathway contributed between 38% and 64% of the total sediment-atmosphere CH_4 flux during low tide.

Ebullition of CH_4 occurs at sites where gas bubbles are present in the first 10–20 cm of the sediment. Ebullition of CH_4 has been reported and quantified in shallow estuarine systems such as the freshwater tidal flats and marshes, and in a saline coastal embayment (Martens and Klump, 1980; Chanton et al., 1986; Middelburg et al., 1996). Ebullition of CH_4 did not occur, for instance, in Tomales Bay where gas bubbles are found 1 m below the sediment-water interface (Sansone et al., 1998). Observed CH_4 ebullition is tightly coupled to the variation of the tidal height and occurs almost exclusively around low tide (Figure 21). This illustrates how hydrostatic pressure at high tide stabilizes gas bubbles in sediments. In deeper systems as, for instance, the Mariager fjord, occurrence of CH_4 ebullition has also been mentioned or observed visually, but has not been measured with bubble capture followed by gas analysis. During the travel in the water column, gas bubbles are affected by pressure changes and partly dissolve. In Cape Lookout Bight, where the water depth is about 8 m, Martens and Klump (1980) evaluated that 15% of the CH_4 contained in the rising bubbles dissolved in the water, the remaining part reaching the atmosphere. In summer, bubble dissolution was similar to sediment-water diffusion as source of CH_4 in the water column. In addition, as bubbles strongly disrupt the physical structure of sediments

when they are released, the surface area for diffusive exchange increases, and sediment-water CH_4 fluxes during high tide in the absence of ebullition were also enhanced. In nontidal systems, changes in atmospheric pressure may influence CH_4 ebullition as observed in freshwaters (Tokida et al., 2007).

The relative importance of diffusion, ebullition, and transport through plants has a major impact on the magnitude of the sediment-water or sediment-atmosphere CH_4 fluxes, because it strongly affects the efficiency of aerobic CH_4 oxidation. Indeed, a large fraction (often >90%) of the diffusive CH_4 fluxes from the sediments is oxidized at the sediment surface, where CH_4 meets oxygen (van der Nat and Middelburg, 1998b; Abril and Iversen, 2002). By contrast, almost all the bubbling CH_4 flux escapes oxidation (Martens and Klump, 1980). When CH_4 is preferentially transported through plants, oxidation is also favored in the plant rhizosphere, and reduces the flux by 5–60%, with a maximum efficiency during the plant-growing period (van der Nat and Middelburg, 1998b). However, in general, rhizospheric CH_4 oxidation is a stronger CH_4 sink than surface CH_4 oxidation, because transport through plants is more important than diffusion. Transport through plants greatly favors CH_4 fluxes in intertidal areas, where the vegetation is aerial. In the sub-tidal area of Tomales Bay, Sansone et al. (1998) reported benthic CH_4 fluxes to the water column 3 times greater inside an eelgrass bed than outside. It was not possible, however, to attribute this difference to CH_4 transport through the plants or to an enhanced methanogenesis and CH_4 diffusion due to the higher levels of organic matter content in the sediments. In general, in sub-tidal areas, sediment-water CH_4 fluxes show an extreme heterogeneity from one system to another, and within a given system (Table 6). Negative downward CH_4 fluxes have also been reported, and are due to intense CH_4 oxidation at the sediment surface (Sansone et al., 1998; Abril and Iversen, 2002).

The last important process for the transport of CH_4 from sediment to the water column and further to the atmosphere is tidal pumping, which consists in a lateral flux of CH_4 from the CH_4 -rich pore waters of intertidal sediments, to the water of creeks and channels, with the water movements due to the tide. This process that has been first described for reduced species other than CH_4 , is due to the loss and replacement of pore waters in intertidal sediments that are drained during ebb (Agosta, 1983). The tidal flushing of CH_4 and DIC from tidal



f0105 **Figure 21** The effect of tidal height on CH_4 ebullition in estuarine shallow waters. (a) freshwater marsh in the White Oak River estuary; (b) coastal marine bay of Cape Lookout Bight; the rise in near-bottom methane concentration due to bubble dissolution is also reported. Redrawn from Chanton, J.P., Martens, C.S., Kelley, C.A., 1989. Gas transport from methane-saturated, tidal freshwater and wetland sediments. *Limnology and Oceanography* 34, 807–819; Martens, C.S., Klump, J.V., 1980. Biogeochemical cycling in an organic-rich coastal marine basin – I. Methane sediment–water exchange processes. *Geochimica et Cosmochimica Acta* 44, 471–490.

t0030 **Table 6** Sediment–water CH_4 fluxes ($\text{mmol m}^{-2} \text{d}^{-1}$) and corresponding salinity in estuarine environments

	Sediment–water CH_4 flux ($\text{mmol m}^{-2} \text{d}^{-1}$)	Salinity	Comment	References
Cape Lookout Bight	14.1	30–35	Total	Martens and Klump (1980)
	2.3		Diffusive flux, yearly average. Benthic chambers nonbubbling periods (high tide)	
Tomales Bay	11.8 –0.0001 to +0.016	10–36	Ebullition (funnels) Seasonal range at three stations, benthic chambers	Sansone et al. (1998)
White Oak River estuary	0.021–0.050 17.1	0.2	Seasonal range at one stations, benthic chambers Sub-tidal station, yearly average, diffusive+ebullitive	Kelley et al (1990)
Randers Fjord (Denmark)	<0.24 –0.019 to –0.253*	18.9 3–7	Sub-tidal station, yearly average Seasonal range at one station, intact core incubation	Abril and Iversen (2002)
Yantze Estuary	0.003–0.4 0.0017–0.0022	17–23 3–6	Seasonal range at one station, intact core incubation Two stations at one season, intact core incubation	Zhang et al. (2008)

* Negative flux due to intense CH_4 oxidation at the sediment surface

marshes to adjacent waters has been evidenced by the temporal change of concentrations during tidal cycles at single-channel stations, a very clear maximum occurring at low tide, even in systems devoid of freshwater inputs (Bartlett et al., 1985; Borges et al., 2003; Neubauer and Anderson, 2003; Barnes et al., 2006; Bouillon et al., 2008; Grunwald et al., 2009; **Figure 22**). Kelley et al. (1995) evaluated that, in a freshwater tidal flat, the loss of CH_4 by horizontal transport by tidal pumping was 2–4 times higher than to the one by diffusion

from sediments to the atmosphere at low tide. In most environments where the intertidal/sub-tidal area is high, CH_4 temporal and spatial distribution in waters is almost exclusively driven by tidal pumping, which may constitute a major evasion pathway at the ecosystem scale (Bartlett et al., 1985; Middelburg et al., 2002; Grunwald et al., 2009).

Finally, geological CH_4 can be released to the water column and/or to the atmosphere through mud volcanoes, via ground-water input, or seeping at pockmarked structures. This has been

AU12

p0165

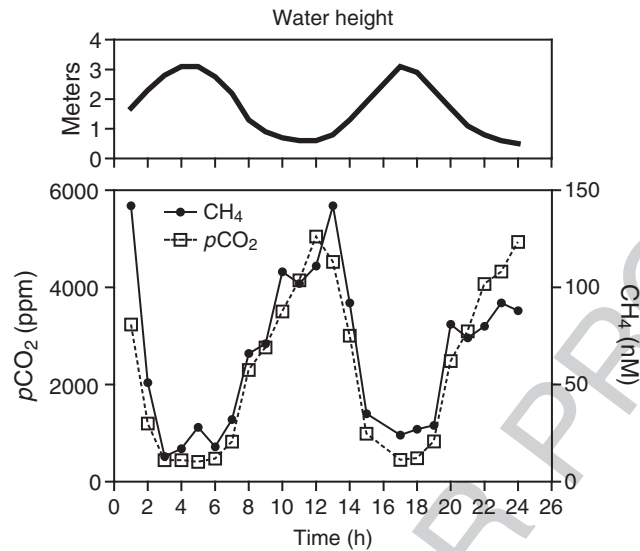


Figure 22 Temporal variation of the CH_4 concentration and partial pressure of CO_2 ($p\text{CO}_2$) in waters of a tidal creek connected to mangrove sediments, illustrating the tidal pumping effect. Adapted from Bouillon, S., Middelburg, J.J., Dehairs, F., Borges, A.V., Abril, G., Flindt, M.R., Ulomi, S., Kristensen, E., 2007c. Importance of intertidal sediment processes and porewater exchange on the water column biogeochemistry in a pristine mangrove creek (Ras Dege, Tanzania). *Biogeosciences* 4, 311–322.

reported in estuarine environments such as the Scheldt plume (Missiaen et al., 2002), the Ría of Vigo (García-Gil et al., 2002), the Firth of Forth (Judd et al., 2002), and the Saint Laurent (Dionne, 1973). However, these features are not specific to estuaries and are not directly related to estuarine biogeochemical C transformations and cycling. As these features are poorly documented, we will not discuss them further, and the related CH_4 fluxes will not be included in the overall evaluation of CH_4 fluxes from estuaries (Section 5.04.5).

5.04.3.3 Distribution and Fate of CH_4 in Estuarine Waters: Oxidation versus Degassing

Concentrations of CH_4 in estuarine waters vary over a wide range and are usually higher than the atmospheric equilibrium (Table 7). In mixed water columns, CH_4 concentrations range from few nmol l^{-1} to a maximum of $1 \mu\text{mol l}^{-1}$ and generally decrease seaward (De Angelis and Lilley, 1987; Scranton and McShane, 1991; De Angelis and Scranton, 1993; Jones and Amador, 1995; Bange et al., 1998; Sansone et al., 1998, 1999; Upstill-Goddard et al., 2000; Jayakumar et al., 2001; Abril and Iversen, 2002; Amouroux et al., 2002; Middelburg et al., 2002; Abril et al., 2007; Ferrón et al., 2007; Zhang et al., 2008; Grunwald et al., 2009). Concentrations of CH_4 in surface waters of estuaries result from the combination of lateral transport with water masses, inputs from sediments, oxidation in the water column, and evasion to the atmosphere, all these processes varying spatially and temporally. Consequently, the plots of CH_4 versus salinity are often nonlinear, but the processes responsible for changes in concentrations are not easy to indentify. The studies by Middelburg et al. (2002), and by Upstill-Goddard et al. (2000), which covered a large variety of European tidal estuaries revealed three major patterns of CH_4 concentrations along salinity gradients (Figure 23): (1) an increase in the very low salinity regions, which reveals the dominance of CH_4

production over CH_4 oxidation and degassing; in these regions, at the limit of the tidal influence, retention and processing of riverine labile material is probably favored (Abril et al., 2007); (2) more downstream in highly dynamic regions with salinities from 1 to 10, which generally coincide with the ETM, CH_4 can decrease very suddenly to values close to the atmospheric equilibrium, and remain very low, as the result of intense evasion and oxidation, and also probably lower accumulation of organic matter and methanogenesis in sediments, due to the strong hydrodynamics; and (3) at salinities around 25, CH_4 peaks were often observed, and were attributed to lateral inputs of CH_4 from tidal flats and marshes (Middelburg et al., 2002). This latter pattern, with highest concentrations at the mouth, was also very marked in the Hudson estuary (De Angelis and Scranton, 1993). It is also possible that lower oxidation and higher sedimentation of phytoplanktonic labile material occur in these areas immediately downstream of the ETM (De Angelis and Scranton, 1993; Abril et al., 2007). Stable isotopic ratios of CH_4 measured along estuarine gradients of six US–Pacific estuaries were consistent with the biogeochemical drivers of these three typical patterns (Sansone et al., 1999).

Together with gas evasion, aerobic oxidation is also a significant sink for CH_4 in estuarine waters. Aerobic CH_4 oxidation rates measured so far in estuarine and coastal waters vary between a maximum of $167 \text{ nmol l}^{-1} \text{ d}^{-1}$ in the freshwater region of the Hudson estuary during summer (De Angelis and Scranton, 1993), to a minimum of $2.3 \times 10^{-4} \text{ nmol l}^{-1} \text{ d}^{-1}$ in the Rhine Plume in the North Sea (Scranton and McShane, 1991), with intermediate values of $6 \text{ nmol l}^{-1} \text{ d}^{-1}$ in the Mariager Fjord (Fenchel et al., 1995). This corresponds to specific oxidation rates between 8.10^{-5} and 0.7 d^{-1} . Using the more sensitive ^{14}C method, De Angelis and Scranton (1993) found that CH_4 oxidation in waters of the Hudson estuary could turnover the CH_4 pool in 1.4–9 days, but only at salinities below 6; CH_4 oxidation rates at higher salinities being

Table 7 Concentrations of CH₄ in surface waters (nmol l⁻¹ and % saturation) and water-air CH₄ fluxes (mmol m⁻² d⁻¹) in estuarine environments

Sites	Range of CH ₄ concentrations in water		CH ₄ flux (mmol m ⁻² d ⁻¹)	Comments/method	References
	nmol l ⁻¹	% saturation			
<i>Inner estuaries main channel</i>					
Yaquina Salmon and Alsea (US-Oregon)	5.7–697	3–290	0.18	Annual average	De Angelis and Lilley (1987)
Hudson (US–New York)	50–940	21–390	0.35	Annual average	De Angelis and Scranton (1993)
Bodden (Germany)	2.4–370	1–155	0.03–0.21	Annual average, spatial range	Bange et al. (1998)
Tomales Bay (US–California)	8–100	3–41	0.007–0.01	Seasonal range, spatial average	Sansone et al. (1998)
Nine European tidal estuaries	2–3600	0.7–1500	0.13	Median all estuaries, 18 cruises, salinity 0 – 33	Middelburg et al. (2002)
Tyne Estuary (UK–North Sea)	13–654	4.5–200	–	One cruise in January 1996	Upstill-Goddard et al. (2000)
Humber Estuary (UK–North Sea)	13–667	3.7–210	–	Five cruises in 1996	Upstill-Goddard et al. (2000)
Randers Fjord estuary (Denmark)	41–420	17–175	0.07–0.41	Annual average, spatial range	Abril and Iversen (2002)
Pulicat Lake estuary (SE India)	94–500	40–213	0.054–0.28	Spatial range in December 2000, calculated water–air flux	Shalini et al. (2006)
Temmesjoki estuary (Finland, Gulf of Botnia)	240–506	102–211	–	Seasonal range, eutrophic estuary	Silvennoinen et al. (2008)
Rio San Pedro, Bay of Cadiz (Spain)	12–87	5.1–50	0.034–0.15	Seasonal range, high salinity estuary	Ferrón et al. (2007)
Adyar River estuary (SE India)	5–6500	2–2700	0.04–114	Spatial and seasonal range, estuary affected by sewage	Nirmal Rajkumar et al. (2008)
Yantze (China)	13–27	5.2–12.8	0.035–0.114	Seasonal range in the region with salinity < 30, mean of 3 gas transfer velocity parameterization	Zhang et al. (2008)
Weser River and Wadden Sea (Germany)	40–1860	22–819	–	Small estuary discharging in a high salinity, tidal flat dominated system	Grunwald et al. (2009)
<i>Estuarine plumes</i>					
Rhine and Scheidt (Southern North Sea)	2.5–370	1–148	0.006–0.6	Spatial range in March 1989	Scranton and McShane (1991)
Orinoco River plume	3.2–176	1.7–87	–	Spatial and temporal range, two cruises, April and October 1988	Jones and Amador (1995)
Amvrakikos bay (Aegean Sea)	11 ± 4	5.2 ± 1.8	0.014	Spatial average in July 1993	Bange et al. (1996)
Danube (Northwestern Black Sea)	131 ± 42	52 ± 17	0.26–0.47	Spatial range in July 1995	Amouroux et al. (2002)
Yantze (China)	3.5–7.1	1.6–3.5	0.006–0.025	Seasonal range in the region with salinity > 30	Zhang et al. (2008)

<i>Stratified fjords and lagoons with anoxic deep waters</i>								
Framvaren Fjord (North Sea)	330	136						Lindstrom (1983)
	20 000	8 700						
Marjaer Fjord (Denmark, Kattegat)	500–900	200–360	0.2–4.9					Fenchel et al. (1995)
	> 30 000	>12 000	-					
Aby-Tendo Lagoons (Ivory Coast)	200–700	71–250	0.8–1.5					Koné et al. (2010)
	13 000 – 31 000	4 640–11 070	-					
<i>Stratified fjords without anoxic deep waters</i>								
Hornsundfjord, Spitsbergen, Norway	19–26	5–7						Damm et al. (2005)
Miljefjord, Spitsbergen, Norway	10–32	3–8						Damm et al. (2005)
<i>Tidal marsh creeks</i>								
Bay Tree Creek Salt Marsh (Virginia)	33–950	13–395	0.17					Bartlett et al. (1985)
<i>Mangrove creeks</i>								
Mtoni (Tanzania)	105–190	43–80	0.09–0.330					Kristensen et al. (2008)
Wright Myo mangrove creek	282–704	115–290	0.4–0.8					Barnes et al. (2006)
Hoogly estuary/Sundarban (Bay of Bengal, India)	11–129	4.6–54	0.002–0.134					Biswas et al. (2007)
Ras Dege (Tanzania)	13–142	5–60	0–0.185					Bouillon et al. (2007c)

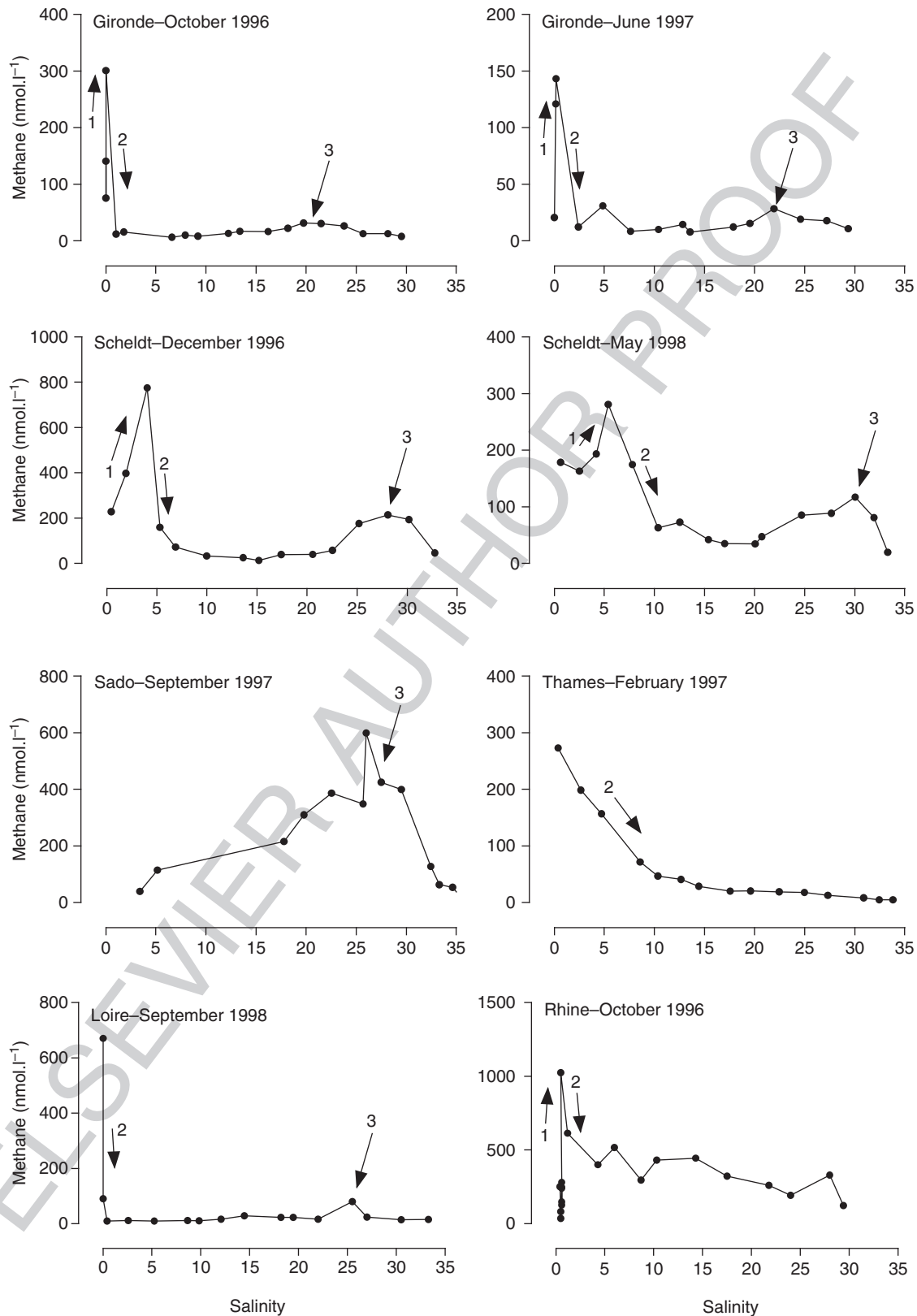


Figure 23 Distribution of CH_4 versus salinity observed in some European tidal estuaries (Middelburg et al., 2002), with three typical patterns: (1) increase at low salinity where CH_4 production fueled by sedimentation of riverine labile material is higher than CH_4 oxidation and degassing; (2) decrease at salinities 1–10 generally associated with the turbidity maximum, due to intense evasion and oxidation, and lower accumulation of organic matter and methanogenesis in sediments, due to strong currents; and (3) increase due to lateral inputs from tidal flats and marshes.

one to two orders of magnitude lower. Adding salt and filtered seawater to the freshwater samples resulted in a strong inhibition of CH_4 oxidation. In the Columbia River estuary, similar oxidation rates were measured by Lilley et al. (1996), consistent with a net shift in $\delta^{13}\text{C}\text{-CH}_4$ at low to intermediate salinities (Sansone et al., 1999). In the Orinoco River plume, CH_4 oxidation was also very variable and the turnover time of CH_4 in the water column relative to oxidation ranged from 2 days to 3.8 years, for CH_4 concentrations of 168 and 68 nmol l^{-1} , respectively (Jones and Amador, 1995). In the low salinity (3–7) region of the Randers Fjord, a microtidal and shallow estuary in Denmark, Abril and Iversen (2002) observed intense CH_4 oxidation at the sediment surface, which resulted in a net uptake of CH_4 from the water by the estuarine sediment (downward CH_4 flux through the sediment–water interface). These authors could not detect any methanotrophic activity at ambient CH_4 concentrations in sediments at salinities 17–23. The sensitivity of methanotrophs to salinity was also observed in hypersaline microbial mats (salinity 90–130), where no CH_4 oxidation activity could be detected even in the presence of oxygen and CH_4 at high concentrations (Conrad et al., 1995). In addition to salinity, suspended matter is another important environmental factor that controls CH_4 oxidation in estuarine waters. Abril et al. (2007) have documented a strong enhancement of CH_4 oxidation in an ETM, leading occasionally to CH_4 concentrations below the atmospheric equilibrium. As the ETM and low salinity coincide geographically, CH_4 oxidation is particularly significant in these regions, and probably accounts for most of the decline (i.e., second pattern in Figure 23). However, more investigations are necessary regarding the microbial ecology in estuaries of methanotrophic bacterial communities, where diversity appears particularly significant (McDonald et al., 2005).

In contrast to tidal and well-mixed estuaries in stratified systems with anoxic deep waters, such as fjords and some lagoons, CH_4 builds up in bottom waters where it can reach concentrations of 30 $\mu\text{mol l}^{-1}$ (Table 7). The thermohaline stratification favors CH_4 oxidation in the water column, and is believed to limit efficiently the CH_4 diffusion to the surface waters and the atmosphere (Lindstrom, 1983; Fenchel et al., 1995). Oxidation of CH_4 occurs in these stratified waters in both oxic and anoxic conditions. In Mariager Fjord, 66% of the CH_4 oxidation was aerobic and occurred just above the oxycline (Fenchel et al., 1995). In Framvaren Fjord, high anaerobic CH_4 oxidation rates were observed in deepest waters, 20 m above the sediment surface, and were 5 times higher than aerobic CH_4 oxidation rates observed above the oxycline at a depth of 20 m. The CH_4 vertical profiles in the water column of two permanently stratified lagoons in Ivory Coast also suggest an efficient CH_4 oxidation above the oxycline (Koné et al., 2010). Despite intense CH_4 oxidation, surface concentrations and diffusive fluxes to the atmosphere are relatively high in these stratified systems (Table 7). In deep systems, dissolution of CH_4 bubbles is generally much stronger than in shallow systems, and up to 100% of the CH_4 bubbles released from the sediment can be dissolved when the water depth exceeds 80 m (McGinnis et al., 2006). This could be an important mechanism for CH_4 to reach the surface waters, and then the atmosphere by diffusion, thus escaping oxidation at the oxycline. It is important to note that Arctic stratified fjords do have anoxic bottom waters, and have lower CH_4 concentrations in

both bottom and surface waters than fjords with anoxic bottom waters (Damm et al., 2005; Table 7).

The contribution of microbial oxidation and atmospheric emission as sinks for dissolved CH_4 is thus extremely variable in estuaries. The percentage of CH_4 oxidized (relative to the sum of evasion and oxidation) was 20% in the Columbia River estuary (Lilley et al., 1996), 10% in the stratified Mariager Fjord (Fenchel et al., 1995), 27% in the Cape Lookout Bight (Sansone and Martens, 1978; Martens and Klump, 1980), from 3% to 70% in the Hudson estuary (De Angelis and Scranton, 1993), and from 24% to 55% in the low salinity regions of the Randers Fjord estuary (Abril and Iversen, 2002). Wind speed has a multiplicative effect on this ratio: at low wind speeds, CH_4 builds up in the water, enhancing microbial oxidation (typically, a first-order process), whereas at high wind speeds, CH_4 is stripped out from the water to the atmosphere, decreasing water concentrations, and inhibiting CH_4 oxidation.

5.04.4 Gas Transfer Velocities of CO_2 and CH_4 in Estuarine Environments: Multiple Drivers and A Large Source of Uncertainty in Flux Evaluations

The gas transfer velocity of CO_2 and CH_4 at the water–air interface (k) depends on turbulence at the aqueous boundary layer. In lakes and in the ocean, wind is the major forcing factor generating turbulence, and k is often parametrized as a function of wind speed at 10 m height (e.g., Wanninkhof, 1992). In streams, turbulence in the aqueous boundary layer is mostly generated by the friction of water flow at the bottom, and k depends on water current velocity, water depth, and bed roughness (O'Connor and Dobbins, 1958; Wanninkhof et al., 1990). Estuaries, and particularly macrotidal estuaries, are unique environments where turbulence is simultaneously generated by wind forcing and boundary friction due to tidal currents at the surface and at the bottom (Zappa et al., 2003, 2007; Borges et al., 2004a, 2004b; Upstill-Goddard, 2006; Abril et al., 2009).

Figure 24 shows how k varies with wind speed across various aquatic environments. In small rivers and streams, the

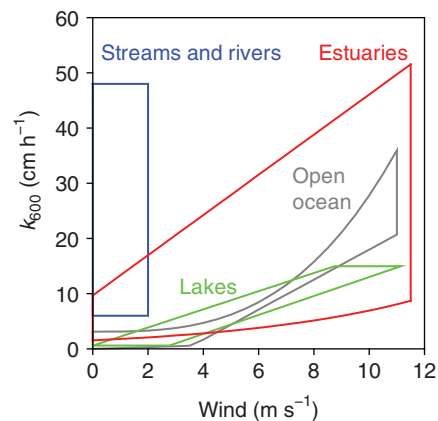


Figure 24 Distribution of the gas transfer velocity (k_{600}) in freshwater, estuarine, and oceanic environments as a function of wind speed. The polygons enclose the maximum and minimal values of k_{600} in streams and rivers (based on Wanninkhof et al. (1990)), lakes (based on Frost and Upstill-Goddard (2002)), oceans (based on Liss and Merlivat (1986) and Wanninkhof and McGillis (1999)), and estuaries (based on Kremer et al. (2003a) and Borges et al. (2004a)).

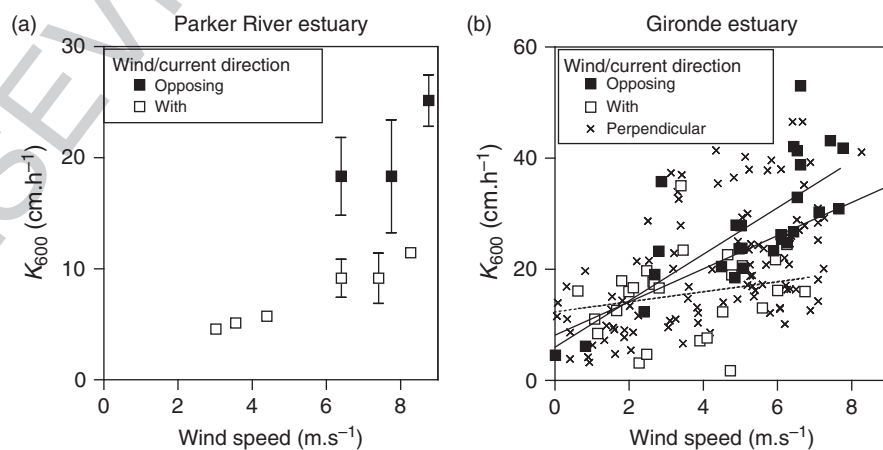
effect of wind speed is limited and the large variability in k values is related to variable depth and water currents (Wanninkhof et al., 1990). Lakes and open ocean show lower scatter in k values as a function of wind speed compared to the other aquatic systems, with k values at high wind speeds higher in the open ocean than in lakes due to fetch limitation in lakes. Estuaries show the largest range of variability in k values as a function of wind speed. As discussed hereafter, this is related to strong fetch limitation in small estuaries (lower boundary), and enhancement of k by tidal currents in macrotidal estuaries (higher boundary). In estuaries, k is further modulated by the interactions between wind and currents (enhancement of turbulence when wind and currents are in opposed directions), and by the dampening of water turbulence by suspended solids at high concentrations.

p0200 To date, there is no method totally satisfactory to quantify k in estuaries, and this question is still a matter of debate between biogeochemists, ecologists and physicists. Although nonintrusive methods such as tracer or micrometeorological techniques should in theory be preferred, their applications in estuarine systems are difficult and scarce (Clark et al., 1994; Carini et al., 1996; Zappa et al., 2003, 2007; Zemmeling et al., 2009), and most of the k parametrizations published so far were derived from floating chamber measurements (Marino and Howarth, 1993; Kremer et al., 2003a, 2003b; Borges et al., 2004a, 2004b; Guérin et al., 2007; Abril et al., 2009). Floating chamber experiments indeed offer the advantage of being easy and cheap, and, most importantly, to be short enough (5–20 min when using infrared gas analyzers) to adequately describe the temporal variability of k driven by wind and current in estuaries. By contrast, tracer methods only provide k -integrated values generally averaged over several tidal cycles. Micrometeorological methods might be affected by surrounding land, and data must be carefully analyzed in terms of wind direction and footprint of measurements. The use of the floating chamber method in estuaries has been criticized by several authors (e.g., Raymond and Cole, 2001), one major critique being that the chamber eliminates wind stress.

However, the fact that turbulence in the aqueous boundary layer, rather than that in the atmospheric boundary layer, is predominant in determining k , and that several experiments with chambers (Kremer et al., 2003b) still support the use of chambers in certain conditions: a chamber that moves relatively to the surface water would disrupt the aqueous boundary layer and artificially enhance gas exchange. Although in environments with low water current but high wind, it is preferable to anchor the chamber to avoid its movement due to the wind, in macrotidal estuaries where water currents can reach values of 2 m s^{-1} , measurements must be made while drifting with the water mass (Frankignoulle et al., 1996; Borges et al., 2004a, 2004b). In the case of tidal estuaries, the use of floating chambers takes advantage of the large $p\text{CO}_2$ gradient between water and air, and of high turbulence in the water generated by both wind and current (Borges et al., 2004a, 2004b; Abril et al., 2009).

Results from floating chamber measurements published so far reveal that k increases significantly with wind speed in estuaries, but the k values versus wind speed show significant scatter (Borges et al., 2004a; Abril et al., 2009); also, with the exception of quiescent embayments (Kremer et al., 2003a), k in estuaries at a given wind speed is generally higher than in oceans or lakes because water current also contributes to k and to its variability (Marino and Howarth, 1993; Zappa et al., 2003; Borges et al., 2004a, 2004b; Abril et al., 2009; Figure 24). When the water current is directed against wind speed, k can be enhanced by a factor of 2, in comparison with situations when wind and current flow in the same direction (Zappa et al., 2007; Abril et al., 2009; Figure 25). When currents are moving against the wind, short waves and microbreaking can emerge, resulting temporarily in much greater k values. Experiments performed with micrometeorological techniques have confirmed these findings based on floating chambers (Zappa et al., 2003, 2007).

When averaged over the tidal cycle and integrating all wind directions, the effect of water currents modulates the value of the y -intercept of the k versus wind speed linear relationship rather than its slope (Borges et al., 2004a; Abril et al., 2009).



f0125 **Figure 25** (a) k_{600} versus wind speed in the Parker River estuary and (b) k_{600} vs. wind speed in the Gironde estuary. At both sites and with both techniques, an enhancement is observed when wind and current flow in the opposite direction. (a) Micro-meteorological data, redrawn from Zappa, C.J., McGillis, W.R., Raymond, P.A., Edson, E.J.B., Hinst, E.J., Zemmeling, H.J., Dacey, J.W.H., Ho, D.T., 2007. Environmental turbulent mixing controls on air–water gas exchange in marine and aquatic systems. *Geophysical Research Letters* 34, GLXXX. doi:10.29/2006GL028790. (b) Chamber data, redrawn from Abril, G., Commarieu, M.V., Sottolichio, A., Bretel, P., Guérin, F., 2009. Turbidity limits gas exchange in a large macrotidal estuary. *Estuarine, Coastal and Shelf Science* 83, 342–348.

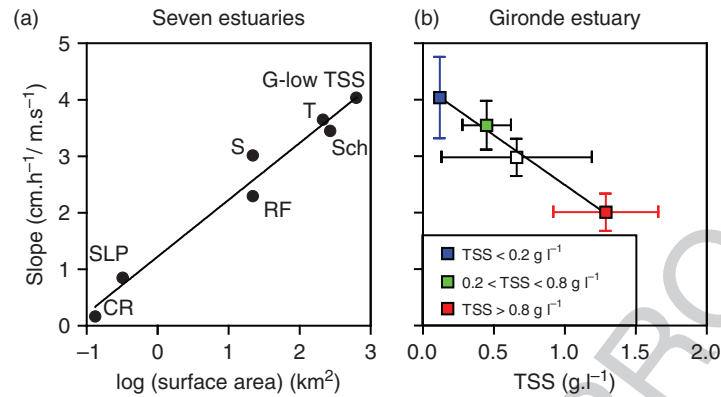


Figure 26 (a) Relationship between the slope of the k_{600} versus wind speed linear regression and the estuarine surface area in seven estuaries: SLP = Sage Lot Pond (Massachusetts, USA) and CR = Childs River (Massachusetts, USA), data from Kremer et al. (2003a); RF = Randers Fjord (Denmark), T = Thames (U.K.) and Sch = Scheldt (Belgium/the Netherlands), data from Borges et al. (2004a); S = Sinnamary (French Guiana), data from Guérin et al. (2007); G-low TSS = Gironde at $\text{TSS} < 0.2 \text{ g.l}^{-1}$, data from Abril et al. (2009). The equation of the regression line in panel (a) is $\text{slope} = 1.00 (\pm 0.08)$. $\text{LOG (surface area)} + 1.23 (\pm 0.14)$ ($r^2 = 0.971$, $p < 0.0001$); (b) Relationship between the slope of the k_{600} versus wind speed linear regression and TSS concentration in the Gironde estuary. The colored symbols correspond to three selected TSS ranges ($\text{TSS} < 0.2 \text{ g.l}^{-1}$; $0.2 < \text{TSS} < 0.8 \text{ g.l}^{-1}$ and $\text{TSS} > 0.8 \text{ g.l}^{-1}$). The open symbol corresponds to the entire data set. Error bars on the TSS values are the standard deviation of the data; error bars on the slope are the 95% confidence intervals around the slope of the linear regression. The equation of the regression line in panel (b) is $\text{slope} = 4.25 (\pm 0.19) - 1.76 (\pm 0.12) \text{TSS}$ ($r^2 = 0.99$, $p < 0.01$, $n = 4$). Redrawn from Abril et al. (2009).

The analysis of k and wind speed data sets from different estuaries revealed that k increases faster with wind speed in large estuaries than in small estuaries due to the fetch limitation effect in smaller estuaries (Borges et al., 2004a; Guérin et al., 2007; Abril et al., 2009; Figure 26(a)). The k -wind speed relationships are thus site specific and a simple linear model appears most appropriate, in which the y -intercept is influenced by the water current and the slope is influenced by the surface area of the estuary (Borges et al., 2004a; Abril et al., 2009). In addition, it has been recently demonstrated that the presence of suspended material in large concentrations ($\text{TSS} > 0.2 \text{ g.l}^{-1}$) had a significant role in attenuating turbulence and, therefore, k . Indeed, in the large and highly turbid Gironde estuary, k was on average significantly lower than in other large estuaries, and decreased linearly with TSS concentrations (Abril et al., 2009; Figure 26(b)). Turbidity can limit k through two processes: first, the formation of vertical density gradients due to TSS stratification in the water column, leading to a limitation of turbulence in the surface layer in the same way as stratification is related to salinity or temperature (Geyer, 1993; Dyer et al., 2004); second, the presence of suspended particles enhances the viscous dissipation of turbulent kinetic energy as flocs are disrupted, or when they collide, interact, and exchange momentum (Dyer et al., 2004). Abril et al. (2009) proposed a generic, empirical equation for all estuaries that parametrizes k as a function of water current velocity, wind speed, estuarine surface area, and the TSS concentration:

$$k_{600} = 1.80e^{-0.0165\nu} + [1.23 + 1.00\text{LOG}(S)] \cdot [1 - 0.44\text{TSS}]U_{10}$$

where k_{600} is the gas transfer velocity normalized to a Schmidt number of 600 in cm.h^{-1} , ν is the water current velocity in m.s^{-1} , S is the surface area of the estuary in km^2 , TSS is the concentration of total suspended solids in g.l^{-1} , and U_{10} is the wind speed at 10 m height in m.s^{-1} .

This equation needs, however, to be verified and improved in the near future for several reasons: (1) it is based exclusively on

floating chamber measurements; micrometeorological measurements are promising in estuaries and capture the short-term variations in k (Zappa et al., 2003, 2007); they should be repeated in different types of estuaries and compared with floating chambers; and (2) there might be differences between sites for the turbidity effect, due to the nature of the suspended particles, their grain size, and their organic content. It is also important to note that this empirical equation has been validated for estuaries with surface areas less than 500 km^2 . It is very unlikely that the slope of the equation (Figure 26(a)) will continue to increase in estuaries with much larger surface areas and different morphologies, especially in microtidal areas where the combined effects of wind and water current are not as effective.

5.04.5 Significance of CO_2 and CH_4 Emission from Estuaries in the Global Carbon Cycle

s0060

We used the estuarine typology given by Dürr et al. (2010) and Laruelle et al. (2010) to scale air-water CO_2 fluxes in estuarine environments. Fjords and fjärds (type IV) are the most extensive estuarine types (~43% of the total surface area and 26% of the worldwide exorheic coast line). They are dominant at latitudes north of 45°N (Scandinavia, Canada, and Alaska) and south of 45°S (southern Chile) (Figure 27). Tidal systems (type II) and lagoons (type III) are the second and third most abundant estuarine types (~26% and 24% of the total surface area, respectively). While no clear spatial pattern is apparent for tidal systems (type II), lagoons (type III) are dominant in the tropics and subtropics of the Northern Hemisphere ($0^\circ - 45^\circ \text{N}$). Small deltas (type I) that represent ~8% of the total surface area do not show a clear latitudinal pattern. Based on this typology, the total surface area of estuaries is $1.1 \times 10^6 \text{ km}^2$ and ~81% is located in the Northern Hemisphere, with ~58% north of 45°N .

AU14

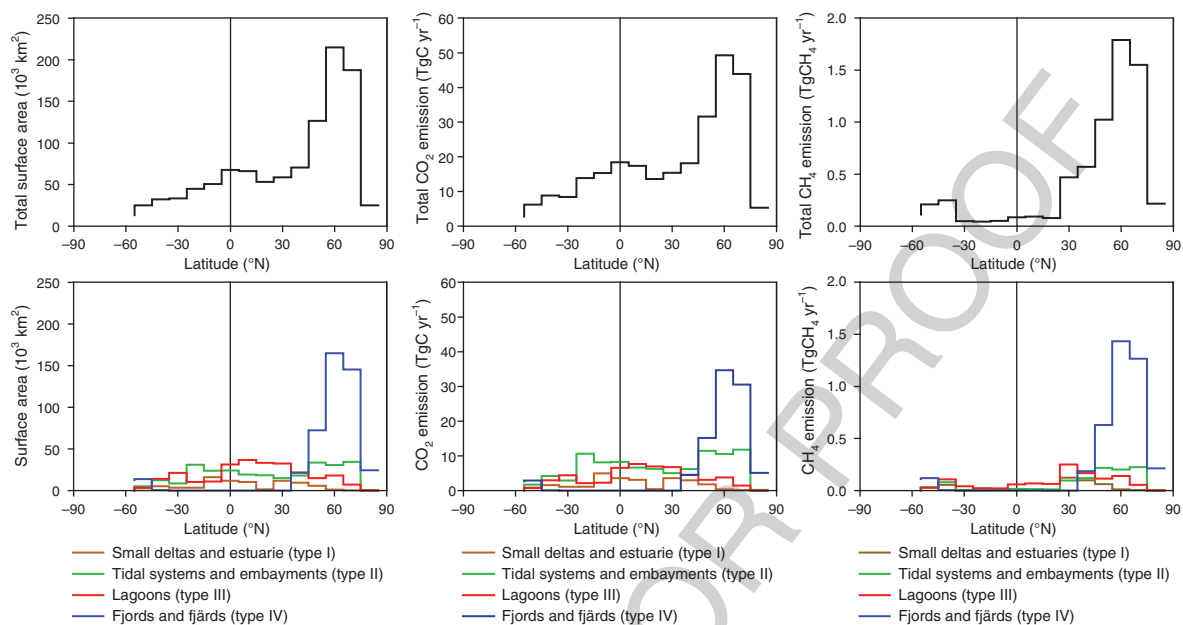


Figure 27 Latitudinal distribution of surface area of estuaries (total and by types; Dürr et al., 2010) and of the scaled emissions to the atmosphere by estuaries of CO₂ (TgC yr⁻¹) and CH₄ (TgCH₄ yr⁻¹) (total and by types, **Table 8**). Adapted from Laruelle et al. (2010).

Table 8 Average surface areas of estuarine types based on the typology of Dürr et al. (2010), average (\pm standard deviation) of air–water CO₂ fluxes (in mol C m⁻² yr⁻¹) based on the data compilation given in **Table 2**, and integrated air–water CO₂ fluxes (in PgC yr⁻¹; adapted from Laruelle et al. 2010), and average CH₄ fluxes (in mmol C m⁻² yr⁻¹) based on the data compilation given in **Tables 5** and **7**, and integrated atmospheric CH₄ fluxes (TgCH₄ yr⁻¹) using the relative surface areas of subsystems given in **Table 10**

	Surface area (10 ⁶ km ²)	Air–water CO ₂ flux		Air–water CH ₄ flux	
		(mol C m ⁻² yr ⁻¹)	(PgC yr ⁻¹)	(mmol C m ⁻² yr ⁻¹)	(TgCH ₄ yr ⁻¹)
Small deltas and estuaries (type I)	0.084	25.7 \pm 15.8	0.026 \pm 0.016	317	0.42
Tidal systems and embayments (type II)	0.276	28.5 \pm 24.9	0.094 \pm 0.082	243	1.07
Lagoons (type III)	0.252	17.3 \pm 16.6	0.052 \pm 0.050	278	1.14
Fjords and fjärds (type IV)	0.456	17.5 \pm 14.0*	0.096 \pm 0.077	544	3.96
Total	1.067	21.0 \pm 17.6	0.268 \pm 0.225	385	6.60

* The standard deviation was estimated as $\pm 80\%$ based on the values of the other three types.

As it not possible to evaluate the uncertainty of the individual air–water CO₂ fluxes given by the different studies, the standard deviations of the means for each estuarine type were propagated to provide an estimate of the uncertainty on the scaled fluxes that mainly reflects the site-to-site variability rather than absolute uncertainty.

Air–water CO₂ fluxes were averaged for each estuarine type, and scaled globally using the respective surface area (**Table 8**). The emission of CO₂ to the atmosphere from estuarine environments shows two maxima, one at the equator and another at $\sim 65^\circ$ N (**Figure 27**). The maximum of CO₂ emission at the equator corresponds to a small peak in surface area (associated to types II and III with high air–water CO₂ fluxes). The maximum of CO₂ emission at $\sim 65^\circ$ N corresponds to a large peak in surface area (associated to type IV with lower air–water CO₂ flux). The overall emission of CO₂ to the atmosphere from estuaries is estimated at 0.27 PgC yr⁻¹. Tidal systems (type II) and fjords and fjärds (type IV) contribute equally ($\sim 35\%$) to the global estuarine CO₂ emission, while lagoons (type III) and small deltas (type I) contribute 20% and 10% to the global estuarine CO₂ emission, respectively. About 79% of the total CO₂ emission to the atmosphere from estuaries occurs in the Northern

Hemisphere. The contribution to the total CO₂ emission by estuaries by climatic zone is similar: 32% for tropical systems (between 25° N and 25° S), 31% for temperate systems (35° N– 55° N; 35° S– 55° S), and 37% for high latitude systems ($>65^\circ$ N).

The emission of CO₂ from estuarine environments of 0.27 \pm 0.23 PgC yr⁻¹ based on the typology of estuarine environments of Dürr et al. (2010) and Laruelle et al. (2010) is lower than previous estimates ranging between 0.36 and 0.60 PgC yr⁻¹ (Abril and Borges, 2004; Borges, 2005; Borges et al., 2005; Chen and Borges, 2009) (**Table 9**). This is due to the fact that previous global scaling attempts of the CO₂ emission from estuaries used the average of air–water CO₂ fluxes across estuarine types, and due to smaller (older) data sets possibly biased towards tidal European (often polluted) systems. Hence, the average air–water CO₂ fluxes used for scaling ranged between 32.1 and 38.2 mol C m⁻² yr⁻¹ (**Table 9**) higher than the global

0045 **Table 9** Comparison of published global CO₂ fluxes and emissions to the atmosphere from estuaries

CO ₂ flux (mol C m ⁻² yr ⁻¹)	Emission of CO ₂ (PgC yr ⁻¹)	Surface area (10 ⁶ km ²)	References
36.5	0.60	1.40 ^a	Abril and Borges (2004)
38.2	0.43	0.94 ^b	Borges (2005)
28.6	0.32	0.94 ^b	Borges et al. (2005)
32.1	0.36	0.94 ^b	Chen and Borges (2009)
21.0	0.27	1.10 ^c	This study

^a Based on Woodwell, G.M., Rich, P.H., Hall, C.A.S., 1973. Carbon in estuaries. In: Woodwell, G.M., Pecan, E.V. (Eds.), Carbon and the Biosphere. Technical Information Center, U.S. Atomic Energy Commission; National Technical Information Service, Springfield, VA, pp. 221–240. including intertidal areas.

^b Based on Woodwell, G.M., Rich, P.H., Hall, C.A.S., 1973. Carbon in estuaries. In: Woodwell, G.M., Pecan, E.V. (Eds.), Carbon and the Biosphere. Technical Information Center, U.S. Atomic Energy Commission; National Technical Information Service, Springfield, VA, pp. 221–240. excluding intertidal areas.

^c Based on Dürr H.H., G.G. Laruelle, C.M. van Kempen, C.P. Slomp, M. Meybeck and H. Middelkoop (2010) World-wide typology of near-shore coastal systems: defining the estuarine filter of river inputs to the oceans, Estuaries and Coasts, submitted.

average value of 21.0 ± 17.6 C mol m⁻²yr⁻¹ given in **Table 8** that takes into account the relative surface area of different estuarine types. Further, the global surface area of estuarine environments based on the typology of Dürr et al. (2010) and Laruelle et al. (2010) of ~1.1 10⁶ km² is lower than the value of 1.4 × 10⁶ km² given by Woodwell et al. (1973) used by Abril and Borges (2004). The scaling of estuarine CO₂ emissions of Borges (2005), Borges et al. (2005), and Chen and Borges (2009) was based on a global estuarine surface area of 0.94 × 10⁶ km², also based on the values given by Woodwell et al. (1973) but excluding intertidal areas associated to marshes and mangroves (**Table 9**).

0235 The emission of CO₂ from estuaries is a nonnegligible component of the global C cycle (**Figure 28**). The emission of CO₂ from estuaries is equivalent to the emission of CO₂ from lakes and rivers, respectively, 0.11 and 0.23 PgCyr⁻¹. The emission of CO₂ from estuaries corresponds to ~100% and 19% of the sink of CO₂ related to the shelf seas and the open ocean, respectively, for a surface area one order of magnitude lower (0.3%, 7.0%, and 63.0% of the Earth's surface for estuaries, shelf seas, and open ocean, respectively). Finally, the emission of CO₂ from estuaries compares to the flux of total organic carbon (TOC) from rivers to estuaries of 0.38 PgCyr⁻¹. Assuming the degradation of 50% of particulate organic carbon (POC) (Abril et al., 2002) and 25% of DOC (Moran et al., 1999; Raymond and Bauer, 2000; Wiegner and Seitzinger, 2001; del Giorgio and Davis, 2003; 00503) during estuarine transit, the potential emission of CO₂ from the degradation of riverine TOC would be ~0.14 PgC yr⁻¹ based on the DOC and POC fluxes reported by Ludwig et al. (1996). This rough estimate compares well with the emission of CO₂ estimated by scaling air–water CO₂ flux values, considering uncertainties on estimates of air–water CO₂ fluxes and estuarine surface area and on organic matter fluxes from rivers and organic matter removal during estuarine transit (e.g., 00502 and 00503). Based on the POC flux from rivers to estuaries of 0.50 PgCyr⁻¹ suggested by Richey (2004) and a removal of 70% of POC during estuarine transit (Keil et al., 1997), it would set the potential emission of CO₂ from the degradation of riverine TOC to 0.40 PgCyr⁻¹. This confirms that the net heterotrophy of estuarine ecosystems strongly contributes to their emission of CO₂ to the atmosphere. However, considering the diversity of C cycling across systems and uncertainties in

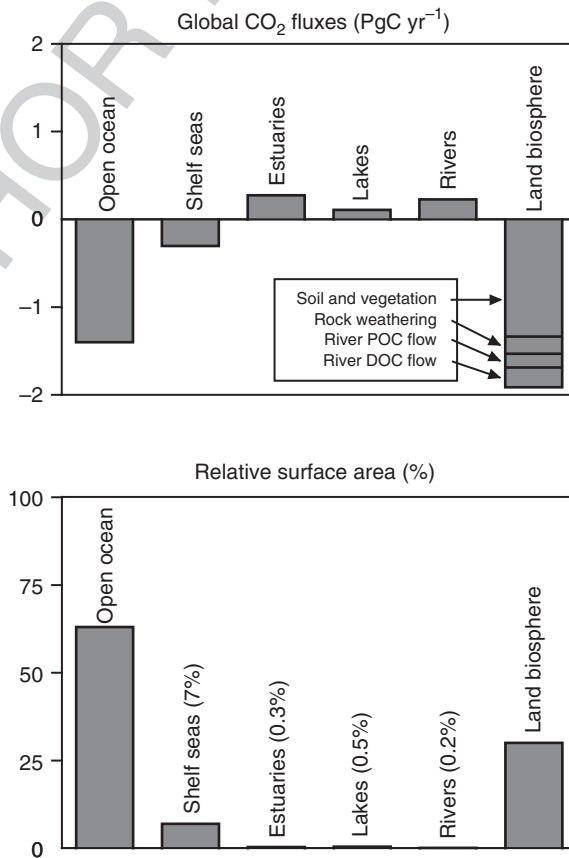


Figure 28 Global CO₂ exchanges with the atmosphere (PgCyr⁻¹) in the f0140 open ocean (Takahashi et al., 2009a, 2009b), continental shelf seas (Chen and Borges, 2009), estuaries (**Table 8**), rivers, and lakes (Cole et al., 2007), and land biosphere (vegetation and soils (Cole et al., 2007), rock weathering (Ludwig et al., 1996), the export of DOC and POC by rivers from land to ocean (Ludwig et al., 1996)), and the relative surface area of continental-shelf seas (Walsh, 1988), estuaries (Woodwell et al., 1973), and rivers, and lakes (Lehner and Döll, 2004). Note that the export of DOC and POC by rivers from land to ocean is a sink of atmospheric CO₂ for the land biosphere and a source of CO₂ from the coastal and open oceans (assuming remineralization to maintain steady state). Note that rock weathering is a sink of atmospheric CO₂ for the land biosphere and a source of CO₂ from the coastal and open oceans (assuming marine calcification to maintain steady state).

AU6

the different estimates, this does not necessarily minimize the role of lateral allochthonous DIC and organic carbon inputs, and the role of input of CO₂ from rivers in sustaining the emission of CO₂ from estuaries to the atmosphere.

p0240 **Figure 17** that summarizes all the processes that drive CH₄ fluxes in estuarine systems shows a high spatial heterogeneity, from $14.5 \pm 17.5 \text{ mmol m}^{-2} \text{ d}^{-1}$ in vegetated freshwater tidal marshes, to $0.04 \pm 0.17 \text{ mmol m}^{-2} \text{ d}^{-1}$ in estuarine plumes offshore. Such spatial heterogeneity makes it difficult to estimate precisely global CH₄ emissions from estuaries. We estimated representative CH₄ fluxes, based on median values of five sub-ecosystem types: (1) well-mixed estuarine water column, which corresponds to estuarine channels and shallow coastal embayments; (2) unvegetated tidal flats, where sediment-air CH₄ fluxes at low tide are on average ~8 times higher than water-air fluxes in adjacent channels (**Tables 5 and 6**); we divided by 2 the median flux to account for the inundation time due to tidal cycles; (3) vegetated tidal marshes show the largest spatial variation of CH₄ fluxes, mainly controlled by salinity (**Figure 20**); hence, we had to assume that the data compiled in **Table 5** are representative of an average situation; because most of the flux occurs through plants, the CH₄ flux from marshes is assumed to be constant throughout the tidal cycle; (4) mangroves, where sediment-air CH₄ fluxes are much less variable than in marshes, the median was divided by 2 to account for inundation time during the tidal cycle; and (5) for stratified systems with anoxic bottom waters, the flux is the average of two systems (**Table 7**). We adapted the estuarine

typology of Dürr et al. (2010) with a percentage of surface area occupied by each estuarine subsystem in each estuarine type (**Table 10**). Mangroves were restricted between 25° N and 25° S, and tidal marshes to other latitudes. The CH₄ fluxes were then scaled by latitudinal bands as for CO₂ fluxes. The resulting total CH₄ flux is $6.6 \text{ TgCH}_4 \text{ yr}^{-1}$, type IV contributing 60% of the total, types II and III contributing equally 17%, and type I contributing 6% (**Table 8**). About 4% of the total CH₄ flux occurs from well-mixed waters, 3% from tidal flats, 36% from tidal marshes, less than 1% from mangrove sediments, and 56% from stratified systems. The estimated CH₄ flux for type IV is probably overestimated. The CH₄ flux of $1.85 \text{ mmol C m}^{-2} \text{ d}^{-1}$ assumed representative of stratified systems is based only on two systems: a relatively shallow fjord and a tropical lagoon, both characterized by anoxic bottom waters and high CH₄ concentrations (Damm et al., 2005). Because the surface area of type IV estuaries is very large (**Table 8**), this has a strong impact on the calculation of the total CH₄ flux, especially at high latitudes (**Figure 27**). The sum of CH₄ emissions of $<3 \text{ TgCH}_4 \text{ yr}^{-1}$ from the other three types is consistent with previous estimates: $0.8\text{--}1.3 \text{ TgCH}_4 \text{ yr}^{-1}$ (Bange et al., 1994), $0.9\text{--}1.7 \text{ TgCH}_4 \text{ yr}^{-1}$ (Upstill-Goddard et al., 2000), and $1.8\text{--}3.0 \text{ TgCH}_4 \text{ yr}^{-1}$ (Middelburg et al., 2002) (**Table 10**). These estimates were based on the total surface area of estuaries given by Woodwell et al. (1973) of $1.4 \times 10^6 \text{ km}^2$, an area ~2.3 higher than the one from the typology of Dürr et al. (2010) for the sum of types I, II, and III (**Table 10**). In previous studies,

AU16

t0050 **Table 10** Ratios used to convert CH₄ fluxes from estuarine subsystems to CH₄ fluxes from estuarine types

	<i>Small deltas and estuaries (type I)</i>	<i>Tidal systems and embayments (type II)</i>	<i>Lagoons (type III)</i>	<i>Fjords and fjärds (type IV)</i>	<i>CH₄ flux per subecosystem (mmol m⁻² yr⁻¹)</i>
Well-mixed estuarine channels and bays	35%	60%	40%	25%	37
Tidal flats	15%	10%	20%	0%	146
Tidal marshes	50%	30%	30%	5%	1241
Mangrove sediments and waters	50%	30%	30%	0%	29
Stratified systems	0%	0%	10%	70%	675
Resulting CH ₄ flux per estuarine type (mmol m ⁻² yr ⁻¹)	318	245	277	544	

The fact that the sum of percentages is >100% is due to the distribution of mangroves limited between 25°N to 25°S latitudes and of tidal marshes at other latitudes.

Calculated CH₄ fluxes per estuarine types account for this latitudinal distribution of marshes and mangroves and are weighted by the surface areas of each type given by Dürr et al. (2010).

t0055 **Table 11** Comparison of published global CH₄ fluxes and emissions to the atmosphere from estuaries

<i>CH₄ flux (mmol C m⁻² yr⁻¹)</i>	<i>Emission of CH₄ (TgCH₄ yr⁻¹)</i>	<i>Surface area (10⁶ km²)</i>	<i>References</i>
36–59	0.8–1.3	1.4 ^a	Bange et al. (2004)
41–47	0.9–1.7	1.4 ^a	Upstill-Goddard et al. (2000)
79–132	1.8–3.0	1.4 ^a	Middelburg et al. (2002)
385	6.6	1.1 ^b	This study (all estuarine types)
266	2.6	0.6 ^b	This study (excluding fjords and fjärds (Type IV))

^a Based on Woodwell, G.M., Rich, P.H., Hall, C.A.S., 1973. Carbon in estuaries. In: Woodwell, G.M., Pecan, E.V. (Eds.), Carbon and the biosphere. Technical Information Center, U.S. Atomic Energy Commission; National Technical Information Service, Springfield, VA, pp. 221-240. including intertidal areas.

^b Based on Dürr H.H., G.G. Laruelle, C.M. van Kempen, C.P. Slomp, M. Meybeck and H. Middelkoop (2010) World-wide typology of near-shore coastal systems: defining the estuarine filter of river inputs to the oceans, Estuaries and Coasts, submitted.

CH₄ fluxes were not discriminated either between estuarine types, which have a relatively homogeneous air–water diffusive CH₄ flux (0.67–1.49 mmolC m⁻¹ d⁻¹; **Table 9**), or between subsystems, which show, on the contrary, a very large heterogeneity (0.1–3.4 mmolC m⁻¹ d⁻¹; **Table 9**). As a consequence, our estimate is very sensitive to the percentage of intertidal areas, in particular by the part occupied by tidal marshes. Tidal marshes alone emit ~2.3 TgCH₄ yr⁻¹, for a surface area of 0.12 × 10⁶ km², a value much higher than the one of 0.34 TgCH₄ yr⁻¹ proposed by Bartlett et al. (1985) for a higher surface area of 0.38 × 10⁶ km². This difference is because we included data from freshwater tidal marshes in the estimate. The inclusion of sediment–air CH₄ flux emissions in our global estimates also explains why the CH₄ flux per surface area (266–385 mmolC m⁻² yr⁻¹, excluding and including fjords and fjärds (type IV), respectively) is higher than previous estimates (36–132 mmolC m⁻² yr⁻¹) that only accounted for the diffusive emissions of CH₄ to the atmosphere from the water column (**Table 10**). Our estimate of CH₄ flux from mangrove sediments is only 0.05 TgCH₄ yr⁻¹, for a surface area of 0.10 × 10⁶ km², a surface only 30% lower than the one given by the Food and Agricultural Organization (FAO, 2003). This CH₄ flux would be 0.11 TgCH₄ yr⁻¹ if we assume similar fluxes at high tide and low tide (Kristensen et al., 2008), but is much lower than the flux of 2.2 TgCH₄ yr⁻¹ proposed by Barnes et al. (2006), who used an overestimated surface area for world mangroves forests and creeks (0.56 × 10⁶ km²). There is a convergence for the magnitude of the total CH₄ flux from estuaries (<3 TgCH₄ yr⁻¹), which is a minor contributor to global atmospheric CH₄ content (~0.5% of global anthropogenic and natural CH₄ emissions, 582 TgCH₄ yr⁻¹ according to the Fourth Assessment Report of the Intergovernmental Panel on Climate Change (Denman et al., 2007)). Note, however, that the flux of CH₄ from estuaries is not taken into account in global budgets, and that the imbalance of total sources and total sinks of CH₄ accounted so far is small (~ 1.0 TgCH₄ yr⁻¹; Denman et al., 2007), and is of the same order of magnitude as estuarine CH₄ emissions. Yet, there are still very large uncertainties concerning the partitioning of CH₄ fluxes between estuarine types and sub-types.

s0065 **5.04.6 Summary and Perspectives**

p0245 Estuarine systems are highly dynamic in terms of C cycling and emit CO₂ to the atmosphere at rates that are quantitatively significant for the global C cycle. This emission of CO₂ to the atmosphere is strongly supported by the net heterotrophic nature of these ecosystems. The robustness of the evaluation of the emission of CO₂ from estuarine ecosystems has increased during the past years due to increasing data availability and improvements in the surface area estimated by estuarine types. The latter can still be improved, for instance, by distinguishing between microtidal and macrotidal systems, as the former are usually highly stratified and are lower sources of CO₂ to the atmosphere than the latter that are usually permanently or partly well mixed. However, the degree of detail in a typology depends on the availability of data to populate the typology. At present, the sparseness of data is the major limitation in the quantification of the spatial and temporal variability of CO₂ fluxes in estuarine environments. There is a fair amount

of data to characterize tidal systems (type II) and small deltas (type I). However, for fjords and fjärds (type IV) that represent 43% of the total estuarine surface area there are data from only one location. For lagoons (type III), most of the available data were obtained from five contiguous systems located in Ivory Coast (~5° N) although these nearshore ecosystems are ubiquitous at all latitudes. Finally, there is a lack of data in estuarine environments at high latitudes, while 52% of the surface area of estuarine ecosystems is located at latitudes >65° N.

Regarding future observational efforts, there is also a need p0250 for sustained measurements to unravel interannual variability and long-term trends of CO₂ and CH₄ in estuarine environments. Due to the strong linkage with river catchments, the interannual variability of CO₂ and CH₄ in estuarine environments is expected to be strong in relation to variability of precipitation and freshwater discharge. Due to changes in land-use on the river catchments that change inputs of C, N, and P (e.g., Smith et al., 2003; Galloway et al. 2005; **00509** and **00506**), in addition to water-diversion activities (Humborg et al., 1997; Vörösmarty and Sahagian, 2000), decadal changes in CO₂ and CH₄ dynamics, and fluxes with the atmosphere in estuarine environments are expected to be significant. For instance, long-term changes in TA from the Mississippi River have been documented possibly due to changes in land use (Raymond and Cole, 2003; Cai et al., 2008; Raymond et al., 2008). In the US, a long-term decrease of pCO₂ in rivers and streams (1973–94) has been reported and attributed to a decline in terrestrial primary production (Jones et al., 2003). In the outer Scheldt estuary (river plume), strong changes in CO₂ fluxes and carbonate chemistry during the last five decades have been modeled in response to changes in nutrient delivery from rivers (Gypens et al., 2009; Borges and Gypens, 2010).

Future increases in organic matter inputs and expanding p0255 hypoxic and anoxic zones could lead to an increase of the CH₄ emissions from estuaries. In continental shelves and upwelling systems, increasing stratification and slowing down of convection are also expected to lead to an increase of CH₄ production, although Naqvi et al. (2009) predict that this will not lead to a major increase in the CH₄ emission from these systems to the atmosphere due to CH₄ oxidation in the water column. Oxidation of CH₄ might not be as effective in decreasing the CH₄ emission from estuaries than in the open ocean, due to shallower water columns (~10 m compared ~100 m for shelves and upwelling systems) and to direct emissions from intertidal sediments to the atmosphere. Yet, the potential feedback on atmospheric composition and climate change will probably be minor, as estuarine CH₄ emissions only represent <1% of the total CH₄ global emissions, although the imbalance of total sources and total sinks of CH₄ accounted so far is small (~ 1.0 TgCH₄ yr⁻¹) and of the same order of magnitude as estuarine CH₄ emissions.

Data used in the present chapter were either obtained by the p0260 authors, data mined from publications, or communicated by colleagues. There is a need for publicly available and quality checked databases for CO₂ and CH₄ in estuarine environments. Not only cross-system meta-analysis of data can be enlightening as explored in the present chapter, but also considering the uncertainties in estimating *k* in estuarine environments (cf. Section 5.04.4), there could be a need in future to re-evaluate air–water CO₂ and CH₄ fluxes, requiring access to the raw pCO₂ and [CH₄] data.

p0265 Unlike CH₄, we did not account for sediment–atmosphere CO₂ fluxes from intertidal areas when scaling CO₂ fluxes between estuaries and the atmosphere. Although several studies report sediment–atmosphere CO₂ fluxes in estuarine intertidal areas measured with dark chambers providing only the benthic respiration term (e.g., Middelburg et al., 1996), there are only a limited number of studies reporting net annual sediment–atmosphere CO₂ fluxes at the community level, that in tidal salt marshes range between -11 and -25 mol C m⁻² yr⁻¹ (Houghton and Woodwell, 1980; Kathilankal et al., 2008). The net annual CO₂ sink over intertidal areas is sustained by the primary production by macrophytes and microphytobenthos. Yet, the primary production at the surface of the sediment that sustains this CO₂ sink fuels organic carbon degradation within the sediment. The CO₂ produced will be partly transferred by tidal pumping to the water column and then emitted to the atmosphere.

p0270 Finally, we did not discuss CO₂ fluxes in river plumes (or outer estuaries). Data with adequate spatial and temporal coverage in these systems to robustly evaluate air–sea CO₂ fluxes are scarce. Some outer estuaries act as sources of CO₂ to the atmosphere such as the Scheldt (1.9 mol m⁻² yr⁻¹; Borges and Frankignoulle, 2002c; Schiettecatte et al., 2006; Borges et al., 2008), the Loire (10.5 mol C m⁻² yr⁻¹; de la Paz et al., 2010), and the Kennebec (0.9 mol C m⁻² yr⁻¹; Salisbury et al., 2009; Vandemark et al., 2009), while others act as sinks for atmospheric CO₂ such as the Amazon (-0.5 mol m⁻² yr⁻¹; Körtzinger, 2003) and the Changjiang (-1.9 mol m⁻² yr⁻¹; Zhai and Dai, 2009). The direction of the annual net flux of CO₂ in outer estuaries could be, to a large extent, related to the presence or the absence of haline stratification that promotes export of organic matter across the pycnocline and enhances light availability for primary production (Borges, 2005). Haline stratification generally occurs in high freshwater discharge systems; hence, large river plumes (Amazon and Changjiang) act as sinks of CO₂, while smaller systems (Scheldt, Loire, and Kennebec) act as sources of CO₂ to the atmosphere. Hence, a typological approach taking into account physical and biogeochemical characteristics that drive a net annual sink or source of CO₂ is required to estimate the global surface of outer estuaries and scale globally the CO₂ fluxes from these environments, in addition to more observations in different systems.

Acknowledgments

M. Frankignoulle coordinated the EU projects BIOGEST and EUROTROPH that generated a large amount of the data and knowledge on CO₂ and CH₄ dynamics in estuarine environments; he was also a source of inspiration for both authors. J.J. Middelburg, S. Bouillon, G.V.M. Gupta, M. Dai, F. Gazeau, M.F. Billet, T. Miyajima, E. Kristensen, W.-J. Cai, P. Raymond, G.G. Laruelle, H.H. Dürr, C.P. Slomp kindly provided part of the data used in this chapter, N. Gypens provided comments during manuscript elaboration, and J.J. Middelburg provided constructive comments on the draft version. This contributes to EU Coordination and support action COCOS (212196) and Fonds National de la Recherche Scientifique (F.N.R.S.) projects CAKI (2.4.598.07) and CASIMIR (2.4.608.09). AVB is a research associate at the F.N.R.S.

References

- Abril, G., Borges, A.V., 2004. Carbon dioxide and methane emissions from estuaries. In: Tremblay, A., Varfalvy, L., Roehm, C., Garneau, M. (Eds.), *Greenhouse Gases Emissions from Natural Environments and Hydroelectric Reservoirs: Fluxes and Processes*. Springer, Berlin, pp. 187–207. [bib0005](#)
- Abril, G., Commarieu, M.V., Etcheber, H., Deborde, J., Deflandre, B., Zivadinovic, M.K., Chaillou, G., Anschutz, P., 2010. *In vitro* simulation of oxic/suboxic diagenesis in an estuarine fluid mud subjected to redox oscillations. *Estuarine, Coastal and Shelf Science* 88, 279–291. [bib0010](#)
- Abril, G., Commarieu, M.-V., Guérin, F., 2007. Enhanced methane oxidation in an estuarine turbidity maximum. *Limnology and Oceanography* 52, 470–475. [bib0015](#)
- Abril, G., Commarieu, M.-V., Maro, D., Fontugne, M., Guérin, F., Etcheber, H., 2004. A massive dissolved inorganic carbon release at spring tide in a highly turbid estuary. *Geophysical Research Letters* 31, L09316. doi:10.1029/2004GL019714. [bib0020](#)
- Abril, G., Commarieu, M.V., Sottolichio, A., Bretel, P., Guérin, F., 2009. Turbidity limits gas exchange in a large macrotidal estuary. *Estuarine, Coastal and Shelf Science* 83, 342–348. [bib0025](#)
- Abril, G., Etcheber, H., Borges, A.V., Frankignoulle, M., 2000. Excess atmospheric carbon dioxide transported by rivers into the Scheldt estuary. *Comptes Rendus de l'Académie des Sciences Série II Fascicule A – Sciences de la Terre et des Planètes* 330 (11), 761–768. [bib0030](#)
- Abril, G., Etcheber, H., Delille, B., Frankignoulle, M., Borges, A.V., 2003. Carbonate dissolution in the turbid and eutrophic Loire estuary. *Marine Ecology Progress Series* 259, 129–138. [bib0035](#)
- Abril, G., Etcheber, H., Le Hir, P., Bassoullet, P., Boutier, B., Frankignoulle, M., 1999. Oxic/anoxic oscillations and organic carbon mineralization in an estuarine maximum turbidity zone (The Gironde, France). *Limnology and Oceanography* 44, 1304–1315. [bib0040](#)
- Abril, G., Iversen, N., 2002. Methane dynamics in a shallow, non-tidal, estuary (Randers Fjord, Denmark). *Marine Ecology Progress Series* 230, 171–181. [bib0045](#)
- Abril, G., Nogueira, E., Etcheber, H., Cabecadas, G., Lemaire, E., Brogueira, M.J., 2002. Behaviour of organic carbon in nine contrasting European estuaries. *Estuarine, Coastal and Shelf Science* 54, 241–262. [bib0050](#)
- Albert, D.B., Martens, C.S., Alperin, M.J., 1998. Biogeochemical processes controlling methane in gassy coastal sediments – part 2. *Groundwater flow control of acoustic turbidity in Eckernförde Bay sediments*. *Continental Shelf Research* 18, 1771–1793. [bib0055](#)
- Alford, D.P., Delaune, R.D., Lindau, C.W., 1997. Methane flux from Mississippi River deltaic plain wetlands. *Biogeochemistry* 37, 227–236. [bib0060](#)
- Algesten, G., Wikner, J., Sobek, S., Tranvik, L.J., Jansson, M., 2004. Seasonal variation of CO₂ saturation in the Gulf of Bothnia: indications of marine net heterotrophy. *Global Biogeochemical Cycles* 18 (4), GB4021. doi:10.1029/2004GB002232. [bib0065](#)
- Allen, D.E., Dalal, R.C., Rennenberg, H., Meyer, R.L., Reeves, S., Schmidt, S., 2007. Spatial and temporal variation of nitrous oxide and methane flux between subtropical mangrove sediments and the atmosphere. *Soil Biology and Biochemistry* 39, 622–631. [bib0070](#)
- Aller, R.C., 1998. Mobile deltaic and continental shelf muds as suboxic, fluidized bed reactors. *Marine Chemistry* 61, 143–155. [bib0075](#)
- Amouroux, D., Roberts, G., Rapsomanikis, S., Andrea, M.O., 2002. Biogenic gas (CH₄, N₂O, DMS) emission to the atmosphere from near-shore and shelf waters of the Northwestern Black sea. *Estuarine, Coastal and Shelf Science* 54, 575–587. [bib0080](#)
- Audry, S., Blanc, G., Schäfer, J., Chaillou, G., Robert, S., 2006. Early diagenesis of trace metals (Cd, Cu, Co, Ni, U, Mo, and V) in the freshwater reaches of a macrotidal estuary. *Geochimica et Cosmochimica Acta* 70, 2264–2282. [bib0085](#)
- Azevedo, I.C., Duarte, P.M., Bordalo, A.A., 2006. Pelagic metabolism of the Douro estuary (Portugal) – factors controlling primary production. *Estuarine, Coastal and Shelf Science* 69, 133–146. [bib0090](#)
- Bange, H.W., 2006. Nitrous oxide and methane in European coastal waters. *Estuarine, Coastal and Shelf Science* 70, 361–374. [bib0095](#)
- Bange, H.W., Bartell, U.H., Rapsomanikis, S., Andrea, M.O., 1994. Methane in the Baltic and North Seas and a reassessment of the marine emissions of methane. *Global Biogeochemical Cycles* 8, 465–480. [bib0100](#)
- Bange, H.W., Dahlke, S., Ramesh, R., Meyer-Reil, L.-A., Rapsomanikis, S., Andrea, M.O., 1998. Seasonal study of methane and nitrous oxide in the coastal waters of the southern Baltic Sea. *Estuarine, Coastal and Shelf Science* 47, 807–817. [bib0105](#)
- Bange, H.W., Rapsomanikis, S., Andrea, M.O., 1996. The Aegean Sea as a source of atmospheric nitrous oxide and methane. *Marine Chemistry* 53, 41–49. [bib0110](#)
- Barnes, J., Ramesh, R., Purvaja, R., Nirmal Rajkumar, A., Senthil Kumar, B., Krithika, K., Ravichandran, K., Uher, G., Upstill-Goddard, R., 2006. Tidal dynamics and rainfall control N₂O and CH₄ emissions from a pristine mangrove creek. *Geophysical Research Letters* 33, doi:10.1029/2006GL026829. [bib0115](#)

- bib0120** Bartlett, K.B., Bartlett, D.S., Harris, R.C., Sebacher, D.I., 1987. Methane emissions along a salt marsh salinity gradient. *Biogeochemistry* 4, 183–202.
- bib0125** Bartlett, K.B., Harris, R.C., Sebacher, D.I., 1985. Methane flux from coastal marshes. *Journal of Geophysical Research* 90, 5710–5720.
- bib0130** Battin, T.J., Kaplan, L.A., Findlay, S., Hopkinson, C.S., Marti, E., Packman, A.I., Newbold, J.D., Sabater, F., 2008. Biophysical controls on organic carbon fluxes in fluvial networks. *Nature Geosciences* 1, 95–100.
- bib0135** Bianchi, T.S., 2007. *Biogeochemistry of Estuaries*. Oxford University Press, Oxford, 720 pp.
- bib0140** Billett, M.F., Garnett, M.H., Harvey, F., 2007. UK peatland streams release old carbon dioxide to the atmosphere and young dissolved organic carbon to rivers. *Geophysical Research Letters* 34, L23401. doi:10.1029/2007GL031797.
- bib0145** Billett, M.F., Moore, T.R., 2008. Supersaturation and evasion of CO₂ and CH₄ in surface waters at Mer Bleue peatland, Canada. *Hydrological Processes* 22, 2044–2054.
- bib0150** Billett, M.F., Palmer, S.M., Hope, D., Deacon, C., Storeton-West, R., Hargreaves, K.J., Flechard, C., Fowler, D., 2004. Linking land–atmosphere–stream carbon fluxes in a lowland peatland system. *Global Biogeochemical Cycles* 18, GB1024. doi:10.1029/2003GB002058.
- bib0155** Biswas, H., Mukhopadhyay, S.K., Sen, S., Jana, T.K., 2007. Spatial and temporal patterns of methane dynamics in the tropical mangrove dominated estuary, NE coast of Bay of Bengal, India. *Journal of Marine Systems* 68, 55–64.
- bib0160** Blair, N.E., Aller, R.C., 1995. Anaerobic methane oxidation on the Amazon shelf. *Geochimica et Cosmochimica Acta* 59, 3707–3715.
- bib0165** Borges, A.V., 2005. Do we have enough pieces of the jigsaw to integrate CO₂ fluxes in the coastal ocean? *Estuaries* 28 (1), 3–27.
- bib0170** Borges, A.V., Delille, B., Frankignoulle, M., 2005. Budgeting sinks and sources of CO₂ in the coastal ocean: diversity of ecosystems counts. *Geophysical Research Letters* 32, L14601. doi:10.1029/2005GL023053.
- bib0175** Borges, A.V., Delille, B., Schiettecatte, L.-S., Gazeau, F., Abril, G., Frankignoulle, M., 2004a. Gas transfer velocity of CO₂ in three European estuaries (Randers Fjord, Scheldt and Thames). *Limnology and Oceanography* 49, 1630–1641.
- bib0180** Borges, A.V., Djenidi, S., Lacroix, G., Theate, J., Delille, B., Frankignoulle, M., 2003. Atmospheric CO₂ flux from mangrove surrounding waters. *Geophysical Research Letters* 30 (11), 1558. doi:10.1029/2003GL017143.
- bib0185** Borges, A.V., Frankignoulle, M., 2002a. Distribution of surface carbon dioxide and air–sea exchange in the upwelling system off the Galician coast. *Global Biogeochemical Cycles* 16 (2), 1020. doi:10.1029/2000GB001385.
- bib0190** Borges, A.V., Frankignoulle, M., 2002b. Aspects of dissolved inorganic carbon dynamics in the upwelling system off the Galician coast. *Journal of Marine Systems* 32, 181–198. doi:10.1016/S0924-7963(02)00031-3.
- bib0195** Borges, A.V., Frankignoulle, M., 2002c. Distribution and air–water exchange of carbon dioxide in the Scheldt plume off the Belgian coast. *Biogeochemistry* 59 (1–2), 41–67. doi:10.1023/A:1015517428985.
- bib0200** Borges, A.V., Gypens, N., 2010. Carbonate chemistry in the coastal zone responds more strongly to eutrophication than to ocean acidification. *Limnology and Oceanography* 55, 346–353.
- bib0205** Borges, A.V., Ruddick, K., Schiettecatte, L.-S., Delille, B., 2008. Net ecosystem production and carbon dioxide fluxes in the Scheldt estuarine plume. *BMC Ecology* 8, 15. doi:10.1186/1472-6785-8-15.
- bib0210** Borges, A.V., Schiettecatte, L.-S., Abril, G., Delille, B., Gazeau, F., 2006. Carbon dioxide in European coastal waters. *Estuarine, Coastal and Shelf Science* 70 (3), 375–387.
- bib0215** Borges, A.V., Vanderborcht, J.-P., Schiettecatte, L.-S., Gazeau, F., Ferron-Smith, S., Delille, B., Frankignoulle, M., 2004b. Variability of the gas transfer velocity of CO₂ in a macrotidal estuary (the Scheldt). *Estuaries* 27, 593–603.
- bib0220** Bouillon, S., Abril, G., Borges, A.V., Dehairs, F., Govers, G., Hughes, H., Merckx, R., Meysman, F.J.R., Nyunja, J., Osburn, C., Middelburg, J.J., 2009. Distribution, origin and cycling of carbon in the Tana River (Kenya): a dry season basin-scale survey from headwaters to the delta. *Biogeochemistry* 6, 2475–2493.
- bib0225** Bouillon, S., Dehairs, F., Schiettecatte, L.-S., Borges, A.V., 2007a. Biogeochemistry of the Tana estuary and delta (northern Kenya). *Limnology and Oceanography* 52 (1), 45–59.
- bib0230** Bouillon, S., Dehairs, F., Velimirov, B., Abril, G., Borges, A.V., 2007b. Dynamics of organic and inorganic carbon across contiguous mangrove and seagrass systems (Gazi bay, Kenya). *Journal of Geophysical Research – Biogeosciences* 112, G02018. doi:10.1029/2006JG000325.
- bib0235** Bouillon, S., Frankignoulle, M., Dehairs, F., Velimirov, B., Eiler, A., Abril, G., Etcheber, H., Borges, A.V., 2003. Inorganic and organic carbon biogeochemistry in the Gautami Godavari estuary (Andhra Pradesh, India) during pre-monsoon: the local impact of extensive mangrove forest. *Global Biogeochemical Cycles* 17 (4), 1114. doi:10.1029/2002GB002026.
- bib0240** Bouillon, S., Middelburg, J.J., Dehairs, F., Borges, A.V., Abril, G., Flindt, M.R., Ulomi, S., Kristensen, E., 2007c. Importance of intertidal sediment processes and porewater exchange on the water column biogeochemistry in a pristine mangrove creek (Ras Dege, Tanzania). *Biogeochemistry* 4, 311–322.
- bib0245** Brunet, F., Dubois, K., Veizer, J., Nkoue Ndong, G.R., Ndam Ngoupayou, J.R., Boeglin, J.L., Probst, J.L., 2009. Terrestrial and fluvial carbon fluxes in a tropical watershed: Nyong basin, Cameroon. *Chemical Geology* 265, 563–572.
- bib0250** Caffrey, J.M., 2004. Factors controlling net ecosystem metabolism in U.S. estuaries. *Estuaries* 27 (1) 90–101.
- bib0255** Cai, W.-J., Guo, X., Chen, C.T.A., Dai, M., Zhang, L., Zhai, W., Lohrenz, S.E., Yin, K., Harrison, P.J., Wang, Y., 2008. A comparative overview of weathering intensity and HCO₃⁻ flux in the world's major rivers with emphasis on the Changjiang, Huanghe, Zhujiang (Pearl) and Mississippi Rivers. *Continental Shelf Research* 28 (1–2), 1538–1549.
- bib0260** Cai, W.-J., Pomeroy, L.R., Moran, M.A., Wang, Y.C., 1999. Oxygen and carbon dioxide mass balance for the estuarine–intertidal marsh complex of five rivers in the southeastern US. *Limnology and Oceanography* 44 (3), 639–649.
- bib0265** Cai, W.-J., Wang, Y., 1998. The chemistry, fluxes, and sources of carbon dioxide in the estuarine waters of the Satilla and Altamaha Rivers, Georgia. *Limnology and Oceanography* 43 (4), 657–668.
- bib0270** Cai, W.-J., Wang, Z.H.A., Wang, Y.C., 2003. The role of marsh-dominated heterotrophic continental margins in transport of CO₂ between the atmosphere, the land–sea interface and the ocean. *Geophysical Research Letters* 30 (16), 1849. doi:10.1029/2003GL017633.
- bib0275** Cai, W.-J., Wiebe, W.J., Wang, Y.C., Sheldon, J.E., 2000. Intertidal marsh as a source of dissolved inorganic carbon and a sink of nitrate in the Satilla River–estuarine complex in the southeastern US. *Limnology and Oceanography* 45 (8), 1743–1752.
- bib0280** Capone, D.G., Kiene, R.P., 1988. Comparison of microbial dynamics in marine and freshwater sediments: contrasts in anaerobic carbon catabolism. *Limnology and Oceanography* 33, 725–749.
- bib0285** Carini, S., Weston, N., Hopkinson, C., Tucker, J., Giblin, A., Vallino, J., 1996. Gas exchange rates in the Parker River estuary, Massachusetts. *Biological Bulletin* 191, 333–334.
- bib0290** Carmouze, J.P., Knoppers, B., Vasconcelos, P., 1991. Metabolism of a subtropical Brazilian lagoon. *Biogeochemistry* 14, 129–148.
- bib0295** Chanton, J.P., Dacey, J.W.H., 1991. Effect of vegetation on methane flux, reservoirs and carbon isotopic composition. In: Sharkey, T., Holland, E., Mooney, H. (Eds.), *Trace Gas Emissions from Plants*. Academic Press, San Diego, CA, pp. 65–92.
- bib0300** Chanton, J.P., Martens, C.S., Kelley, C.A., 1989. Gas transport from methane-saturated, tidal freshwater and wetland sediments. *Limnology and Oceanography* 34, 807–819.
- bib0305** Chanton, J.P., Whiting, G., 1995. Trace gas exchange in freshwater and coastal marine systems: ebullition and plant transport. In: Matson, P., Harriss, R. (Eds.), *Methods in Ecology: Biogenic Trace Gases: Measuring Emissions from Soil and Water*. Blackwell, Cambridge, pp. 98–125.
- bib0310** Chavez, F.P., Messié, M., 2009. A comparison of Eastern Boundary Upwelling Ecosystems. *Progress in Oceanography* 83 (1–4), 80–96.
- bib0315** Chen, C.T.A., Borges, A.V., 2009. Reconciling opposing views on carbon cycling in the coastal ocean: continental shelves as sinks and near-shore ecosystems as sources of atmospheric CO₂. *Deep-Sea Research II* 56 (8–10), 578–590.
- bib0320** Chen, C.-T.A., Wang, S.-L., Lu, X.-X., Zhang, S.-R., Lui, H.-K., Tseng, H.-C., Wang, B.-J., Huang, H.-I., 2008. Hydrogeochemistry and greenhouse gases of the Pearl River, its estuary and beyond. *Quaternary International* 186 (1), 79–90.
- bib0325** Cheng, X., Luo, Y., Xu, Q., Lin, G., Zhang, Q., Chen, J., Li, B., 2009. Seasonal variation in CH₄ emission and its ¹³C-isotopic signature from *Spartina alterniflora* and *Scirpus mariqueter* soils in an estuarine wetland. *Plant Soil*, doi:10.1007/s1104-009-0033-y.
- bib0330** Ciavatta, S., Pastres, R., Badetti, C., Ferrari, G., Beck, M.B., 2008. Estimation of phytoplanktonic production and system respiration from data collected by a real-time monitoring network in the Lagoon of Venice. *Ecological Modelling* 212, 28–36.
- bib0335** Clark, C.D., Hiscock, W.T., Millero, F.J., Hitchcock, G., Brand, L., Miller, W.L., Ziolkowski, L., Chen, R.F., Zika, R.G., 2004. CDOM distribution and CO₂ production on the Southwest Florida Shelf. *Marine Chemistry* 89, 145–167.
- bib0340** Clark, J.F., Wanninkhof, R., Schlosser, P., Simpson, H.J., 1994. Gas exchange rates in the tidal Hudson River using a dual tracer technique. *Tellus, Series B* 46, 274–285.
- bib0345** Cloern, J.E., Jassby, A.D., 2008. Complex seasonal patterns of primary producers at the land–sea interface. *Ecology Letters* 11, 1294–1303.
- bib0350** Cole, J.J., Caraco, N.F., 2001. Carbon in catchments: connecting terrestrial carbon losses with aquatic metabolism. *Marine and Freshwater Research* 52 (1), 101–110.
- bib0355** Cole, J.J., Caraco, N.F., Kling, G.W., Kratz, T.K., 1994. Carbon dioxide supersaturation in the surface waters of lakes. *Science* 265 (5178), 1568–1570.
- bib0360** Cole, J.J., Prairie, Y.T., Caraco, N.F., McDowell, W.H., Tranvik, L.J., Striegl, R.G., Duarte, C.M., Kortelainen, P., Downing, J.A., Middelburg, J.J., Melack, J., 2007. Plumbing the global carbon cycle: integrating inland waters into the terrestrial carbon budget. *Ecosystems* 10, 171–184.

- bib0365** Collins, K.J., 1978. Fluxes of Organic Carbon and Nutrients in Southampton Waters. Ph.D. Dissertation, University of Southampton.
- bib0370** Conrad, R., 1989. Control of methane production in terrestrial ecosystems. In: Andrea, M.O., Schimel, D.S. (Eds.), *Exchange of Trace Gases between Terrestrial Ecosystems and the Atmosphere*. Wiley, Chichester, pp. 39–58.
- bib0375** Conrad, R., Frenzel, P., Cohen, Y., 1995. Methane emission from hypersaline microbial mats: lack of aerobic methane oxidation activity. *FEMS Microbiology and Ecology* 16, 297–306.
- bib0380** Crill, P.M., Martens, C.S., 1983. Spatial and temporal fluctuations of methane production in anoxic coastal marine sediments. *Limnology and Oceanography* 28, 1117–1130.
- bib0385** Damm, E., Mackensen, A., Budéus, G., Faber, E., Hanfland, C., 2005. Pathways of methane in seawaters: plume spreading in an Arctic shelf environment (SW-Spitsbergen). *Continental Shelf Research* 25, 1453–1472.
- bib0390** Davies, J.L., 1964. A morphogenic approach to world shore-lines. *Zeitschrift für Geomorphologie* 8, 127–142.
- bib0395** Dawson, J.J.C., Billett, M.F., Hope, D., 2001. Diurnal variations in the carbon chemistry of two acidic peatland streams in north-east Scotland. *Freshwater Biology* 46, 1309–1322.
- bib0400** Dawson, J.J.C., Billett, M.F., Hope, D., Palmer, S.M., Deacon, C.M., 2004. Sources and sinks of aquatic carbon linked to a peatland stream continuum. *Biogeochemistry* 70, 71–92.
- bib0405** Dawson, J.J.C., Billett, M.F., Neal, C., Hill, S., 2002. A comparison of particulate, dissolved and gaseous carbon in two contrasting upland streams in the UK. *Journal of Hydrology* 257, 226–246.
- bib0410** Day, J.W., Jr., Madden, C.J., Ley-Lou, F., Wetzel, R.L., Navarro, A.M., 1988. Aquatic primary productivity in Terminos lagoon region. In: Yáñez-Arancibia, A., Day, J.W. Jr., (Eds.), *Ecology of Coastal Ecosystems in the Southern Gulf of Mexico: The Terminos Lagoon Region*. Universidad Nacional Autónoma de Mexico, Mexico City, pp. 221–236.
- bib0415** De Angelis, M.A., Lilley, M.D., 1987. Methane in surface waters of Oregon estuaries and rivers. *Limnology and Oceanography* 32, 716–722.
- bib0420** De Angelis, M.A., Scranton, M.I., 1993. Fate of methane in the Hudson River and Estuary. *Global Biogeochemical Cycles* 7, 509–523.
- bib0425** de la Paz, M., Gómez-Parra, A., Forja, J., 2007. Inorganic carbon dynamic and air–water CO₂ exchange in the Guadalquivir Estuary. *Journal of Marine Systems* 68, 265–277.
- bib0430** de la Paz, M., Padín, X.A., Ríos, A.F., Pérez, F.F., 2010. Surface fCO₂ variability in the Loire plume and adjacent shelf waters: high spatio-temporal resolution study using ships of opportunity. *Marine Chemistry* 118, 108–118.
- bib0435** Deborde, J., Abril, G., Guérin, F., Poirier, P., Marty, B., Boucher, G., Thouzeau, G., Canton, M., Anschutz, P., 2010. Methane sources, sinks and fluxes in a temperate tidal lagoon: the Arcachon Lagoon (SW France). *Estuarine, Coastal and Shelf Science* (in revision).
- bib0440** del Giorgio, P.A., Cole, J.J., Caraco, N.F., Peters, R.H., 1999. Linking planktonic biomass and metabolism to net gas fluxes in northern temperate lakes. *Ecology* 80, 1422–1431.
- bib0445** del Giorgio, P.A., Davis, J., 2003. Patterns in dissolved organic matter lability and consumption across aquatic systems. In: Findlay, S.E.G., Sinsabaugh, R.L. (Eds.), *Aquatic Ecosystems, Interactivity of Dissolved Organic Matter*. Academic Press/Elsevier, San Diego, CA, pp. 399–424.
- bib0450** DeLaune, R.D., Smith C.J., Patrick, W.H., Jr., 1983. Methane release from Gulf Coast wetlands. *Tellus* 35B, 8–15.
- bib0455** Denman, K.L., Brasseur, G., Chidthaisong, A., Ciais, P., Cox, P.M., Dickinson, R.E., Hauglustaine, D., Heinze, C., Holland, E., Jacob, D., Lohmann, U., Ramachandran, S., da Silva Dias, P.L., Woisy S.C., Zhang, X., 2007. Couplings between changes in the climate system and biogeochemistry. In: Solomon, S., D. Qin, M. Manning, Z. Chen, M. Marquis, K.B. Averyt, M.Tignor and H.L. Miller (eds.) *Climate Change 2007: The Physical Science Basis. Contribution of Working Group I to the Fourth Assessment Report of the Intergovernmental Panel on Climate Change*. Cambridge University Press, Cambridge, United Kingdom and New York, NY, USA.
- bib0460** Depetris, P.J., Kempe, S., 1993. Carbon dynamics and sources in the Paraná River. *Limnology and Oceanography* 38 (2), 382–395.
- bib0465** Diaz, R.J., Rosenberg, R., 2008. Spreading dead zones and consequences for marine ecosystems. *Science* 321, 926–929.
- bib0470** Dionne, J.-C., 1973. Monroes: a type of so-called mud volcanoes in tidal flats. *Journal of Sedimentary Petrology* 43, 848–856.
- bib0475** Duarte, C.M., Agusti, S., 1998. The CO₂ balance of unproductive aquatic ecosystems. *Science* 281, 234–236.
- bib0480** Dürr H.H., Laruelle, G.G. van Kempen, C.M. Slomp, C.P. Meybeck, M. Middelkoop, H., 2010. World-wide typology of near-shore coastal systems: defining the estuarine filter of river inputs to the oceans. *Estuaries and Coasts* (submitted).
- bib0485** Dyer, K.R., Christie, M.C., Manning, A.J., 2004. The effects of suspended sediments on turbulence within an estuarine turbidity maximum. *Estuarine, Coastal and Shelf Science* 59, 237–248.
- Elliott, M., McLusky, D.S., 2002. The need for definitions in understanding estuaries. *Estuarine, Coastal and Shelf Science* 55 (6), 815–827.
- bib0490** Emerson, S., Bender, M.L., 1981. Carbon fluxes at the sediment–water interface: calcium carbonate preservation. *Journal of Marine Research* 39, 139–162.
- bib0495** Fairbridge, R.W., 1980. The estuary: its definition and geochemical role. In: Olausson, E., Cato, I. (Eds.), *Chemistry and Biogeochemistry of Estuaries*. Wiley, New York, NY, pp. 1–35.
- bib0500** Fenchel, T., Bernard, C., Esteban, G., Findlay, B.J., Hansen, P.J., Iversen, N., 1995. Microbial diversity and activity in a Danish fjord with anoxic deep waters. *Ophelia* 43, 45–100.
- bib0505** Ferrón, S., Ortega, T., Gómez-Parra, A., Forja, J.M., 2007. Seasonal study of CH₄, CO₂ and N₂O in a shallow tidal system of the bay of Cádiz (SW Spain). *Journal of Marine Systems* 66, 244–257.
- bib0510** FAO (Food and Agriculture Organization of the United Nations) 2003. State of the World's Forests (SOFO). Report. FAO, Rome, 100 pp.
- bib0515** Frankignoulle, M., Abril, G., Borges, A., Bourge, I., Canon, C., Delille, B., Libert, E., Thèate, J.-M., 1998. Carbon dioxide emission from European estuaries. *Science* 282 (5388), 434–436.
- bib0520** Frankignoulle, M., Borges, A.V., 2001. European continental shelf as a significant sink for atmospheric carbon dioxide. *Global Biogeochemical Cycles* 15, 569–576.
- bib0525** Frankignoulle, M., Bourge, I., Wollast, R., 1996. Atmospheric CO₂ fluxes in a highly polluted estuary (The Scheldt). *Limnology and Oceanography* 41 (2), 365–369.
- bib0530** Frankignoulle, M., Middelburg, J.J., 2002. Biogases in tidal European estuaries: the BIOGEST project. *Biogeochemistry* 59 (1–2), 1–4.
- bib0535** Friederich, G.E., Ledesma, J., Ulloa, O., Chavez, F.P., 2008. Air–sea carbon dioxide fluxes in the coastal southeastern tropical Pacific. *Progress in Oceanography* 79 (2–4), 156–166.
- bib0540** Friederich, G.E., Walz, P.M., Burczynski, M.G., Chavez, F.P., 2002. Inorganic carbon in the central California upwelling system during the 1997–1999 El Niño-La Niña event. *Progress in Oceanography* 54 (1–4), 185–203.
- bib0545** Frithsen, J.B., Keller, A.A., Pilson, M.E.Q., 1985. Data Report 3, Vol. 1. Marine Ecosystems Research Laboratory Service, University of Kingston.
- bib0550** Frost, T., Upstill-Goddard, R.C., 2002. Meteorological controls of gas exchange at a small English lake. *Limnology and Oceanography* 47, 1165–1174.
- bib0555** Galloway, J.N., Dentener, F.J., Capone, D.G., Boyer, E.W., Howarth, R.W., Seitzinger, S.P., Asner, G.P., Cleveland, C.C., Green, P.A., Holland, E.A., Karl, D.M., Michaels, A.F., Porter, J.H., Townsend, A.R., Vöörsmarty, C.J., 2005. Nitrogen cycles: past, present, and future. *Biogeochemistry* 70, 153–226.
- bib0560** Gao, X.L., Song, J.M., Li, X.Q., Yuan, H.M., Li, N., 2005. Spatial and temporal variations in pH and total alkalinity at the beginning of the rainy season in the Changjiang Estuary, China. *Acta Oceanologica Sinica* 24 (5), 68–77.
- bib0565** García-Gil, S., Vilas, F., García-García, A., 2002. Shallow gas features in incised-valley fills (Ría de Vigo, NW Spain): a case study. *Continental Shelf Research* 22, 2303–2315.
- bib0570** García-Muñoz, M., Aristegui, J., Pelegrí, J.L., Antoranz, A., Ojeda, A., Torres, M., 2005. Exchange of carbon by an upwelling filament off Cape Ghir (NW Africa). *Journal of Marine Systems* 54, 83–95.
- bib0575** Garside, C., Malone, T.C., 1978. Monthly oxygen and carbon budgets of the New York Bight Apex. *Estuarine, Coastal and Shelf Science* 6, 93–104.
- bib0580** Gattuso, J.-P., Frankignoulle, M., Wollast, R., 1998. Carbon and carbonate metabolism in coastal aquatic ecosystems. *Annual Review of Ecology and Systematics* 29, 405–434.
- bib0585** Gazeau, F., Borges, A.V., Barrón, C., Duarte, C.M., Iversen, N., Middelburg, J.J., Delille, B., Pizay, M.-D., Frankignoulle, M., Gattuso, J.-P., 2005a. Net ecosystem metabolism in a micro-tidal estuary (Randers Fjord, Denmark): evaluation of methods. *Marine Ecology Progress Series* 301, 23–41.
- bib0590** Gazeau, F., Gattuso, J.-P., Middelburg, J.J., Brion, N., Schiettecatte, L.-S., Frankignoulle, M., Borges, A.V., 2005b. Planktonic and whole system metabolism in a nutrient-rich estuary (the Scheldt estuary). *Estuaries* 28 (6), 868–883.
- bib0595** Gazeau, F., Gentili, B., Smith, S.V., Frankignoulle, M., Gattuso, J.-P., 2004. The European coastal zone: characterization and first assessment of ecosystem metabolism. *Estuarine, Coastal and Shelf Science* 60 (4), 673–694.
- bib0600** Gazeau, F., Middelburg, J.J., Loijens, M., Vanderborcht, J.-P., Pizay, M.-D., Gattuso, J.-P., 2007. Planktonic primary production in estuaries: a comparison of the ¹⁴C, O₂ and ¹⁸O methods. *Aquatic Microbial Ecology* 46, 95–106.
- bib0605** Gerard, G., Chanton, J.P., 1993. Quantification of methane oxidation in the rhizosphere of emergent aquatic macrophytes – defining upper limits. *Biogeochemistry* 23, 79–97.
- bib0610** Geyer, W.R., 1993. The importance of suppression of turbulence by stratification on the estuarine turbidity maximum. *Estuaries* 16, 113–125.
- bib0615** Ghosh, S., Jana, T.K., Singh, B.N., Choudhury, A., 1987. Comparative study of carbon dioxide system in virgin and reclaimed mangrove waters of Sundarbans during freshet. *Mahasagar: Bulletin of the National Institute of Oceanography* 20 (3), 155–161.

- bib0625** Goyet, C., Millero, F.J., O'Sullivan, D.W., Eiseheid, G., McCue, S.J., Bellerby, R.G.J., 1998. Temporal variations of $p\text{CO}_2$ in surface seawater of the Arabian Sea in 1995. *Deep-Sea Research Part I* 45 (4–5), 609–623.
- bib0630** Grunwald, M., Dellwig, O., Beck, M., Dippner, J.W., Freund, J.A., Kohlmeier, C., Schnetger, B., Brumsack, H.-J., 2009. Methane in the southern North Sea: sources, spatial distribution and budgets. *Estuarine, Coastal and Shelf Science* 81, 445–456.
- bib0635** Guérin, F., Abril, G., Serça, D., Delon, C., Richard, S., Delmas, R., Tremblay, A., Varfalvy L., 2007. Gas transfer velocities of CO_2 and CH_4 in a tropical reservoir and its river downstream. *Journal of Marine Systems* 66, 161–172.
- bib0640** Guo, X., Dai, M., Zhai, W., Cai, W.-J., Chen, B., 2009. CO_2 flux and seasonal variability in a large subtropical estuarine system, the Pearl River Estuary, China. *Journal of Geophysical Research* 114, G03013. doi:10.1029/2008JG000905.
- bib0645** Gupta, G.V.M., Sarma, V.V.S.S., Robin, R.S., Raman, A.V., Jai Kumar, M., Rakesh, M., Subramanian, B.R., 2008. Influence of net ecosystem metabolism in transferring riverine organic carbon to atmospheric CO_2 in a tropical coastal lagoon (Chilka Lake, India). *Biogeochemistry* 87, 265–285.
- bib0650** Gupta, G.V.M., Thottathil, S.D., Balachandran, K.K., Madhu, N.V., Madheswaran, P., Nair, S., 2009. CO_2 supersaturation and net heterotrophy in a tropical estuary (Cochin, India): influence of anthropogenic effect. *Ecosystems* 12 (7), 1145–1157.
- bib0655** Gypens, N., Borges, A.V., Lancelot, C., 2009. Effect of eutrophication on air–sea CO_2 fluxes in the coastal Southern North Sea: a model study of the past 50 years. *Global Change Biology* 15 (4), 1040–1056.
- bib0660** Heip, C., Goosen, N.K., Herman, P.M.J., Kromkamp, J., Middelburg, J.J., Soetaert, K., 1995. Production and consumption of biological particles in temperate tidal estuaries. *Oceanography and Marine Biology: An Annual Review* 33, 1–149.
- bib0665** Hofmann, A.F., Middelburg, J.J., Soetaert, K., Meysman, F.J.R., 2009. pH modelling in aquatic systems with time-variable acid–base dissociation constants applied to the turbid, tidal Scheldt estuary. *Biogeosciences* 6, 1539–1561.
- bib0670** Hofmann, A.F., Soetaert, K., Middelburg, J.J., 2008. Present nitrogen and carbon dynamics in the Scheldt estuary using a novel 1-D model. *Biogeosciences* 5, 981–1006.
- bib0675** Hope, D., Palmer, S.M., Billett, M.F., Dawson, J.J.C., 2001. Carbon dioxide and methane evasion from a peatland stream. *Limnology and Oceanography* 46, 847–857.
- bib0680** Hopkinson, C.S., Jr., 1985. Shallow-water benthic and pelagic metabolism: evidence of heterotrophy in the nearshore Georgia Bight. *Marine Biology* 87, 19–32.
- bib0685** Hopkinson, C.S., Jr., 1988. Patters of organic carbon exchange between coastal ecosystems: the mass balance approach in salt marsh ecosystems. In: Jansson, B.O. (Ed.), *Coastal–Offshore Ecosystems Interactions*. Springer, Berlin, pp. 122–154.
- bib0690** Hopkinson, C.S., Vallino, J.J., 1995. The relationships among Man's activities in the watersheds and estuaries: a model of runoff effects on patterns of estuarine community metabolism. *Estuaries* 18, 598–621.
- bib0695** Hoppema, J.M.J., 1991. The oxygen budget of the Western Wadden Sea, The Netherlands. *Estuarine, Coastal and Shelf Science* 32, 483–502.
- bib0700** Houghton, R.A., Woodwell, G.M., 1980. The Flax Pond ecosystem study: exchanges of CO_2 between a salt marsh and the atmosphere. *Ecology* 61 (6), 1434–1445.
- bib0705** Humborg, C., Ittekköt, V., Cociasu, A., Bodungen, B.V., 1997. Effect of Danube River dam on Black Sea biogeochemistry and ecosystem structure. *Nature* 386, 385–388.
- bib0710** Hunt, C.W., Salisbury, J.E., Vandemark, D., McGillis, W., 2010. Sub-estuary scale contrasts of carbon dioxide exchange, response to freshwater input variability, and inorganic carbon dynamics. *Estuaries and Coasts* (submitted).
- bib0715** Ivanov, M.V., Pimenov, N.V., Rusanov, I.I., Lein, A.Yu., 2002. Microbial processes of the methane cycle at the North-western shelf of the Black Sea. *Estuarine, Coastal and Shelf Science* 54, S589–S599.
- bib0720** Jassby, A.D., Cloern, J.E., Powell, T.P., 1993. Organic carbon sources and sinks in San Francisco Bay: variability induced by a river flow. *Marine Ecology Progress Series* 93, 39–54.
- bib0725** Jayakumar, D.A., Naqvi, S.W.A., Narvekar, P.V., George, M.D., 2001. Methane in coastal and offshore water of the Arabian Sea. *Marine Chemistry* 74, 1–13.
- bib0730** Jiang, L.-Q., Cai, W.-J., Wang, Y., 2008. A comparative study of carbon dioxide degassing in river- and marine-dominated estuaries. *Limnology and Oceanography* 53(6), 2603–2615.
- bib0735** Jones, J.B., Mulholland, P.J., 1998. Influence of drainage basin topography and elevation on carbon dioxide and methane supersaturation of stream water. *Biogeochemistry* 40, 57–72.
- bib0740** Jones, J.B., Jr., Stanley, E.H., Mulholland, P.J., 2003. Long-term decline in carbon dioxide supersaturation in rivers across the contiguous United States. *Geophysical Research Letters* 30 (10), 1495. doi:10.1029/2003GL017056.
- bib0745** Jones, R.D., Amador, J.A., 1995. Methane and carbon monoxide production, oxidation and turnover times in the Caribbean Sea as influenced by the Orinoco River. *Journal of Geophysical Research* 98, 2353–2359.
- bib0750** Judd, A.G., Sim, R., Kingston, P., McNally, J., 2002. Gas seepage on an intertidal site: Torry Bay, Firth of Forth, Scotland. *Continental Shelf Research* 22, 2317–2331.
- bib0755** Kathilankal, J.C., Mozdzler, T.J., Fuentes, J.D., D'Odorico, P., McGlathery, K.J., Ziemann, J.C., 2008. Tidal influences on carbon assimilation by a salt marsh. *Environmental Research Letters* 3, 044010. doi:10.1088/1748-9326/3/4/044010.
- bib0760** Kaul, L.W., Froelich, P.N., 1984. Modeling estuarine nutrient geochemistry in a simple system. *Geochimica et Cosmochimica Acta* 48, 1417–1733.
- bib0765** Keil, R.G., Mayer, L.M., Quay, P.D., Richey, J.E., Hedges, J.I., 1997. Loss of organic matter from riverine particles in deltas. *Geochimica et Cosmochimica Acta* 61 (7), 1507–1511.
- bib0770** Kelley, C.A., Martens, C.S., Chanton, J.P., 1990. Variations in sedimentary carbon remineralization rates in the White Oak River estuary, North Carolina. *Limnology and Oceanography* 35, 372–383.
- bib0775** Kelley, C.A., Martens, C.S., Ussler, W., III, 1995. Methane dynamics across a tidally flooded riverbank margin. *Limnology and Oceanography* 40, 1112–1129.
- bib0780** Kelly, C.A., Fee, E., Ramlal, P.S., Rudd, J.W.M., Hesselin, R.H., Anema, C., Schindler, E.U., 2001. Natural variability of carbon dioxide and net epilimnetic production in the surface waters of boreal lakes of different sizes. *Limnology and Oceanography* 46, 1054–1064.
- bib0785** Kemp, W.M., Smith, E.M., Marvin-DiPasquale, M., Boynton, W.R., 1997. Organic carbon-balance and net ecosystem metabolism in Chesapeake Bay. *Marine Ecology Progress Series* 150, 229–248.
- bib0790** Kenney, B.E., Litaker, W., Duke, C.S., Ramus, J., 1988. Community oxygen metabolism in a shallow tidal estuary. *Estuarine, Coastal and Shelf Science* 27, 33–43.
- bib0795** King, G.M., 1994. Association of methanotrophs with the roots and rhizomes of aquatic vegetation. *Applied and Environmental Microbiology* 60, 3220–3227.
- bib0800** Koné, Y.J.M., Abril, G., Delille, B., Borges, A.V., (2010) Seasonal variability of methane in the rivers and lagoons of Ivory Coast (West Africa). *Biogeochemistry* (in press).
- bib0805** Koné, Y.J.M., Abril, G., Kouadio, K.N., Delille, B., Borges, A.V., 2009. Seasonal variability of carbon dioxide in the rivers and lagoons of Ivory Coast (West Africa). *Estuaries and Coasts* 32, 246–260.
- bib0810** Koné, Y.J.M., Borges, A.V., 2008. Dissolved inorganic carbon dynamics in the waters surrounding forested mangroves of the Ca Mau Province (Vietnam). *Estuarine, Coastal and Shelf Science* 77 (3), 409–421.
- bib0815** Körtzinger, A., 2003. A significant CO_2 sink in the tropical Atlantic Ocean associated with the Amazon River plume. *Geophysical Research Letters* 30 (24), 2287. doi:10.1029/2003GL018841.
- bib0820** Kremer, J.N., Nixon, S.W., Buckley, B., Roques, P., 2003b. Technical note: conditions for using the floating chamber method to estimate air–water gas exchange. *Estuaries* 26, 985–990.
- bib0825** Kremer, J.N., Reischauer, A., D'Avanzo, C., 2003a. Estuary-specific variation in the air–water gas exchange coefficient for oxygen. *Estuaries* 26, 829–836.
- bib0830** Kristensen, E., Flindt, M.R., Ulomi, S., Borges, A.V., Abril, G., Bouillon, S., 2008. Emission of CO_2 and CH_4 to the atmosphere by sediments and open waters in two Tanzanian mangrove forests. *Marine Ecology Progress Series* 370, 53–67.
- bib0835** Kuliński, K., Pempkowiak, J., 2008. Dissolved organic carbon in the southern Baltic Sea: quantification of factors affecting its distribution. *Estuarine, Coastal and Shelf Science* 78, 38–44.
- bib0840** Laruelle G.G., Dürr, H.H., Slomp, C.P., Borges, A.V., 2010. Evaluation of sinks and sources of CO_2 in the global coastal ocean using a spatially-explicit typology of estuaries and continental shelves. *Geophysical Research Letters* (submitted).
- bib0845** Le Mer, J., Roger, P., 2001. Production, oxidation, emissions and consumption of methane in soils: a review. *European Journal of Soil Biology* 37, 25–50.
- bib0850** Lehner, B., Döll, P., 2004. Development and validation of a global database of lakes, reservoirs and wetlands. *Journal of Hydrology* 296 (1–4), 1–22.
- bib0855** Lindstrom, M.E., 1983. Methane consumption in Framvaren, an anoxic marine fjord. *Limnology and Oceanography* 28, 1247–1251.
- bib0860** Lilley, M.D., De Angelis, M.A., Olson, E.J., 1996. Methane concentrations and estimated fluxes from Pacific northwest rivers. In: Adams, D.D., Seitzinger, S.P., Crill, P.M. (Eds.), *Cycling of Reduced Gases in the Hydrosphere*. E. Schweizerbart'sche Verlagbuchhandlung, Stuttgart, pp. 187–196.
- bib0865** Lipschultz, F., 1981. Methane release from a brackish intertidal salt-marsh embayment of Chesapeake Bay, Maryland. *Estuaries* 4, 143–145.
- bib0870** Liss, P.S., Merlivat, L., 1986. Air–sea exchange rates: introduction and synthesis. In: Buat-Ménard, P. (Ed.), *The Role of Air–Sea Exchange in Geochemical Cycling*. Reidel, Dordrecht, pp. 113–127.
- bib0875** Ludwig, W., Probst, J.L., Kempe, S., 1996. Predicting the oceanic input of organic carbon by continental erosion. *Global Biogeochemical Cycles* 10 (1), 23–41.
- bib0880** Magenheimer, J.F., Moore, T.R., Chmura, G.L., Daoust, R.J., 1996. Methane and carbon dioxide flux from a macrotidal salt marsh, Bay of Fundy, New Brunswick. *Estuaries* 19, 139–145.
- bib0885** Marino, R., Howarth, R.W., 1993. Atmospheric oxygen exchange in the Hudson River: dome measurements and comparison with other natural waters. *Estuaries* 16, 433–445.
- bib0890** Martens, C.S., Albert, D.B., Alperin, M.J., 1998. Biogeochemical processes controlling methane in gassy coastal sediments – part 1. A model coupling organic matter flux

- to gas production, oxidation and transport. *Continental Shelf Research* 18, 1741–1770.
- [bib0895](#) Martens, C.S., Benner, R.A., 1977. Interstitial water chemistry of anoxic Long Island Sound sediments. 1. Dissolved gases. *Limnology and Oceanography* 22, 10–25.
- [bib0900](#) Martens, C.S., Goldhaber, M.B., 1978. Early diagenesis in transitional sedimentary environments of the White Oak River estuary, North Carolina. *Limnology and Oceanography* 23, 428–441.
- [bib0905](#) Martens, C.S., Klump, J.V., 1980. Biogeochemical cycling in an organic-rich coastal marine basin – I. Methane sediment–water exchange processes. *Geochimica et Cosmochimica Acta* 44, 471–490.
- [bib0910](#) Martins, O., 1982. Geochemistry of the Niger River. In: Degens, E.T. (Ed.), *Transport of Carbon and Minerals in Major World Rivers, Part 1*, SCOPE/JUNEP Sonderband 52, Mitt. Geologisch-Paläontologisches Institut, Universität Hamburg, pp. 397–418.
- [bib0915](#) McDonald, I.R., Smith, K., Lidstrom, M.E., 2005. Methanotrophic populations in estuarine sediment from Newport Bay, California. *FEMS Microbiology Letters* 250, 287–293.
- [bib0920](#) McGinnis, D.F., Greinert, J., Artemov, Y., Beaubien, S.E., Wüest, A., 2006. Fate of rising methane bubbles in stratified waters: how much methane reaches the atmosphere? *Journal of Geophysical Research* 111, doi:10.1029/2005JC003183.
- [bib0925](#) Mee, L.D., 1977. *The Chemistry and Hydrography of Some Tropical Coastal Lagoons – Pacific Coast of Mexico*. Ph.D. Dissertation, University of Liverpool, 125 pp.
- [bib0930](#) Meybeck, M., Abril, G., Roussennac, S., Behrendt, H., Billett, M.F., Billen, G., Borges, A.V., Casper, P., Garnier, J., Hinderer, M., Huttunen, J., Johansson, T., Kastowski, M.F., Manó, S., 2006. Specific study on freshwater greenhouse gas budget. CarboEurope – GHG – Concerted Action: Synthesis of the European Greenhouse Gas Budget. Report 1.1.5.
- [bib0935](#) Middelburg, J.J., Klaver, G., Nieuwenhuize, J., Wielemaker, A., Haas, W., Vlut, T., Van der Nat, F.J.W.A., 1996. Organic matter mineralization in intertidal sediments along an estuarine gradient. *Marine Ecology Progress Series* 132, 157–168.
- [bib0940](#) Middelburg, J.J., Nieuwenhuize, J., Iversen, N., Høgh, N., de Wilde, H., Helder, W., Seifert, R., Christof, O., 2002. Methane distribution in tidal estuaries. *Biogeochemistry* 59, 95–119.
- [bib0945](#) Millero, F.J., Graham, T.B., Huang, F., Bustos-Serrano, H., Pierrot, D., 2006. Dissociation constants of carbonic acid in sea water as a function of salinity and temperature. *Marine Chemistry* 100, 80–94.
- [bib0950](#) Millero, F.J., Hiscock, W.T., Huang, F., Roche, M., Zhang, J.Z., 2001. Seasonal variation of the carbonate system in Florida Bay. *Bulletin of Marine Science* 68, 101–123.
- [bib0955](#) Missiaen, T., Murphy, S., Loncke, L., Henriët, J.-P., 2002. Very high-resolution seismic mapping of shallow gas in the Belgian coastal zone. *Continental Shelf Research* 22, 2291–2301.
- [bib0960](#) Miyajima, T., Tsuboi, Y., Tanaka, Y., Koike, I., 2009. Export of inorganic carbon from two Southeast Asian mangrove forests to adjacent estuaries as estimated by the stable isotope composition of dissolved inorganic carbon. *Journal of Geophysical Research* 114, G01024. doi:10.1029/2008JG000861.
- [bib0965](#) Moran, M.A., Sheldon, W.M., Sheldon, J.E., 1999. Biodegradation of riverine dissolved organic carbon in five estuaries of the southeastern United States. *Estuaries* 22, (1) 55–64.
- [bib0970](#) Mukhopadhyay, S.K., Biswas, H., De, T.K., Sen, S., Jana, T.K., 2002. Seasonal effects on the air–water carbon dioxide exchange in the Hooghly estuary, NE coast of Gulf of Bengal, India. *Journal of Environmental Monitoring* 4 (4), 549–552.
- [bib0975](#) Naqvi, S.W.A., Bange, H.W., Farías, L., Monteiro, P.M.S., Scramton, M.J., Zhang, J., 2009. Coastal hypoxia/anoxia as a source of CH₄ and N₂O. *Biogeosciences Discussion* 6, 9455–9523.
- [bib0980](#) Neal, C., House, W.A., Jarvie, H.P., Eatherall, A., 1998. The significance of dissolved carbon dioxide in major rivers entering the North Sea. *Science of the Total Environment* 210–211, 187–203.
- [bib0985](#) Neubauer, S.C., Anderson, I.C., 2003. Transport of dissolved inorganic carbon from a tidal freshwater marsh to the York River estuary. *Limnology and Oceanography* 48 (1), 299–307.
- [bib0990](#) Nirmal Rajkumar, A., Barnes, J., Ramesh, R., Purvaja, R., Upstill-Goddard, R.C., 2008. Methane and nitrous oxide fluxes in the polluted Adyar River and estuary, SE India. *Marine Pollution Bulletin* 56, 2043–2051.
- [bib0995](#) O'Connor, D.J., Dobbins, W.E., 1958. Mechanism of reaeration in natural streams. *Transactions of the American Society of Civil Engineering* 123, 641–684.
- [bib1000](#) Odum, H.T., Hoskin, C.M., 1958. Comparative studies of the metabolism of Texas Bays. *Publications of the Institute of Marine Science, University of Texas* 5, 16–46.
- [bib1005](#) Odum, H.T., Wilson, R., 1962. Further studies on the reaeration and metabolism of Texas Bays. *Publications of the Institute of Marine Science, University of Texas* 8, 23–55.
- [bib1010](#) Okkonen, S.R., Schmidt, G.M., Cokelet, E.D., Stabeno, P.J., 2004. Satellite and hydrographic observations of the Bering Sea 'Green Belt'. *Deep-Sea Research II* 51, 1033–1051.
- Oremland, R.S., Polcin, S., 1982. Methanogenesis and sulfate reduction: competitive and non-competitive substrates in estuarine sediments. *Applied and Environmental Microbiology* 44, 1270–1276.
- [bib1020](#) Ortega, T., Ponce, R., Forja, J., Gómez-Parra, A., 2005. Fluxes of dissolved inorganic carbon in three estuarine systems of the Cantabrian Sea (north of Spain). *Journal of Marine Systems* 53 (1–4), 125–142.
- [bib1025](#) Ovalle, A.R.C., Rezende, C.E., Lacerda, L.D., Silva, C.A.R., 1990. Factors affecting the hydrochemistry of a mangrove tidal creek, Sepetiba bay, Brazil. *Estuarine, Coastal and Shelf Science* 31 (5), 639–650.
- [bib1030](#) Park, P.K., Hager, S.W., Cissel, M.C., 1969. Carbon dioxide partial pressure in the Columbia River. *Science* 166, 867–868.
- [bib1035](#) Perillo, G.M.E., 1995. Definition and geomorphologic classifications of estuaries. In: Perillo, G.M.E. (Ed.), *Geomorphology and Sedimentology of Estuaries. Developments in Sedimentology Elsevier, Amsterdam* vol. 53, pp. 17–47.
- [bib1040](#) Prego, R., 1993. General aspects of carbon biogeochemistry in the Ria of Vigo, northwestern Spain. *Geochimica et Cosmochimica Acta* 57 (9), 2041–2052.
- [bib1045](#) Pritchard, D.W., 1952. Salinity distribution and circulation in the Chesapeake Bay estuarine system. *Journal of Marine Research* 11, 107–123.
- [bib1050](#) Pritchard, D.W., 1955. Estuarine circulation patterns. *Proceedings of the American Society of Civil Engineers* 81 (717), 1–11.
- [bib1055](#) Pritchard, D.W., 1967. Observation of circulation in coastal plain estuaries. In: Lauff, G.H. (Ed.), *Estuaries. American Association for the Advancement of Science, Washington, DC*, pp. 3–5.
- [bib1060](#) Raimbault, P., Garcia, N., Cerutti, F., 2007. Distribution of inorganic and organic nutrients in the South Pacific Ocean – evidence for long-term accumulation of organic matter in nitrogen-depleted waters. *Biogeosciences Discussion* 4, 3041–3087.
- [bib1065](#) Ralison, O.H., Borges, A.V., Dehairs, F., Middelburg, J.J., Bouillon, S., 2008. Carbon biogeochemistry of the Betsiboka Estuary (north-western Madagascar). *Organic Geochemistry* 39, 1649–1658.
- [bib1070](#) Randall, J.M., Day, J.W., Jr., 1987. Effects of river discharge and vertical circulation on aquatic primary production in a turbid Louisiana (USA) estuary. *Netherlands Journal of Sea Research* 21, 231–242.
- [bib1075](#) Raymond, P.A., Bauer, J.E., 2000. Bacterial consumption of DOC during transport through a temperate estuary. *Aquatic Microbial Ecology* 22, 1–12.
- [bib1080](#) Raymond, P.A., Bauer, J.E., Cole, J.J., 2000. Atmospheric CO₂ evasion, dissolved inorganic carbon production, and net heterotrophy in the York River estuary. *Limnology and Oceanography* 45 (8), 1707–1717.
- [bib1085](#) Raymond, P.A., Cole, J.J., 2001. Gas exchange in rivers and estuaries: choosing a gas transfer velocity. *Estuaries* 24, 312–317.
- [bib1090](#) Raymond, P.A., Cole, J.J., 2003. Increase in the export of alkalinity from North America's largest river. *Science* 301 (5629), 88–91.
- [bib1095](#) Raymond, P.A., Hopkins, C.S., 2003. Ecosystem modulation of dissolved carbon age in a temperate marsh-dominated estuary. *Ecosystems* 6, 694–705.
- [bib1100](#) Raymond, P.A., Oh, N.H., Turner, R.E., Broussard, W., 2008. Anthropogenically enhanced fluxes of water and carbon from the Mississippi River. *Nature* 451, 449–452.
- [bib1105](#) Reeburgh, W.S., 1969. Observation of gases in Chesapeake Bay sediments. *Limnology and Oceanography* 14, 368–375.
- [bib1110](#) Revilla, M., Ansoategui, A., Iriarte, A., Madariaga, I., Orive, E., Sarobe, A., Trigueros, J.M., 2002. Microplankton metabolism along a trophic gradient in a shallow-temperate estuary. *Estuaries* 25 (1), 6–18.
- [bib1115](#) Reyes, E., Merino, M., 1991. Diel dissolved oxygen dynamics and eutrophication in a shallow, well-mixed tropical lagoon (Cancun, Mexico). *Estuaries* 14 (4), 372–381.
- [bib1120](#) Richey, J.E., 2004. Pathways of atmospheric CO₂ through fluvial systems. In: Field, C.B., Raupach, M.R. (Eds.), *The Global Carbon Cycle, Integrating Humans, Climate, and the Natural World*. Island Press, Washington, DC, pp. 329–340.
- [bib1125](#) Riera, J.L., Schindler, J.E., Kratz, T.K., 1999. Seasonal dynamics of carbon dioxide and methane in two clear-water lakes and two bogs lakes in northern Wisconsin, U.S.A. *Canadian Journal of Fisheries and Aquatic Sciences* 56, 265–274. doi:10.1139/cjfas-56-2-265.
- [bib1130](#) Robert, S., Blanc, G., Schaefer, J., Lavaux, G., Abril, G., 2004. Metal mobilization in the Gironde Estuary (France): the role of the soft mud layer in the maximum turbidity zone. *Marine Chemistry* 87, 1–13.
- [bib1135](#) Rochelle-Newall, E.J., Winter, C., Barrón, C., Borges, A.V., Duarte, C.M., Elliott, M., Frankignoulle, M., Gazeau, F., Middelburg, J.J., Pizay, M.-D., Gattuso, J.-P., 2007. An artificial neural network analysis of factors controlling ecosystem metabolism in the coastal ocean. *Ecological Applications* 17 (5, supplement), S185–S196.
- [bib1140](#) Roehm, C.L., Prairie, Y.T., del Giorgio, P.A., 2009. The pCO₂ dynamics in lakes in the boreal region of northern Québec, Canada. *Global Biogeochemical Cycles* 23, GB3013. doi:10.1029/2008GB003297.
- [bib1145](#) Rowe, G.T., Smith, S., Falkowski, P., Whitledge, T., Teroux, R., Phoel, W., Ducklow, H., 1986. Do continental shelves export organic matter? *Nature* 324, 559–561.

- bib1150** Russell, M.J., Montagna, P.A., 2007. Spatial and temporal variability and drivers of net ecosystem metabolism in Western Gulf of Mexico estuaries. *Estuaries and Coasts* 30 (1), 137–153.
- bib1155** Salisbury, J., Green, M., Hunt, C., Campbell, J., 2008. Coastal acidification by rivers: a new threat to shellfish? *EOS, Transactions, American Geophysical Union* 89, 513–514.
- bib1160** Salisbury, J., Vandemark, D., Hunt, C., Campbell, J., Jonsson, B., Mahadevan, A., McGillis, W., Xue, H., 2009. Episodic riverine influence on surface DIC in the coastal Gulf of Maine. *Estuarine, Coastal and Shelf Science* 82, 108–118.
- bib1165** Sansone, F.J., Holmes, M.E., Popp, B.N., 1999. Methane stable isotopic ratios and concentrations as indicators of methane dynamics in estuaries. *Global Biogeochemical Cycles* 13, 463–474.
- bib1170** Sansone, F.J., Martens, C.S., 1977. Methane oxidation in Cape Lookout Bight, North Carolina. *Limnology and Oceanography* 23, 349–355.
- bib1175** Sansone, F.J., Rust, T.M., Smith, S.V., 1998. Methane distribution and cycling in Tomales Bay, California. *Estuaries* 21, 66–77.
- bib1180** Santos, R., Silva, J., Alexandre, A., Navarro, N., Barrón, C., Duarte, C.M., 2004. Ecosystem metabolism and carbon fluxes of a tidally dominated coastal lagoon. *Estuaries* 27 (6), 977–985.
- bib1185** Sarma, V.V.S.S., Kumar, M.D., Manerikar, M., 2001. Emission of carbon dioxide from a tropical estuarine system, Goa, India. *Geophysical Research Letters* 28 (7), 1239–1242.
- bib1190** Schiettecatte, L.-S., Gazeau, F., Van der Zee, C., Brion, N., Borges, A.V., 2006. Time series of the partial pressure of carbon dioxide (2001–2004) and preliminary inorganic carbon budget in the Scheldt plume (Belgian coast waters). *Geochemistry, Geophysics, Geosystems* (G3) 7, Q06009. doi:10.1029/2005GC001161.
- bib1195** Scholten, H., Klepper, O., Nienhuis, P.H., Knoester, M., 1990. Oosterschelde estuary (SW Netherlands): a self-sustaining ecosystem? *Hydrobiologia* 195, 201–215.
- bib1200** Scranton, M.I., McShane, K., 1991. Methane fluxes in the southern North Sea: the role of European rivers. *Continental Shelf Research* 11, 37–52.
- bib1205** Seitzinger, S.P., Harrison, J.A., Dumont, E., Beusen, A.H.W., Bouwman, A.F., 2005. Sources and delivery of carbon, nitrogen, and phosphorus to the coastal zone: an overview of Global Nutrient Export from Watersheds (NEWS) models and their application. *Global Biogeochemical Cycles* 19, GB4S01. doi:10.1029/2005GB002606.
- bib1210** Shalini, A., Ramesh, R., Purvaja, R., Barnes, J., 2006. Spatial and temporal distribution of methane in an extensive shallow estuary, south India. *Journal of Earth System Science* 115 (4), 451–460.
- bib1215** Shin, K.-H., Tanaka, N., 2004. Distribution of dissolved organic matter in the eastern Bering Sea, Chukchi Sea (Barrow Canyon) and Beaufort Sea. *Geophysical Research Letters* 31, L24304. doi:10.1029/2004GL021039.
- bib1220** Silvennoinen, H., Liikanen, A., Rintala, J., Martikainen, P.J., 2008. Greenhouse gas fluxes from the eutrophic Temmesjoki River and its Estuary in the Liminganlahti Bay (the Baltic Sea). *Biogeochemistry* 90, 193–208.
- bib1225** Small, L.F., McIntire, C.D., MacDonald, K.B., Lara-Lara, J.R., Frey, B.E., Amspoker, M.C., Wenfield, T., 1990. Primary production, plant and detrital biomass and particle transport in the Columbia River. *Progress in Oceanography* 25, 175–210.
- bib1230** Smith, S.V., Hollibaugh, J.T., 1993. Coastal metabolism and the oceanic carbon balance. *Reviews of Geophysics* 31, 75–89.
- bib1235** Smith, S.V., Hollibaugh, J.T., 1997. Annual cycle and interannual variability of ecosystem metabolism in a temperate climate embayment. *Ecological Monographs* 67, 509–533.
- bib1240** Smith, S.V., Kimmerer, W.J., Laws, E.A., Brock, R.E., Walsh, T.W., 1981. Kaneohe Bay sewage diversion experiment: perspectives on ecosystem responses to nutritional perturbation. *Pacific Science* 35, 279–395.
- bib1245** Smith, S.V., Swaney, D.P., Talaue-McManus, L., Bartley, J.D., Sandhei, P.T., McLaughlin, C.J., Dupra, V.C., Crossland, C.J., Buddemeier, R.W., Maxwell, B.A., Wulff, F., 2003. Humans, hydrology, and the distribution of inorganic nutrient loading to the ocean. *BioScience* 53 (3), 235–245.
- bib1250** Smith, S.V., Veeh, H.H., 1989. Mass balance of biogeochemically active materials (C, N, P) in a hypersaline gulf. *Estuarine, Coastal and Shelf Science* 29, 195–215.
- bib1255** Sobek, S., Algesten, G., Bergström, A.-K., Jansson, M., Tranvik, L.J., 2003. The catchment and climate regulation of $p\text{CO}_2$ in boreal lakes. *Global Change Biology* 9, 630–641. doi:10.1046/j.1365-2486.2003.00619.x.
- bib1260** Sobek, S., Tranvik, L.J., Cole, J.J., 2005. Temperature independence of carbon dioxide supersaturation in global lakes. *Global Biogeochemical Cycles* 19, GB2003. doi:10.1029/2004GB002264.
- bib1265** Soetaert, K., Herman, P.M.J., 1995. Carbon flows in the Westerschelde estuary (The Netherlands) evaluated by means of an ecosystem model (MOSES). *Hydrobiologia* 311, 247–266.
- bib1270** Sotomayor, D., Corredor, J.E., Morell, J.M., 1994. Methane flux from mangrove sediments along the southwestern coast of Puerto Rico. *Estuaries* 17, 140–147.
- bib1275** Souza, M.F.L., Gomes, V.R., Freitas, S.S., Andrade, R.C.B., Knoppers, B., 2009. Net ecosystem metabolism and nonconservative fluxes of organic matter in a tropical mangrove estuary, Piauí River (NE of Brazil). *Estuaries and Coasts* 32, 111–122.
- Takahashi, T., Sutherland, S.C., Wanninkhof, R., Sweeney, C., Feely, R.A., Chipman, D.W., Hales, B., Friederich, G., Chavez, F., Sabine, C., Watson, A., Bakker, D.C.E., Schuster, U., Metzl, N., Yoshikawa-Inoue, H., Ishii, M., Midorikawa, T., Nojiri, Y., Körtzinger, A., Steinhoff, T., Hoppema, M., Olafsson, J., Amarnson, T.S., Tilbrook, B., Johannessen, T., Olsen, A., Bellerby, R., Wong, C.S., Delille, B., Bates, N.R., de Baar, H.J.W., 2009a. Climatological mean and decadal change in surface ocean $p\text{CO}_2$, and net sea-air CO_2 flux over the global oceans. *Deep-Sea Research II* 56 (8–10), 554–577.
- bib1285** Takahashi, T., Sutherland, S.C., Wanninkhof, R., Sweeney, C., Feely, R.A., Chipman, D.W., Hales, B., Friederich, G., Chavez, F., Sabine, C., Watson, A., Bakker, D.C.E., Schuster, U., Metzl, N., Yoshikawa-Inoue, H., Ishii, M., Midorikawa, T., Nojiri, Y., Körtzinger, A., Steinhoff, T., Hoppema, M., Olafsson, J., Amarnson, T.S., Tilbrook, B., Johannessen, T., Olsen, A., Bellerby, R., Wong, C.S., Delille, B., Bates, N.R., de Baar, H.J.W., 2009b. Corrigendum to “Climatological mean and decadal change in surface ocean $p\text{CO}_2$, and net sea-air CO_2 flux over the global oceans.” *Deep-Sea Research I* 56 (11), 2075–2076.
- bib1290** Teodoru, C., del Giorgio, P.A., Prairie, Y.T., 2009. Patterns in $p\text{CO}_2$ in boreal streams and rivers of northern Quebec, Canada. *Global Biogeochemical Cycles* 23, GB2012. doi:10.1029/2008GB003404.
- bib1295** Tokida, T., Miyazaki, T., Mizoguchi, M., Nagata, O., Takakai, F., Kagimoto, A., Hatano, R., 2007. Falling atmospheric pressure as a trigger for methane ebullition from peatland. *Global Biogeochemical Cycles* 21, doi:10.1029/2006GB002790.
- bib1300** Upstill-Goddard, R.C., 2006. Air–sea gas exchange in the coastal zone. *Estuarine, Coastal and Shelf Science* 70, 388–404.
- bib1305** Upstill-Goddard, R.C., Barnes, J., Frost, T., Punshon, S., Owens, N.J.P., 2000. Methane in the Southern North Sea: low salinity inputs, estuarine removal and atmospheric flux. *Global Biogeochemical Cycles* 14, 1205–1217.
- bib1310** Van der Maarel, M.J.E.C., Hansen, T.A., 1997. Dimethylsulfoniopropionate in anoxic intertidal sediment: a precursor of methanogenesis via dimethyl sulfide, methanethiol, and methylpropionate. *Marine Geology* 137, 5–12.
- bib1315** van der Nat, F.J.W.A., Middelburg, J.J., 1998a. Effect of two common macrophytes on methane dynamics in freshwater sediments. *Biogeochemistry* 43, 79–104.
- bib1320** van der Nat, F.J.W.A., Middelburg, J.J., 1998b. Seasonal variation in methane oxidation by the rhizosphere of *Phragmites australis* and *Scirpus lacustris*. *Aquatic Botany* 61, 95–110.
- bib1325** van der Nat, F.J.W.A., Middelburg, J.J., 2000. Methane emissions from tidal freshwater marshes. *Biogeochemistry* 49, 103–121.
- bib1330** van der Nat, F.J.W.A., Middelburg, J.J., van Meteren, D., Wielemakers, A., 1998. Diel methane emission patterns from *Scirpus lacustris* and *Phragmites australis*. *Biogeochemistry* 41, 1–22.
- bib1335** Van Es, F.B., 1977. A preliminary carbon budget for a part of the Ems estuary: the Dollard. *Helgolander Wiss. Meeresunters* 30, 283–294.
- bib1340** Vandemark, D., Salisbury, J., Irish, J., Hunt, C., Shellito, S., Chai, F., 2009. Examination of Interannual Ocean CO_2 and Air–Sea CO_2 Flux in the Western Gulf of Maine. RARGOM Gulf of Maine Symposium. St. Andrews-by-the-Sea, New Brunswick, 4–9 October.
- bib1345** Vanderborght, J.P., Wollast, R., Loijens, M., Regnier, P., 2002. Application of a transport-reaction model to the estimation of biogas fluxes in the Scheldt estuary. *Biogeochemistry* 59, 207–237.
- bib1350** Vannote, R.L., Minshall, G.W., Cummins, K.W., Sedell, J.R., Cushing, C.E., 1980. The river continuum concept. *Canadian Journal of Fisheries and Aquatic Sciences* 37, 130–137.
- bib1355** Vörösmarty, C.J., Sahagian, D., 2000. Anthropogenic disturbance of the terrestrial water cycle. *BioScience* 50 (9), 753–765.
- bib1360** Walsh, J.J., 1988. *On the Nature of Continental Shelves*. Academic Press, San Diego, CA.
- bib1365** Wang, X.U., Lee, C., 1994. Sources and distribution of aliphatic amines in salt marsh sediments. *Organic Geochemistry* 22, 1005–1021.
- bib1370** Wang, Z.A., Cai, W.-J., 2004. Carbon dioxide degassing and inorganic carbon export from a marsh-dominated estuary (the Duplin River): a marsh CO_2 pump. *Limnology and Oceanography* 49 (2), 341–354.
- bib1375** Wanninkhof, R., 1992. Relationship between wind speed and gas exchange over the ocean. *Journal of Geophysical Research* 97, 7373–7382.
- bib1380** Wanninkhof, R., McGillis, W.R., 1999. A cubic relationship between air–sea CO_2 exchange and wind speed. *Geophysical Research Letters* 26, 1889–1892.
- bib1385** Wanninkhof, R., Mulholland, P.J., Elwood, J.W., 1990. Gas exchange rates for a first-order stream determined with deliberate and natural tracers. *Water Resources Research* 26, 1621–1630.
- bib1390** Wassmann, P., Naas, K.E., Johannessen, P.J., 1986. Annual supply and loss of particulate organic carbon in Nordasvannet, a eutrophic, land-locked fjord in Western Norway. *Rapports et Procès Verbaux des Réunions Conseil International pour l’Exploration de la Mer* 186, 423–431.
- bib1395** Wiegner, T.N., Seitzinger, S.P., 2001. Photochemical and microbial degradation of external dissolved organic matter inputs to rivers. *Aquatic Microbial Ecology* 24, 27–40.
- bib1400** Wollast, R., 1983. Interaction in estuaries and coastal waters. In: Bolin, B., Cook, R.B. (Eds.), *The Major Biogeochemical Cycles and Their Interactions*. SCOPE. Wiley, Chichester, pp. 385–407.
- bib1405** Woodwell, G.M., Rich, P.H., Hall, C.A.S., 1973. Carbon in estuaries. In: Woodwell, G.M., Pecan, E.V. (Eds.), *Carbon and the Biosphere*. Technical Information Center, U.S.

- Atomic Energy Commission; National Technical Information Service, Springfield, VA, pp. 221–240.
- [bib1410](#) Zappa, C.J., McGillis, W.R., Raymond, P.A., Edson, E.J.B., Hinst, E.J., Zemmeling, H.J., Dacey, J.W.H., Ho, D.T., 2007. Environmental turbulent mixing controls on air–water gas exchange in marine and aquatic systems. *Geophysical Research Letters* 34, GLXXX. doi:10.29/2006GL028790.
- [bib1415](#) Zappa, C.J., Raymond, P.A., Terray, E.A., McGillis, W.R., 2003. Variation in surface turbulence and the gas transfer velocity over a tidal cycle in a macro-tidal estuary. *Estuaries* 26, 1401–1415.
- [bib1420](#) Zemmeling, H.J., Slagter, H.A., van Slooten, C., Snoek, J., Heusinkveld, B., Elbers, J., Bink, N.J., Klaassen, W., Philippart, C.J.M., de Baar, H.J.W., 2009. Primary production and eddy correlation measurements of CO₂ exchange over an intertidal estuary. *Geophysical Research Letters* 36, L19606. doi:10.1029/2009GL039285.
- Zhai, W., Dai, M., 2009. On the seasonal variation of air–sea CO₂ fluxes in the outer Changjiang (Yangtze River) Estuary, East China Sea. *Marine Chemistry* 117 (1–4), 2–10. [bib1425](#)
- Zhai, W., Dai, M., Guo, X., 2007. Carbonate system and CO₂ degassing fluxes in the inner estuary of Changjiang (Yangtze) River, China. *Marine Chemistry* 107 (3), 342–356. [bib1430](#)
- Zhang, G., Zhang, J., Lui, S., Ren, J., Xu, J., Zhang, F., 2008. Methane in the Changjiang (Yangtze River) Estuary and its adjacent marine area: riverine input, sediment release and atmospheric fluxes. *Biogeochemistry* 91, 71–84. [bib1435](#)
- Ziegler, S., Benner, R., 1998. Ecosystem metabolism in a subtropical, seagrass-dominated lagoon. *Marine Ecology Progress Series* 173, 1–12. [bib1440](#)

ELSEVIER AUTHOR PROFILE